DANMARKS OG GRØNLANDS GEOLOGISKE UNDERSØGELSE **RAPPORT 2023/48**

Whole-rock geochemistry and geochronology of granitic intrusions from Clavering Ø, Hudson Land and Gauss Halvø, North-East Greenland. Version 2

Thomas F. Kokfelt, Diogo Rosa,
Kristine Thrane & Agnete Steenfelt

GEOLOGICAL SURVEY OF DENMARK AND GREENLAND
DANISH MINISTRY OF CLIMATE, ENERGY AND UTILITIES

G E U S

DANMARKS OG GRØNLANDS GEOLOGISKE UNDERSØGELSE **RAPPORT 2023/48**

Whole-rock geochemistry and geochronology of granitic intrusions from Clavering Ø, Hudson Land and Gauss Halvø, North-East Greenland. Version 2

Thomas F. Kokfelt, Diogo Rosa, Kristine Thrane & Agnete Steenfelt

GEOLOGICAL SURVEY OF DENMARK AND GREENLAND
DANISH MINISTRY OF CLIMATE, ENERGY AND UTILITIES

G E U S

Content

Introduction 3

Geological Setting 5

Clavering Ø 5
Hudson Land and Gauss Halvø 6

Previous investigations of granites and rhyolites 7

Ages of granites and rhyolites 8

Samples 10

Analytical Method 12

Whole-rock chemistry 12
Zircon U-Pb dating by LA-ICPMS 12

Results 14

Geochemical data 14

Discussion based on total geochemical dataset 26

Rock alteration 26
Rock classification and tectonic setting 27
Major elements 27
Trace elements 29
Magma fertility 34

Geochronology results 38

523813 – Augen granite (Tonian) 38
521688 – Augen granite (Tonian) 40
521649 – Monzonite (Caledonian) 42
523808 – Monzonite (Caledonian) 44
567268 – Porphyritic granite (Caledonian) 46
587001 – Medium-grained equigranular two-mica granite (Caledonian) 48
523816 - Granitic vein (Caledonian) 50
546917 – Two-mica granite (Caledonian) 53
567232 – Aplitic granite (Devonian) 55
Summary of ages 57

Summary and evaluation/further studies 58

References 60

Introduction

This report represents an update of the recent GEUS report on East Greenland granite chemistry by Thrane et al. (2021), by adding 82 new samples characterised for whole-rock chemistry and nine samples for U-Pb geochronology. The total dataset thereby amounts to 188 samples that are geochemically characterised. The newly added samples were collected in Hudson Land in 2022 under the GEUS mapping campaign in the area. The samples included for U-Pb geochronology come from Clavering Ø and Hudson Land.

The overall aim of this project is to characterise the Neoproterozoic and Palaeozoic magmatic rocks, based on their geochemistry, to explore ways to effectively discriminate and group the granitoids. In turn, this will help to better understand the genesis of these granite groups, their spatial and temporal distribution, their structural and tectonic setting and predict which granites may be associated with mineralisation and understand their control on such mineralisation.

The Caledonian orogen in North-East Greenland is generally understood as a collisional orogen composed by a stack of nappes thrusted westwards over a basement of Archaean and Palaeoproterozoic ortho- and paragneiss units (Higgins et al. 2004; Kalsbeek et al. 2008a). Much of the geochemical and geochronological data obtained to support the present understanding is derived from the western part of the orogen, whereas the central and eastern parts are less well documented. This study focuses on Neoproterozoic and Palaeozoic felsic and intermediate magmatic rocks from the central part of the Caledonian orogen and forms part of a GEUS-project initiated in 2018 dealing with geological mapping and evaluation of the mineral potential of an area including Clavering Ø, Hudson Land and Gauss Halvø (Figure 1).

In the overall dataset the magmatic rocks are divided into three groups according to formation age: (1) a Tonian group, previously referred to as “Grenville” (c. 950-900 Ma), (2) a Caledonian, Middle Ordovician to Silurian group (c. 465-425 Ma) and (3) a Devonian (c. 380 Ma) group (Kalsbeek et al. 2000, 2001a,b, 2008b). In the field it can be difficult, if not impossible, to distinguish the different generations of magmatic rocks apart. However, certain characteristics can be of help in determining the relative age, such as extent or lack of deformation and cross-cutting relationships; as where granites intrude Devonian sedimentary rocks, the ages of the intrusive rocks can be surmised. Because of the inherent difficulty in distinguishing the different age groups of apart in the field, and because age dating cannot be applied to all rock samples, we apply geochemical characterisation as an alternative constraint to distinguish the different rock groups.

The initial report by Thrane et al (2021) contained geochemical data for 106 samples in total, including granites *sensu lato* (105) and Devonian evolved volcanics, mainly rhyolites (11). This report expands the database with an additional 82 entries, including 64 granite samples, *sensu lato*, of Caledonian to Devonian age, and 18 Devonian volcanics. The total database hereby includes 188 samples, including 159 granites, *sensu lato*, and 29 Devonian volcanics.

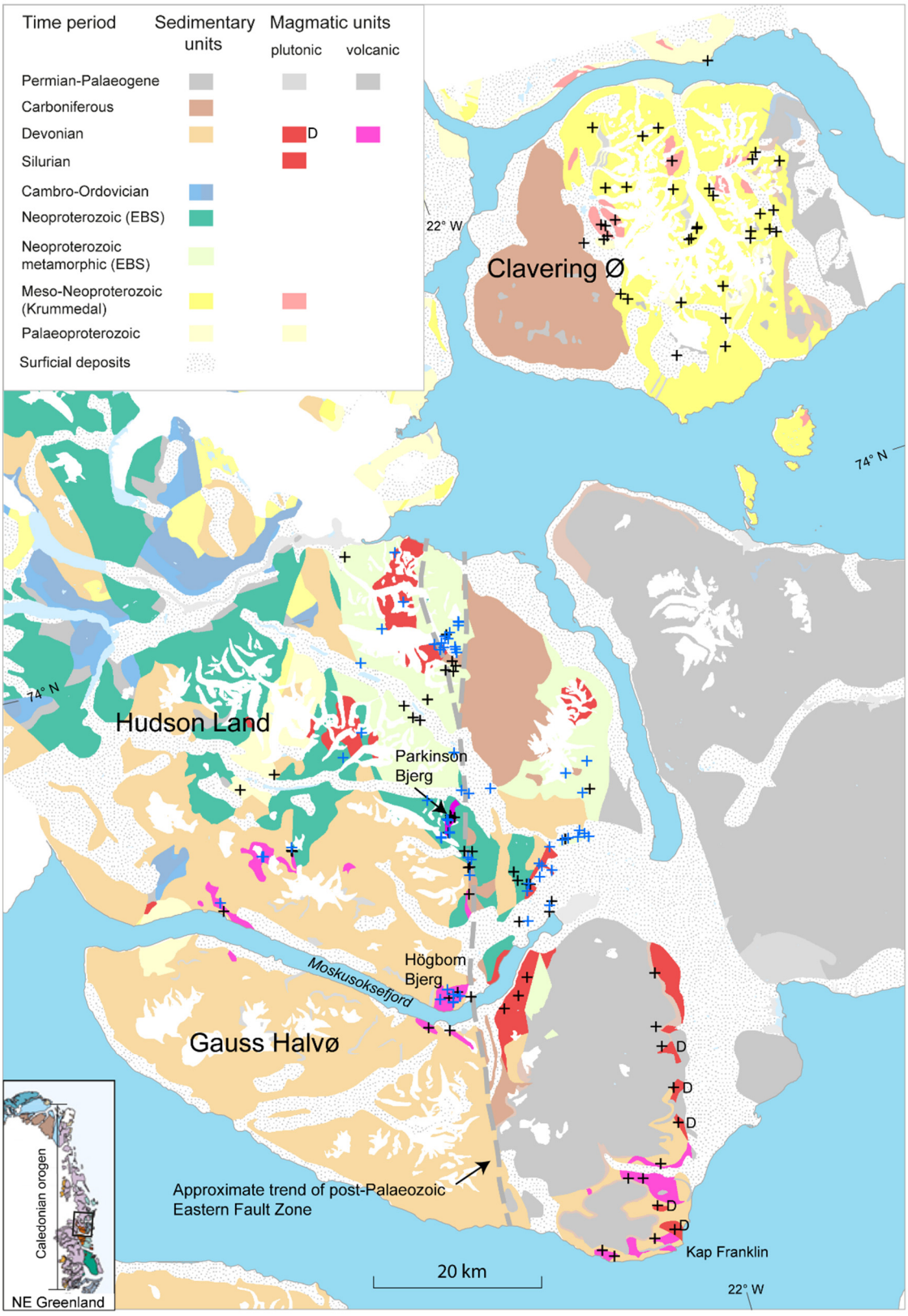

Figure 1: *Geological map of study region with sample sites, indicated (+); in blue the newly added samples, in black the existing data from Thrane et al. (2021). Geology is simplified and modified from Escher (2001). D marks granites regarded as Devonian by Koch & Haller (1971).*

Geological Setting

Most of the study area is composed of rocks affected by the Caledonian collisional orogeny (Higgins et al. 2004; Kalsbeek et al. 2008a). Palaeoproterozoic basement and Neoproterozoic to Ordovician sedimentary rocks were highly deformed by folding and thrusting and were variably metamorphosed during the orogeny. The area has also previously been affected by an Early Neoproterozoic high-grade metamorphic and magmatic event at c. 950-920 Ma, related to an orogenic event (Kalsbeek et al. 2000; Watt & Thrane 2001).

The region of Clavering Ø, Hudson Land and Gauss Halvø exhibits a complex pattern of Proterozoic to Palaeogene rocks (Figure 1). The underlying Palaeoproterozoic orthogneiss basement (Kalsbeek et al. 1993) is only recognised in few places. More dominant, especially at Clavering Ø, is the overlying Meso- to Neoproterozoic migmatised metasedimentary rocks of the Krummedal supracrustal sequence. Neoproterozoic basinal sediments of the Eleonore Bay Supergroup (EBS) as well as platformal Cambro-Ordovician limestone are thrusted on top of the Krummedal sequence. The Krummedal sequence and EBS are intruded by granites of presumed Tonian, Caledonian and Devonian ages.

Unmetamorphosed Devonian and Carboniferous continental sediments have been deposited in down-faulted basins during the waning and extensional stages of the orogen. Permian, Triassic, Jurassic, and Cretaceous sedimentary successions are preserved in downfaulted blocks in the eastern part of the region. These rocks are, in turn, overlain by Paleogene basalts.

The region is transected by numerous faults of various ages. The most prominent tectonic feature is the several hundred metres wide Post-Devonian Eastern Fault Zone (EFZ) that transects Hudson Land and Gauss Halvø as a regional N-S trending brittle structure (Figure 1). Within the fault zone, rocks (including some granites and rhyolites) are fractured and hydrothermally altered with extensive hematisation, epidotisation and argillisation (Harpøth et al. 1986). In addition, the EFZ hosts numerous quartz veins with Ag-Au-Pb-Zn-Cu sulphides and fluorite.

Clavering Ø

The crystalline complex of Clavering Ø forms a 22 km wide N-S trending belt in the centre of Clavering Ø. This area has previously been studied by Mittelholzer (1941), Haller (1971) and Jones & Escher (1999).

In the west, the crystalline complex is unconformably overlain by Carboniferous sediments and Palaeogene volcanic rocks, whereas in the east, they are overlain by Triassic to Cretaceous sediments and Palaeogene volcanic rocks. Outliers of Carboniferous to Cretaceous sediments and Palaeogene volcanic rocks also overlie the crystalline complexes in the central region. The crystalline complexes mainly comprise migmatitic supracrustal rocks, presumed to belong to the geographically widespread Krummedal sequence (Escher 2001). The

underlying Palaeoproterozoic orthogneiss is only recognised in the very northern part of the island. The ortho- and paragneiss complex is intruded by three generations of granites described in this report.

Hudson Land and Gauss Halvø

Hudson Land and Gauss Halvø comprise highly metamorphosed ortho- and paragneisses, Neoproterozoic EBS, and Devonian sediments that are intercalated with felsic and mafic extrusive rocks. Carboniferous sediments occur east of the EFZ. Likewise, Permian, Triassic, Cretaceous sediments and Palaeogene volcanic rocks only occur east of the EFZ.

Western Hudson Land are dominated by successions of the upper part of the EBS, Cambro-Ordovician and Devonian sediments. N-S and NW-SE trending faults transect all these sequences (Koch & Haller 1971; Stendal 1999). The crystalline complex and the Devonian sediments were intruded by several generations of granites.

Geological maps of Hudson Land and eastern part of Gauss Halvø show granite bodies up to 10-20 km in diameter and more or less conspicuous bodies are seen in unpublished field maps from Hudson Land. Ages of the granites are unknown, but most are termed ‘Caledonian’ i.e. Silurian (c. 430 Ma), except the few intruding into Devonian sediments, that must be Devonian or younger. The large granite body in northern Hudson Land is foliated and could be of Tonian age. The rhyolitic lavas shown on the map are Devonian.

Previous investigations of granites and rhyolites

Granite bodies in North-East Greenland are shown in several earlier maps where they are divided into age groups, Archaean, Palaeoproterozoic, Neoproterozoic, Silurian, Devonian and Palaeogene based on field relations and scarce age dating (Koch & Haller 1971; Bengaard 1992, Escher 2001). Geochemical investigations have been conducted outside the study area and it was shown that most Neoproterozoic and Silurian granites are peraluminous and interpreted to have formed by melting of Meso-Neoproterozoic metasediment (Kalsbeek et al. 2000, 2001a,b, 2008b).

The study area has been mapped several times and the number and character of magmatic rocks vary among the maps. The 1:250 000 scale map by Koch & Haller (1971) distinguishes between syn-tectonic, post-tectonic and Devonian granites. However, the Meso-Neoproterozoic age of the Krummedal sequence and Tonian age of some of the granites hosted by this sequence were not known in 1971. The Devonian magmatism is described and studied in some detail by scientists of the Lauge Koch expeditions, see Haller (1971), and no equally comprehensive study has been published later.

A five-year project, the Stordal campaign 1973-1977, performed an aeroradiometric survey over North-East Greenland from 72° to 76°N (Nielsen & Larsen 1974). The survey indicated that some presumed Tonian as well as many Silurian and Devonian granites were enriched in K, Th and U, relative to their host rocks and to many other common granites (Nielsen & Steenfelt 1977). The highest number of measured U anomalies including some indicating U-mineralisation was found in Hudson Land and Gauss Halvø, particularly associated within Devonian rhyolites and granites. Following this recognition, almost all previously known and new occurrences of rhyolite found during the radiometric survey in interior Hudson Land and Gauss Halvø were visited and sampled (Ryan & Sandwall 1975). New granite occurrences discovered along and across the Eastern Fault Zone (Figure 1) were also sampled (Cooper 1976). The majority of the samples (several hundreds) were analysed for U; the Devonian magmatic rocks also for a few other elements (Steenfelt 1982). It was clarified that the Devonian acid magmatic rocks comprise lavas, dykes and larger bodies with porphyries, aplites, pegmatites and granites, and that the occurrence at Parkinson Bjerg is granite, not rhyolite as in the Koch-Haller map (Figure 1). It was also noticed that in some of the outcrop areas of presumed Devonian granitic rocks, different and presumably older granites were also present (Ryan & Sandwall 1975; Thyrsted 1975).

A 1:250 000 scale map covering the western part of Hudson Land and Gauss Halvø resulted from new stratigraphic studies of the upper Proterozoic to Devonian rocks (Olsen & Larsen 1993; Bengaard 1992). This map includes some, but not all, rhyolite occurrences that were discovered during the Stordal campaign. The studies agree with Haller (1971) that the Devonian magmatic activity that also produced thin basaltic flows took place during the Upper Devonian.

The most recent map covering the study area is the 1:500 000-scale map of Escher (2001). In this map, all granites at Clavering Ø are depicted as granites of unknown age (930 or 430

Ma), whilst granites in Hudson Land are shown as Caledonian, including the ones previously mapped as Devonian. Devonian rhyolites are shown with much less accuracy than in previous maps. Figure 1 is based on this rather simple map, since the Koch & Haller map (1971) has not been digitised.

Exploration by Nordisk Mineselskab A/S, GEUS, Arc Mining and 21st North have suggested that the Parkinson Bjerg granite could host Sn-W-Mo-Nb-REE greisen-type mineralisation, in addition to the known abundant fluorite-tourmaline-quartz veining. Anomalous concentrations of these metals were detected in secondary material, i.e., floats, stream sediment and heavy mineral concentrates extending from Parkinson Bjerg to further to the south, possibly implying the existence of a hidden granite body (Harpøth et al. 1986; Thomassen & Tukiainen 2010; Arc Mining 2014; C. Østergaard, 21th North, Pers. Com. 2016).

Ages of granites and rhyolites

In North-East Greenland, Tonian and Caledonian granites are described by Kalsbeek et al. (2008b) as intruding the metasedimentary rocks of the Late Mesoproterozoic-Neoproterozoic Krummedal supracrustal sequence and the overlying Neoproterozoic Eleonore Bay Supergroup (EBS). Most of them are S-type muscovite-biotite leucogranites and interpreted as having been formed by anatexis of schists and paragneisses of the Krummedal supracrustal sequence. The intrusions occur as plutons, sheets, pegmatites and aplites. Archaean and Palaeoproterozoic gneisses that form the crystalline basement underlying the supracrustal rocks seem not to have participated in the generation of these granites. Most of the Caledonian intrusive bodies are reported as Silurian of age (435-425 Ma) and leucogranitic, but some intrusions have more mafic compositions and include monzonites, diorites, granodiorites with minor amounts of granite. These types of intrusions are interpreted as I-type with geochemical and isotopic signatures typical of arc magmas and they span a larger age range from Middle Ordovician to Silurian (465-430 Ma). These relatively mafic granitoids were originally discovered and investigated by Kalsbeek et al. (2008) in the southernmost segment of the East Greenland Caledonides (in Milne Land, Renland and Liverpool Land), and have only recently been discovered on Clavering Ø (Bernstein & Thrane, 2019; Kokfelt 2019; Rosa 2019).

Prior to this report only a single Devonian granite from the study area has been dated. A K-Ar analysis of mica was obtained from the granite at Kap Franklin, yielding an age of 395 ± 10 Ma (Haller 1971). Age determinations from granite samples from Clavering Ø and Hudson Land are underway, and some preliminary ages are presented below. The ages of the remaining samples are mostly inferred. However, few granites are demonstrably Devonian or younger as indicated by their stratigraphic levels. For example, the small intrusion that outcrops at Kap Franklin (Figure 1) and intrude Devonian sediments and, therefore, must be Devonian or younger. Other granites on the eastern part of Gauss Halvø were considered Devonian (D in Figure 1). The rhyolitic lavas and pyroclastic rocks are embedded into Devonian sediments. The stratigraphy of the sediments shows that eruptions took place intermittently over Middle and Upper Devonian in time (Haller 1971).

Several other granitic bodies and dykes were mapped as Devonian granites or rhyolites by Koch & Haller (1971). On the north side of inner Moskusoksefjord, at Högboms Bjerg a granite occurring together with rhyolite was considered Devonian. This assumption is verified by new age dating presented below. Other granites in Hudson Land are mapped as syn- or post-tectonic granites in relation to the Silurian deformation by Koch & Haller (1971).

In summary, previous studies have not clarified the ages and origins of granitic magmatism within the study region, and none of the previous maps reliably depict the setting and distribution of variably aged magmatic rocks.

Samples

The overall sample set was grouped as either Tonian, Caledonian or Devonian magmatic rocks, based on available cross-cutting relationships, deformation intensity, previous map legends and preliminary unpublished U-Pb geochronology. Through an iterative process, a final classification was obtained by comparing the whole-rock geochemistry of these preliminary groups, creating six distinct groups based on age and geochemical signatures (Thrane et al. 2021). From this iterative exercise, it emerged that the Devonian granitoids have two distinct geochemical signatures, justifying division into two groups, whose context is discussed below. The six groups are: (1) Tonian granites (Clavering Ø, only), (2) Caledonian monzonites (Clavering Ø, only), (3) Caledonian S-type granites, (4) Intermediate Devonian granites, (5) Devonian rhyolites and (6) Devonian evolved granites. For the new samples presented in this report only three of the originally defined groups are present, namely groups (2), (5) and (6).

Figure 2 shows the distribution of the samples included in this report for whole-rock geochemistry (82) and zircon U-Pb dating (9). The samples are divided into three categories based on their known geology and based on field relations, as (1) Caledonian (Ordovician to Silurian) granites, *sensu lato*, (2) Devonian rhyolites, or (3) Devonian evolved granites.

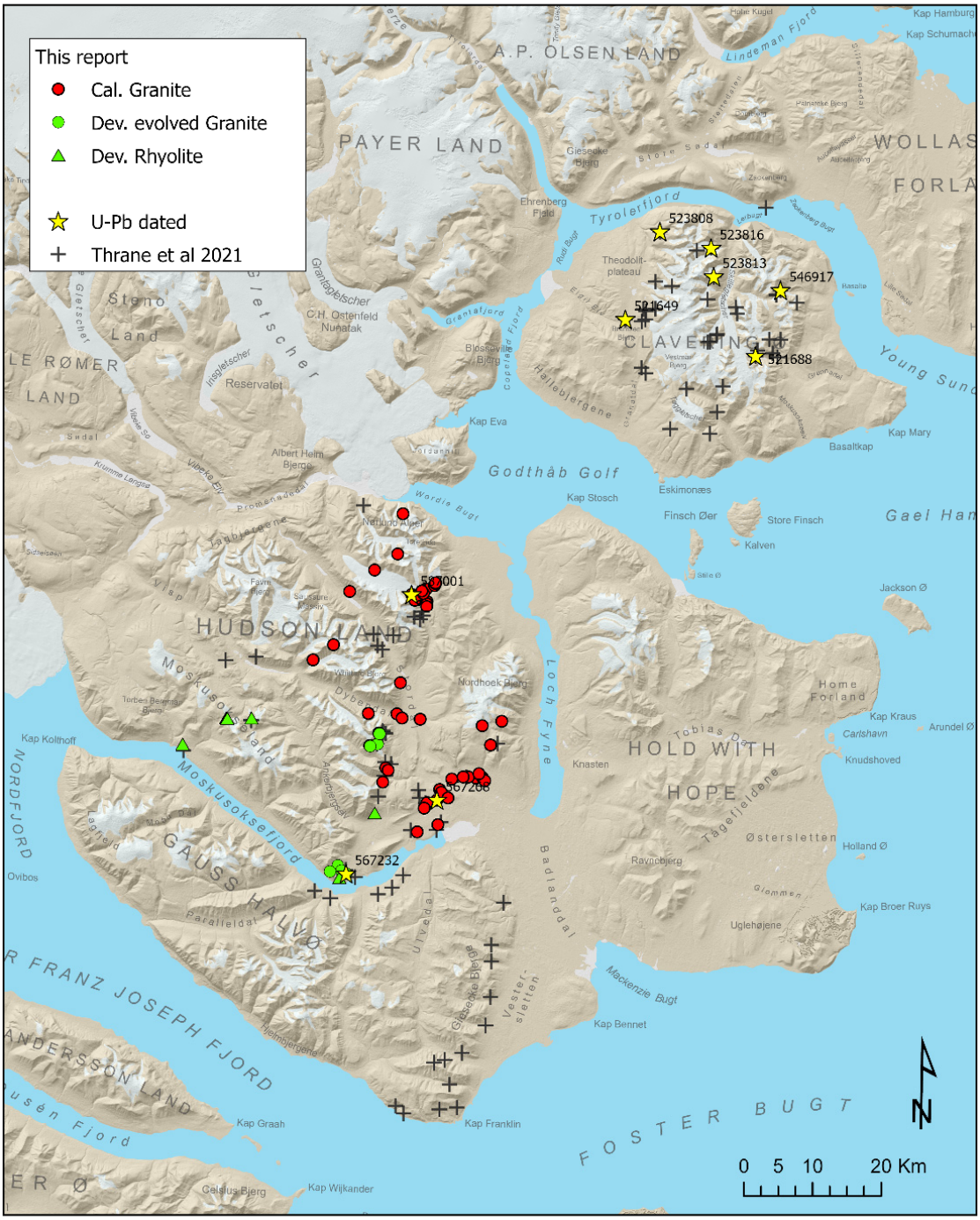

Figure 2: Topographic map showing the localities of samples presented in the current report (colored symbols) and samples presented by Thrane et al. (2021) ('+').

Analytical Method

Whole-rock chemistry

A total of 82 whole-rock chemical analyses were carried out by Bureau Veritas Commodities Canada Ltd. (formerly ACME laboratory) using the analytical code LF600, which comprises determination of major elements by XRF (XF700), total carbon determination (TC000) and trace elements by ICP-MS (LF100-EXT). Additional analytical packages for selected samples include determination of FeO by titration (GC806) for 49 samples and lithium determination (PF370) for 77 samples.

Zircon U-Pb dating by LA-ICPMS

Zircon analyses were conducted at the Department of Geological mapping and economic Geology, Geological Survey of Denmark and Greenland (GEUS). Hand-hammered chips from the rock samples were crushed directly in a tungsten-carbide disc mill. The crushed material was poured onto a Wilfley shaking table where the heavy mineral grains were separated. The heavy mineral fraction was transferred to disposable plastic Petri dishes using ethanol, and magnetic minerals were removed using a hand magnet. Zircon grains were subsequently hand-picked from the final heavy mineral concentrate in the Petri dish. The hand-picked zircon grains were cast into epoxy and polished to expose a central cross-section of each grain. The mount was documented prior to ablation using backscattered electron imaging in a scanning electron microscope. The mount was subsequently cleaned in an ultrasonic bath with propanol, and then loaded into the sample cell of the laser ablation system for age dating.

All U–Pb age data were acquired by laser ablation - single collector - magnetic sector field - inductively coupled plasma - mass spectrometry (LA-SF-ICP-MS) employing a Thermo Finnigan Element2 mass spectrometer coupled to a New Wave Research UP213 frequency-quintupled solid state Nd:YAG laser system, employing a two-volume cell technology. The principle setup is very similar to described by Frei and Gerdes (2009) and is described as follows. The laser was operated at a repetition rate of 10 Hz and nominal energy output of 55%, corresponding to a laser fluency of c. 8 J cm^{-2}. All data were acquired with a single spot analysis on each individual zircon grain with a beam diameter of 30 µm and a crater depth of approximately 15–20 µm. For the spot diameter of 30 µm and ablation times of 30 s the amount of ablated material approximates 200–300 ng. The ablated material was analysed on an Element2 (Thermo Finnigan, Bremen) single-collector, double focussing, magnetic sector-field ICP-MS with a fast field regulator for increased scanning speed. The mass spectrometer was equipped with a Fassel type quartz torch shielded with a grounded Pt electrode and a quartz bonnet. The total acquisition time for each analysis was 60 s, with the first 30 s used to measure the gas blank. The instrument was tuned to give large, stable signals for the ^{206}Pb and ^{238}U peaks, low background count rates (typically around 150 counts

per second for ^{207}Pb) and low oxide production rates ($^{238}U^{16}O/^{238}U$ generally below 0.5 %). ^{202}Hg, $^{204}(Pb + Hg)$, ^{206}Pb, ^{207}Pb, ^{208}Pb, ^{232}Th and ^{238}U intensities were determined through peak jumping using electrostatic scanning in low resolution mode and with the magnet resting at ^{202}Hg. Each peak was determined at four slightly different masses and integrated sampling and a settling time of 1 ms for each isotope. The elemental fractionation induced by the laser ablation and the instrumental mass bias on measured isotopic ratios were corrected through standard-sample bracketing using the GJ-1 zircon (Jackson et al., 2004). Samples were analysed in sequences where three standards bracket each set of ten samples. Data processing and calculation of abundances, isotopic ratios and dates were carried out off-line through the software Iolite version 2.5 (Paton et al. 2011), using for the U-Pb dating the Iolite add-on data reduction scheme VizualAge by Petrus & Kamber (2012), and for the trace elements determination the integral Trace Elements IS data reduction scheme. The VizualAge data reduction scheme includes a correction routine for down-hole isotopic fractionation and provides routines for data that require correction for common Pb, although this option was not used in the data processing. All diagrams for further statistical analysis and interpretation were produced through the IsoPlotR software package. Two uncertainty measures are reported in the dates, of which the first one is the 2σ which is an output from the IsoPlotR software of Vermeesch (2018, 2021). After correcting the data for the effects of mass bias fractionation and Hg-interference a filtering of the data was applied by which analyses with 2σ errors > 10% (abs) for the $^{206}Pb/^{238}U$ ratio were removed from the data set. Data with significant amounts of common Pb (cPb) were not included in calculating the ages. A cross-over age for $^{238}U/^{206}Pb$ vs. $^{207}Pb/^{206}Pb$ based ages are set at 1100 Ma and the reported errors are internal errors at the 2σ level or 95% confidence interval. Long-term external reproducibility was monitored by repeated analyses of the Plešovice zircon standard (Sláma et al., 2008).

Results

Geochemical data

The new whole-rock geochemistry analyses are presented in Table 1 on the following pages, along with sample locality and short descriptions. The presented chemical plots (Figures 3-13) are based on the complete whole-rock geochemical dataset presented in the current report and that presented by Thrane (2021). Further information about all samples can be found in the appendix.

Table 1. Major and trace elements on East Greenland granites and rhyolites

Sample	567204	567205	567206	567207	567208	567209	567210	567211
Group name	Devonian rhyolite, altered	Devonian rhyolite, altered	Devonian rhyolite, altered	Devonian rhyolite, altered	Devonian rhyolite, altered	Devonian rhyolite, altered	Devonian rhyolite, altered	Devonian rhyolite, altered
Rock name *	phonolite	phonolite	phonolite	phonolite	trachyte	phonolite	phonolite	phonolite
Collector [§]	TFK	TFK	TFK	TFK	TFK	TFK	TFK	TFK
Year	2022	2022	2022	2022	2022	2022	2022	2022
Latitude (N)	73.7695	73.7695	73.7695	73.7695	73.7695	73.7695	73.7695	73.7695
Longitude (W)	-23.3156	-23.3156	-23.3156	-23.3156	-23.3156	-23.3156	-23.3130	-23.3130
Locality	OK fjeld	OK fjeld	OK fjeld	OK fjeld	OK fjeld	OK fjeld	OK fjeld	OK fjeld
Major elements:								
SiO2 (wt-%)	80.20	80.82	75.36	78.54	94.65	77.34	78.99	76.62
TiO2 (wt-%)	0.06	0.08	0.08	0.08	0.06	0.08	0.08	0.07
Al2O3 (wt-%)	14.14	12.91	16.84	13.95	3.21	15.12	13.38	14.59
Fe2O3T (wt-%)	0.53	0.73	2.24	2.82	0.57	1.81	2.41	3.58
FeO (wt-%) [#]								
MnO (wt-%)	0.01	0.01	0.03	0.03	0.01	0.03	0.03	0.02
MgO (wt-%)	0.04	0.07	0.07	0.05	0.03	0.04	0.08	0.03
CaO (wt-%)	0.22	0.19	0.17	0.11	0.51	0.09	0.21	0.06
Na2O (wt-%)	0.03	0.03	0.02	0.01	0.03	0.01	0.03	0.02
K2O (wt-%)	0.58	1.48	1.28	0.74	0.33	0.42	2.59	0.40
P2O5 (wt-%)	0.01	0.01	0.01	0.01	0.01	0.01	0.01	0.01
LOI (wt-%)	4.66	3.56	4.74	4.27	1.17	4.91	2.63	4.87
Total	100.48	99.89	100.84	100.61	100.58	99.86	100.44	100.27
Trace elements:								
Co (ppm)	0.2	0.5	0.2	0.3	0.2	0.2	0.2	0.3
Ni (ppm)	1.0	1.4	0.9	1.6	1.3	0.6	1.1	0.8
Cu (ppm)	5.5	2.2	4.7	6.1	7.2	5.7	3.0	2.7
Zn (ppm)	5.0	5.0	8.0	22.0	4.0	14.0	12.0	16.0
Ga (ppm)	20.8	24.9	28.7	27.9	5.0	28.9	20.5	23.7
Rb (ppm)	41.7	108.2	90.0	60.1	25.5	34.9	177.7	34.0
Sr (ppm)	9.5	43.5	53.3	27.4	40.1	15.7	32.1	9.2
Y (ppm)	8.1	16.3	7.3	7.8	24.4	11.4	9.5	9.4
Zr (ppm)	132.6	191.3	172.9	193.2	141.4	191.4	175.9	166.0
Nb (ppm)	39.9	56.5	54.4	53.9	65.3	58.2	53.3	46.3
Mo (ppm)	0.3	1.0	0.5	1.7	1.0	2.1	1.7	2.0
Cs (ppm)	0.7	1.3	0.7	0.9	1.5	0.5	1.3	1.0
Ba (ppm)	14.0	18.0	14.0	15.0	30.0	10.0	17.0	11.0
La (ppm)	0.80	12.60	11.60	13.70	26.20	8.30	2.60	11.60
Ce (ppm)	2.60	17.80	15.20	15.70	34.40	13.60	6.60	17.10
Pr (ppm)	0.19	1.09	1.09	1.04	2.78	1.26	0.42	1.13
Nd (ppm)	0.60	2.30	2.40	2.20	4.60	3.10	1.10	2.40
Sm (ppm)	0.20	0.52	0.42	0.42	0.86	0.59	0.35	0.44
Eu (ppm)	0.02	0.02	0.02	0.02	0.02	0.02	0.02	0.02
Gd (ppm)	0.36	1.11	0.54	0.47	0.99	0.74	0.52	0.61
Tb (ppm)	0.08	0.25	0.10	0.11	0.26	0.16	0.13	0.11
Dy (ppm)	0.68	2.01	0.87	0.94	1.97	1.19	1.04	0.95
Ho (ppm)	0.21	0.47	0.23	0.26	0.56	0.34	0.30	0.26
Er (ppm)	0.75	1.62	0.87	0.94	1.86	1.16	1.28	1.02
Tm (ppm)	0.14	0.28	0.15	0.19	0.32	0.21	0.21	0.20
Yb (ppm)	1.09	1.89	1.30	1.35	2.09	1.66	1.86	1.56
Lu (ppm)	0.17	0.30	0.22	0.24	0.31	0.27	0.30	0.24
Hf (ppm)	7.1	10.0	9.2	10.0	7.7	10.6	9.6	8.8
Ta (ppm)	2.9	4.1	4.0	4.5	2.7	4.3	4.3	3.8
Pb (ppm)	5.0	6.3	12.1	17.6	15.8	14.5	11.2	30.4
Th (ppm)	27.7	32.0	35.2	51.6	128.6	47.2	37.1	42.8
U (ppm)	6.1	14.8	10.3	10.3	13.9	14.6	11.3	10.2
Li (wt-%)	0.011	0.012	N.A.	0.012	0.003	0.033	0.005	0.021
V (ppm)	8.0	9.0	8.0	8.0	17.0	8.0	8.0	8.0
As (ppm)	8.6	14.4	26.0	16.2	23.1	4.0	2.1	3.9
Ag (ppm)	0.1	0.1	0.1	0.1	0.1	0.1	0.1	0.1
Sn (ppm)	1.0	17.0	6.0	4.0	3.0	1.0	3.0	5.0
Sb (ppm)	0.1	0.6	0.3	0.8	0.5	0.3	0.3	0.7
W (ppm)	3.4	7.7	6.7	8.2	14.2	6.7	3.0	17.2
Bi (ppm)	0.1	0.1	0.1	0.1	0.6	0.1	0.1	0.1
Cd (ppm)	0.1	0.1	0.1	0.1	0.1	0.1	0.1	0.1
Au (p.p.b.)	0.5	0.5	0.5	0.5	0.5	0.5	0.5	0.5
Se (ppm)	0.5	0.5	0.5	0.5	0.5	0.5	0.5	0.5
Hg (ppm)	0.0	0.0	0.0	0.0	0.2	0.0	0.0	0.0
Be (ppm)	2.0	2.0	10.0	4.0	1.0	4.0	1.0	1.0

Sample	567212	567214	567215	567218	567220	567222	567223	567229
Group name	Devonian rhyolite, altered	Devonian rhyolite	Devonian rhyolite	Devonian rhyolite	Devonian rhyolite	Devonian rhyolite	Devonian rhyolite	Devonian rhyolite
Rock name *	phonolite	alkali rhyolite	alkali rhyolite	andesite, basaltic andesite	rhyolite, dacite	rhyolite, dacite	andesite, basaltic andesite	alkali rhyolite
Collector §	TFK	TFK	TFK	TFK	TFK	TFK	TFK	TFK
Year	2022	2022	2022	2022	2022	2022	2022	2022
Latitude (N)	73.7691	73.7706	73.7706	73.7706	73.7706	73.7706	73.7706	73.7333
Longitude (W)	-23.3103	-23.1974	-23.1974	-23.1974	-23.1974	-23.1974	-23.1974	-23.5141
Locality	OK fjeld	Hochwacht	Hochwacht	Hochwacht	Hochwacht	Hochwacht	Hochwacht	Moskusokselandet, Unit B
Major elements:								
SiO2 (wt-%)	78.15	77.78	79.40	57.16	85.21	80.05	60.35	76.14
TiO2 (wt-%)	0.07	0.08	0.07	1.05	0.58	0.47	0.79	0.11
Al2O3 (wt-%)	14.69	11.78	12.08	17.40	7.57	6.97	13.44	12.19
Fe2O3T (wt-%)	1.52	1.26	1.89	7.04	1.26	1.14	5.38	2.14
FeO (wt-%) #								
MnO (wt-%)	0.01	0.04	0.02	0.09	0.02	0.04	0.13	0.02
MgO (wt-%)	0.03	0.03	0.17	1.24	0.38	0.33	1.90	0.03
CaO (wt-%)	0.11	0.44	0.09	2.60	0.29	4.50	3.95	0.39
Na2O (wt-%)	0.02	3.53	2.56	6.50	0.38	0.69	5.26	2.63
K2O (wt-%)	0.16	5.08	3.84	2.70	2.67	2.52	3.38	6.13
P2O5 (wt-%)	0.01	0.01	0.01	0.17	0.16	0.13	0.11	0.01
LOI (wt-%)	5.17	0.46	0.79	4.69	1.61	2.66	6.01	0.48
Total	99.94	100.49	100.92	100.64	100.13	99.50	100.70	100.27
Trace elements:								
Co (ppm)	0.4	0.2	0.3	19.7	1.9	1.7	16.1	0.4
Ni (ppm)	1.2	1.7	1.5	20.9	2.9	5.7	20.7	1.4
Cu (ppm)	4.7	4.6	4.4	24.1	13.5	8.3	11.3	7.6
Zn (ppm)	16.0	49.0	6.0	53.0	29.0	77.0	54.0	30.0
Ga (ppm)	21.8	17.6	20.6	17.8	10.3	10.1	12.1	18.9
Rb (ppm)	13.1	249.2	268.3	147.0	219.8	218.3	166.3	367.3
Sr (ppm)	7.3	31.8	31.4	192.9	37.3	53.7	299.6	13.0
Y (ppm)	16.8	71.1	79.3	32.4	44.9	84.8	29.8	78.4
Zr (ppm)	155.5	163.6	138.6	197.8	373.1	342.0	160.0	247.5
Nb (ppm)	49.3	29.3	45.4	17.1	15.5	18.3	17.6	41.4
Mo (ppm)	1.0	0.8	1.1	0.1	0.3	1.1	0.3	2.1
Cs (ppm)	0.5	0.6	5.0	1.8	6.1	6.2	1.0	3.4
Ba (ppm)	12.0	206.0	87.0	187.0	249.0	285.0	354.0	14.0
La (ppm)	5.80	44.10	39.40	45.50	49.60	59.60	30.40	90.00
Ce (ppm)	13.50	82.60	80.00	90.60	97.30	86.30	64.60	181.30
Pr (ppm)	1.19	11.00	10.48	9.60	11.84	14.31	6.91	18.74
Nd (ppm)	3.90	42.10	39.30	33.40	44.00	53.00	25.90	62.80
Sm (ppm)	1.07	10.49	10.32	6.25	9.27	12.23	5.24	13.24
Eu (ppm)	0.02	0.10	0.03	1.07	0.95	0.72	0.87	0.08
Gd (ppm)	1.26	10.90	11.47	5.52	8.72	13.44	4.92	12.11
Tb (ppm)	0.29	1.89	2.07	0.87	1.31	2.13	0.80	2.11
Dy (ppm)	2.32	11.76	12.94	5.49	7.75	12.23	4.94	12.46
Ho (ppm)	0.61	2.54	2.72	1.20	1.57	2.36	1.07	2.74
Er (ppm)	2.20	8.10	7.97	4.10	4.52	6.06	2.95	8.30
Tm (ppm)	0.35	1.17	1.18	0.60	0.58	0.71	0.41	1.19
Yb (ppm)	2.80	7.59	7.58	3.96	3.73	4.37	2.97	7.47
Lu (ppm)	0.42	1.08	1.11	0.61	0.54	0.63	0.44	1.09
Hf (ppm)	8.8	8.2	7.4	5.7	9.9	9.0	4.7	9.9
Ta (ppm)	3.7	2.9	3.4	1.4	0.6	0.7	0.8	2.4
Pb (ppm)	14.1	31.7	14.6	6.0	13.9	151.3	9.3	35.4
Th (ppm)	21.3	49.5	53.0	23.6	13.5	13.1	18.7	44.1
U (ppm)	7.5	15.1	4.1	6.0	9.5	17.8	4.8	7.8
Li (wt-%)	0.017	0.001	0.001	0.001	0.004	0.004	0.001	0.002
V (ppm)	8.0	8.0	8.0	97.0	33.0	25.0	70.0	8.0
As (ppm)	3.4	6.4	1.5	0.7	2.0	4.5	0.8	2.6
Ag (ppm)	0.1	0.1	0.1	0.1	0.1	0.1	0.1	0.1
Sn (ppm)	10.0	10.0	10.0	3.0	1.0	2.0	2.0	7.0
Sb (ppm)	0.4	0.3	0.3	0.1	0.1	0.4	0.3	0.3
W (ppm)	8.1	2.9	2.4	2.2	3.4	3.2	1.9	4.1
Bi (ppm)	0.1	0.1	0.1	0.1	0.3	0.8	0.1	0.1
Cd (ppm)	0.1	0.1	0.1	0.1	0.1	0.1	0.1	0.1
Au (p.p.b.)	0.5	0.5	0.5	0.5	0.8	0.5	0.5	0.5
Se (ppm)	0.5	0.5	0.5	0.5	0.5	0.5	0.5	0.5
Hg (ppm)	0.0	0.1	0.0	0.0	0.0	0.0	0.0	0.0
Be (ppm)	4.0	1.0	10.0	5.0	5.0	14.0	7.0	7.0

Sample	567230	567231	567203	567232	567233	567235	567236	567237
Group name	Devonian rhyolite	Devonian rhyolite	Devonian evol. granite	Devonian evol. granite	Devonian evol. granite	Devonian evol. granite	Devonian evol. granite	Devonian evol. granite
Rock name *	andesite, basaltic andesite	andesite, basaltic andesite	granite	granite	granite	granite	granite	granite
Collector §	TFK	TFK	TFK	TFK	TFK	TFK	TFK	TFK
Year	2022	2022	2022	2022	2022	2022	2022	2022
Latitude (N)	73.5665	73.5665	73.5813	73.5708	73.5711	73.5747	73.5747	73.5747
Longitude (W)	-22.7651	-22.7652	-22.7740	-22.7340	-22.7345	-22.7556	-22.7556	-22.7556
Locality	Høgboms Bjerg	Høgboms Bjerg	Høgboms Bjerg	Høgboms Bjerg	Høgboms Bjerg	Høgboms Bjerg	Høgboms Bjerg	Høgboms Bjerg
Major elements:								
SiO2 (wt-%)	62.23	64.19	75.63	76.29	75.07	72.70	78.93	74.14
TiO2 (wt-%)	0.72	0.76	0.25	0.18	0.22	0.25	0.21	0.25
Al2O3 (wt-%)	12.28	11.84	12.50	11.79	10.28	13.10	10.76	12.90
Fe2O3T (wt-%)	4.85	5.79	2.71	2.25	1.93	3.96	2.11	2.32
FeO (wt-%) #			0.32	0.57	1.35	0.37		0.63
MnO (wt-%)	0.09	0.08	0.02	0.03	0.05	0.02	0.02	0.03
MgO (wt-%)	3.65	3.58	0.08	0.07	1.24	0.29	0.25	0.11
CaO (wt-%)	6.86	3.57	0.09	0.69	3.07	0.14	0.12	0.39
Na2O (wt-%)	2.60	0.25	2.29	2.70	2.09	0.16	0.33	3.09
K2O (wt-%)	3.22	5.87	6.50	5.97	5.66	8.18	6.49	6.24
P2O5 (wt-%)	0.16	0.15	0.03	0.03	0.12	0.03	0.02	0.03
LOI (wt-%)	3.35	3.54	0.37	0.49	0.72	1.09	0.95	0.60
Total	100.01	99.62	100.47	100.49	100.45	99.92	100.19	100.10
Trace elements:								
Co (ppm)	13.1	16.1	0.8	0.7	2.5	1.2	1.1	1.9
Ni (ppm)	30.7	44.8	1.6	1.7	3.1	1.1	2.1	1.5
Cu (ppm)	21.1	32.6	4.8	14.8	8.3	4.3	12.4	8.9
Zn (ppm)	53.0	92.0	15.0	104.0	14.0	22.0	23.0	39.0
Ga (ppm)	14.1	12.0	16.5	24.1	9.4	19.5	15.9	18.4
Rb (ppm)	145.6	381.1	365.2	248.0	213.3	502.9	406.6	313.2
Sr (ppm)	275.2	163.0	59.1	27.5	190.2	22.8	21.2	36.6
Y (ppm)	27.8	27.9	46.7	96.1	11.6	95.1	47.0	55.5
Zr (ppm)	262.2	227.4	272.3	232.7	100.4	276.8	266.0	271.2
Nb (ppm)	12.6	13.6	25.0	37.2	5.7	27.3	22.5	25.8
Mo (ppm)	0.8	0.3	2.7	1.3	0.7	1.5	3.6	1.6
Cs (ppm)	2.6	2.5	4.2	0.9	1.1	6.9	6.3	4.0
Ba (ppm)	588.0	584.0	300.0	42.0	703.0	349.0	273.0	308.0
La (ppm)	41.60	39.40	71.20	62.70	21.90	88.90	55.50	84.70
Ce (ppm)	80.60	79.80	137.10	133.20	42.80	182.40	108.10	165.20
Pr (ppm)	9.12	8.84	13.64	14.53	4.98	17.24	9.95	16.59
Nd (ppm)	34.40	34.00	47.80	55.30	18.70	55.20	31.90	55.40
Sm (ppm)	6.89	6.26	7.96	12.55	3.35	9.51	5.65	9.98
Eu (ppm)	1.24	1.34	0.49	0.15	0.70	0.55	0.32	0.60
Gd (ppm)	5.66	5.94	7.62	13.28	2.81	8.85	5.00	9.15
Tb (ppm)	0.89	0.92	1.29	2.57	0.41	1.73	0.97	1.54
Dy (ppm)	5.18	5.52	8.21	15.62	2.24	12.99	6.83	9.64
Ho (ppm)	1.06	1.04	1.71	3.52	0.42	3.09	1.73	2.11
Er (ppm)	2.92	3.13	5.58	10.84	1.20	10.21	5.74	6.16
Tm (ppm)	0.41	0.41	0.77	1.58	0.18	1.57	0.82	0.92
Yb (ppm)	2.95	3.08	5.23	10.28	1.18	10.63	5.90	6.12
Lu (ppm)	0.42	0.45	0.81	1.43	0.17	1.45	0.87	0.85
Hf (ppm)	6.6	6.0	9.1	9.7	2.9	9.8	9.3	8.9
Ta (ppm)	0.7	0.9	1.8	2.6	0.4	1.8	1.7	2.3
Pb (ppm)	7.8	9.0	15.8	31.3	11.5	9.5	42.0	19.0
Th (ppm)	11.2	11.9	37.3	39.4	8.5	39.4	34.3	42.7
U (ppm)	3.0	2.8	4.7	7.2	3.4	4.1	9.3	7.5
Li (wt-%)	0.006	0.010	0.002	0.001	0.001	0.001	N.A.	0.001
V (ppm)	68.0	57.0	13.0	8.0	22.0	11.0	9.0	8.0
As (ppm)	0.8	0.8	4.1	0.7	1.1	1.6	3.0	0.5
Ag (ppm)	0.1	0.1	0.1	0.1	0.1	0.1	0.1	0.1
Sn (ppm)	2.0	2.0	12.0	5.0	3.0	27.0	16.0	11.0
Sb (ppm)	0.1	0.1	0.5	0.1	0.1	1.2	0.4	0.1
W (ppm)	2.2	3.7	8.5	1.3	0.9	8.0	5.8	2.2
Bi (ppm)	0.2	0.1	0.2	0.1	0.1	0.1	0.2	0.1
Cd (ppm)	0.1	0.1	0.1	0.5	0.1	0.1	0.1	0.1
Au (p.p.b.)	0.5	0.5	0.5	0.5	0.5	0.5	1.7	0.5
Se (ppm)	0.5	0.5	0.5	0.5	0.5	0.5	0.5	0.5
Hg (ppm)	0.0	0.0	0.0	0.0	0.0	0.0	0.0	0.0
Be (ppm)	3.0	1.0	2.0	5.0	1.0	5.0	5.0	7.0

Sample	567248	587064	587065	587066	587067	587069	587074	587077
Group name	Devonian evol. granite	Devonian evol. granite	Devonian evol. granite	Devonian evol. granite	Devonian evol. granite	Devonian evol. granite	Devonian evol. granite	Devonian evol. granite
Rock name *	granite	granite	granite	granite	granodiorite	granite	granite	granite
Collector [§]	TFK	DRO	DRO	DRO	DRO	DRO	DRO	DRO
Year	2022	2022	2022	2022	2022	2022	2022	2022
Latitude (N)	73.5732	73.7415	73.7409	73.7409	73.7409	73.7409	73.7380	73.7542
Longitude (W)	-22.8094	-22.6054	-22.6047	-22.6047	-22.6047	-22.6047	-22.6398	-22.5975
Locality	Høgboms Bjerg	Blokadedal	Blokadedal	Blokadedal	Blokadedal	Blokadedal	Blokadedal	Blokadedal
Major elements:								
SiO2 (wt-%)	77.56	77.88	77.67	78.93	65.10	75.44	77.29	76.72
TiO2 (wt-%)	0.11	0.05	0.06	0.05	0.02	0.13	0.05	0.05
Al2O3 (wt-%)	12.41	12.05	12.21	12.02	3.98	12.94	11.83	12.26
Fe2O3T (wt-%)	1.32	1.35	1.53	0.89	1.04	1.54	1.47	1.51
FeO (wt-%) [#]	0.71							
MnO (wt-%)	0.02	0.02	0.01	0.01	0.01	0.02	0.01	0.01
MgO (wt-%)	0.07	0.04	0.08	0.07	0.05	0.45	0.06	0.04
CaO (wt-%)	0.19	0.43	0.29	0.11	19.02	0.77	0.68	0.56
Na2O (wt-%)	3.41	3.66	3.06	2.75	0.51	3.06	3.33	3.70
K2O (wt-%)	5.21	4.69	5.17	4.91	1.71	5.00	4.97	4.72
P2O5 (wt-%)	0.01	<0.01	<0.01	<0.01	<0.01	0.15	<0.01	<0.01
LOI (wt-%)	0.18	0.34	0.57	0.52	4.94	0.93	0.61	0.52
Total	100.49	100.51	100.65	100.26	96.38	100.43	100.30	100.09
Trace elements:								
Co (ppm)	0.9	0.3	<0.2	<0.2	0.7	2.5	0.4	<0.2
Ni (ppm)	1.4	1.7	1.6	2.3	1.0	2.4	1.8	1.7
Cu (ppm)	50.6	2.9	4.5	4.7	4.0	21.6	4.9	3.0
Zn (ppm)	39.0	16.0	15.0	9.0	16.0	36.0	22.0	18.0
Ga (ppm)	18.8	27.9	28.4	26.1	10.9	18.7	27.2	28.6
Rb (ppm)	246.2	816.7	699.1	686.5	226.9	329.0	585.9	678.6
Sr (ppm)	26.9	5.4	8.3	5.7	22.7	67.5	11.1	10.0
Y (ppm)	63.3	136.2	105.9	52.2	140.1	26.8	177.6	150.7
Zr (ppm)	166.7	115.3	122.7	113.7	33.7	47.1	130.6	146.2
Nb (ppm)	24.7	57.5	50.0	47.8	19.3	7.0	48.4	52.6
Mo (ppm)	1.7	1.7	1.0	2.2	1.2	0.5	2.0	2.0
Cs (ppm)	2.4	16.2	11.7	6.5	11.7	11.3	27.6	4.6
Ba (ppm)	98.0	31.0	56.0	69.0	34.0	371.0	114.0	28.0
La (ppm)	69.40	51.30	55.60	19.50	18.30	17.30	57.40	51.00
Ce (ppm)	139.70	117.80	111.20	30.30	38.00	31.20	121.00	118.00
Pr (ppm)	13.19	14.55	13.50	4.46	4.87	4.24	14.65	13.22
Nd (ppm)	42.10	53.40	45.90	14.40	17.40	15.20	52.80	45.20
Sm (ppm)	7.91	13.55	10.92	3.67	4.73	3.23	14.66	12.87
Eu (ppm)	0.19	0.05	0.07	0.04	0.03	0.35	0.02	<0.02
Gd (ppm)	7.79	14.65	9.87	4.24	6.78	3.68	17.71	14.17
Tb (ppm)	1.38	3.07	1.98	0.99	1.56	0.66	3.75	3.04
Dy (ppm)	9.03	20.34	13.20	7.79	11.47	4.25	25.18	21.05
Ho (ppm)	2.10	4.78	3.19	2.00	2.75	0.88	6.07	4.85
Er (ppm)	7.14	16.30	11.53	7.56	9.21	2.72	19.16	16.58
Tm (ppm)	1.12	2.66	1.99	1.30	1.51	0.32	2.76	2.73
Yb (ppm)	7.52	18.96	14.88	10.01	10.08	1.75	18.07	18.61
Lu (ppm)	1.13	2.82	2.17	1.49	1.47	0.23	2.55	2.69
Hf (ppm)	6.9	7.8	7.1	7.6	2.1	1.6	7.7	8.7
Ta (ppm)	2.8	6.8	6.5	6.6	2.0	0.8	5.4	5.5
Pb (ppm)	273.2	7.2	10.1	4.7	6.8	9.5	14.5	11.3
Th (ppm)	58.9	57.7	59.2	22.5	16.8	8.3	66.5	69.0
U (ppm)	9.4	28.6	7.8	8.1	6.0	4.2	13.0	22.9
Li (wt-%)	0.001	0.009	0.001	0.002	0.007	N.A.	0.002	0.004
V (ppm)	9.0	<8	8.0	<8	28.0	<8	<8	<8
As (ppm)	0.5	2.1	2.1	2.5	2.3	13.4	1.3	1.2
Ag (ppm)	0.5	<0.1	<0.1	0.2	<0.1	<0.1	<0.1	<0.1
Sn (ppm)	8.0	14.0	15.0	14.0	6.0	9.0	36.0	45.0
Sb (ppm)	0.1	0.1	0.1	0.1	0.1	<0.1	0.2	<0.1
W (ppm)	1.9	2.8	5.1	2.7	1.9	2.4	4.6	5.2
Bi (ppm)	0.1	<0.1	0.6	0.5	0.6	2.1	0.5	<0.1
Cd (ppm)	0.1	<0.1	<0.1	<0.1	<0.1	<0.1	<0.1	<0.1
Au (p.p.b.)	0.6	13.2	<0.5	<0.5	1.6	<0.5	<0.5	<0.5
Se (ppm)	0.5	<0.5	<0.5	<0.5	<0.5	<0.5	<0.5	<0.5
Hg (ppm)	0.0	<0.01	<0.01	<0.01	<0.01	<0.01	<0.01	<0.01
Be (ppm)	2.0	17.0	4.0	6.0	<1	3.0	2.0	17.0

Sample	567249	567250	567251	567254	567257	567259	567260	567262
Group name	Caledonian granite	Caledonian granite	Caledonian granite	Caledonian granite	Caledonian granite	Caledonian granite	Caledonian granite	Caledonian granite
Rock name *	granite	syenite	granite	granite	granite	granite	granite	granite
Collector [§]	TFK	TFK	TFK	TFK	TFK	TFK	TFK	TFK
Year	2022	2022	2022	2022	2022	2022	2022	2022
Latitude (N)	73.6995	73.7008	73.7008	73.7007	73.6965	73.7055	73.7430	73.7741
Longitude (W)	-22.1431	-22.1790	-22.2033	-22.1148	-22.1027	-22.1299	-22.0782	-22.0288
Locality	Storelv N	Storelv N	Storelv N	Storelv N	Storelv N	Storelv N	Storelv N	Storelv N
Major elements:								
SiO2 (wt-%)	73.36	58.79	69.68	73.91	70.68	69.73	73.73	76.04
TiO2 (wt-%)	0.22	1.18	0.34	0.05	0.27	0.44	0.14	0.04
Al2O3 (wt-%)	14.85	18.90	15.43	15.73	15.63	15.72	14.70	14.83
Fe2O3T (wt-%)	1.63	6.13	2.34	0.71	1.88	2.89	1.24	0.58
FeO (wt-%) [#]	0.70	3.84	1.67		1.10	2.13	0.48	0.43
MnO (wt-%)	0.02	0.06	0.03	0.02	0.02	0.04	0.02	0.01
MgO (wt-%)	0.20	1.46	0.59	0.16	0.33	0.81	0.13	0.22
CaO (wt-%)	0.77	1.22	1.41	1.01	0.87	1.62	0.65	2.06
Na2O (wt-%)	3.25	3.36	3.44	6.72	3.18	3.68	3.80	5.62
K2O (wt-%)	5.65	7.07	5.61	1.35	6.68	4.78	4.68	1.04
P2O5 (wt-%)	0.22	0.07	0.16	0.06	0.25	0.19	0.20	0.01
LOI (wt-%)	0.68	1.11	0.67	0.92	0.68	0.78	0.74	0.22
Total	100.85	99.35	99.70	100.64	100.47	100.68	100.03	100.67
Trace elements:								
Co (ppm)	1.5	13.6	3.4	0.4	1.8	5.6	0.7	0.6
Ni (ppm)	2.6	33.9	5.6	1.7	3.1	6.0	2.0	2.0
Cu (ppm)	19.4	214.2	10.6	13.0	44.2	5.5	6.8	18.3
Zn (ppm)	36.0	210.0	44.0	11.0	44.0	65.0	31.0	5.0
Ga (ppm)	21.1	29.8	20.0	22.7	22.7	22.9	23.3	12.2
Rb (ppm)	326.0	409.3	272.6	114.3	301.5	270.9	357.9	12.8
Sr (ppm)	64.3	156.9	152.3	42.8	91.7	138.5	48.8	610.9
Y (ppm)	11.0	15.9	14.1	6.4	14.1	15.4	13.0	0.7
Zr (ppm)	75.9	384.5	141.8	3.5	117.9	140.0	63.0	58.7
Nb (ppm)	11.4	25.5	12.6	7.9	9.9	14.9	12.4	5.0
Mo (ppm)	1.2	1.1	1.2	1.1	0.6	0.7	1.2	1.0
Cs (ppm)	27.2	35.6	15.8	7.7	12.7	25.6	21.8	0.2
Ba (ppm)	256.0	582.0	444.0	27.0	403.0	351.0	190.0	510.0
La (ppm)	19.20	62.00	28.90	3.00	28.30	34.30	14.20	1.10
Ce (ppm)	43.90	127.80	60.60	5.30	63.80	72.80	31.20	1.70
Pr (ppm)	4.92	14.05	6.76	0.50	7.42	7.96	3.47	0.11
Nd (ppm)	18.00	51.00	25.00	2.00	28.80	28.60	12.80	0.50
Sm (ppm)	4.64	8.77	4.60	0.43	6.78	5.47	3.26	0.07
Eu (ppm)	0.50	1.30	0.92	0.20	0.83	0.92	0.40	0.16
Gd (ppm)	4.46	6.54	4.29	0.70	6.23	4.59	3.43	0.08
Tb (ppm)	0.63	0.78	0.58	0.14	0.85	0.62	0.57	0.01
Dy (ppm)	2.93	3.64	3.12	1.00	3.57	2.95	2.65	0.08
Ho (ppm)	0.42	0.65	0.54	0.20	0.49	0.59	0.36	0.02
Er (ppm)	0.95	1.84	1.37	0.53	0.98	1.42	0.88	0.12
Tm (ppm)	0.10	0.23	0.20	0.10	0.12	0.20	0.11	0.01
Yb (ppm)	0.71	1.72	1.36	0.52	0.60	1.34	0.67	0.20
Lu (ppm)	0.09	0.26	0.20	0.07	0.08	0.16	0.08	0.02
Hf (ppm)	2.4	9.8	4.1	0.1	3.6	3.9	2.1	1.8
Ta (ppm)	1.3	1.7	0.9	0.6	0.4	1.6	1.5	0.1
Pb (ppm)	23.0	90.8	13.8	9.9	22.1	14.3	11.4	3.5
Th (ppm)	12.1	19.6	13.3	2.0	18.8	15.6	9.2	0.2
U (ppm)	15.0	13.2	8.1	6.0	15.4	8.5	18.7	0.5
Li (wt-%)	0.012	0.016	0.009	0.009	0.008	0.011	0.004	0.001
V (ppm)	15.0	112.0	29.0	8.0	12.0	34.0	8.0	8.0
As (ppm)	0.8	2.7	0.5	0.5	1.4	1.4	0.5	0.5
Ag (ppm)	0.1	0.4	0.1	0.1	0.1	0.1	0.1	0.1
Sn (ppm)	25.0	21.0	10.0	18.0	9.0	14.0	31.0	1.0
Sb (ppm)	0.1	0.1	0.1	0.1	0.1	0.1	0.1	0.1
W (ppm)	3.5	2.5	0.9	2.3	2.2	1.4	3.9	0.5
Bi (ppm)	2.0	2.6	0.8	3.4	1.7	0.8	2.2	0.1
Cd (ppm)	0.1	0.1	0.1	0.1	0.1	0.1	0.1	0.1
Au (p.p.b.)	0.5	0.7	0.5	0.5	0.9	0.5	0.7	0.5
Se (ppm)	0.5	0.5	0.5	0.5	0.5	0.5	0.5	0.5
Hg (ppm)	0.0	0.0	0.0	0.0	0.0	0.0	0.0	0.0
Be (ppm)	30.0	13.0	6.0	19.0	4.0	10.0	17.0	2.0

Sample	567265	567266	567268	567269	567271	567272	567276	567277
Group name	Caledonian granite	Caledonian granite	Caledonian granite	Caledonian granite	Caledonian granite	Caledonian granite	Caledonian granite	Caledonian granite
Rock name *	granite	granite	quartz monzonite	granite	granite	granite	granite	granite
Collector [$]	TFK	TFK	TFK	TFK	TFK	TFK	TFK	TFK
Year	2022	2022	2022	2022	2022	2022	2022	2022
Latitude (N)	73.7679	73.6837	73.6699	73.6660	73.6802	73.6731	73.8218	73.6977
Longitude (W)	-22.1189	-22.3115	-22.3227	-22.3689	-22.3037	-22.2719	-22.5066	-22.2560
Locality	Storelv N	Storelv S	Storelv S	Storelv S	Storelv S	Storelv S	Storelv S	Storelv S
Major elements:								
SiO2 (wt-%)	73.09	73.74	68.90	68.72	68.61	70.94	72.73	71.24
TiO2 (wt-%)	0.25	0.36	0.49	0.56	0.52	0.44	0.29	0.43
Al2O3 (wt-%)	14.61	14.02	15.60	15.22	15.49	15.00	14.39	14.50
Fe2O3T (wt-%)	1.63	2.45	3.18	3.63	3.36	2.24	1.89	2.18
FeO (wt-%) [#]	1.15	1.87	2.56	2.89	2.62	1.10	1.17	0.50
MnO (wt-%)	0.03	0.04	0.04	0.05	0.04	0.03	0.02	0.02
MgO (wt-%)	0.53	0.67	0.94	1.15	1.05	0.46	0.28	0.28
CaO (wt-%)	0.81	0.65	1.74	1.20	1.57	1.09	0.67	1.20
Na2O (wt-%)	3.63	3.97	3.53	4.12	3.77	3.98	4.01	3.10
K2O (wt-%)	5.20	3.74	5.02	3.72	4.15	4.48	4.91	5.78
P2O5 (wt-%)	0.09	0.09	0.21	0.24	0.22	0.19	0.12	0.26
LOI (wt-%)	0.41	0.94	0.87	1.25	1.42	1.38	0.80	1.54
Total	100.28	100.67	100.52	99.86	100.20	100.23	100.11	100.53
Trace elements:								
Co (ppm)	2.3	3.5	4.8	6.5	5.6	3.0	1.3	1.7
Ni (ppm)	4.9	5.4	7.1	7.7	7.3	3.2	1.5	2.1
Cu (ppm)	7.8	5.6	7.4	13.9	5.9	8.7	3.8	5.1
Zn (ppm)	24.0	41.0	64.0	74.0	66.0	54.0	52.0	79.0
Ga (ppm)	14.3	19.3	19.0	21.7	21.4	22.6	23.0	21.5
Rb (ppm)	121.6	214.7	213.9	188.5	206.9	250.9	289.1	254.2
Sr (ppm)	264.3	98.9	204.4	203.6	199.3	493.0	84.3	280.9
Y (ppm)	5.9	15.4	14.1	17.8	19.4	14.2	6.4	9.5
Zr (ppm)	214.7	102.3	155.0	193.4	191.9	163.8	180.4	217.3
Nb (ppm)	6.9	11.3	10.9	14.7	18.3	14.2	15.1	8.5
Mo (ppm)	0.3	1.3	1.4	0.8	0.8	1.1	0.3	1.4
Cs (ppm)	1.0	10.1	11.9	9.6	11.9	5.3	2.9	2.6
Ba (ppm)	1454.0	186.0	415.0	371.0	409.0	683.0	308.0	630.0
La (ppm)	44.00	27.90	34.80	39.00	44.10	51.50	77.60	72.00
Ce (ppm)	77.40	57.40	68.60	79.90	90.90	105.70	165.60	158.50
Pr (ppm)	8.17	6.57	8.17	9.16	9.78	11.55	17.73	17.80
Nd (ppm)	26.50	24.70	29.50	32.70	35.40	41.10	61.00	63.10
Sm (ppm)	3.56	4.49	5.49	6.35	6.93	6.60	9.84	10.71
Eu (ppm)	0.65	0.65	1.00	0.98	1.22	1.20	0.62	0.96
Gd (ppm)	2.33	3.52	4.34	5.12	5.92	4.45	5.62	6.75
Tb (ppm)	0.26	0.55	0.61	0.73	0.76	0.57	0.58	0.66
Dy (ppm)	1.33	2.93	3.07	3.85	4.14	2.89	2.13	2.59
Ho (ppm)	0.23	0.54	0.53	0.66	0.59	0.47	0.21	0.28
Er (ppm)	0.57	1.64	1.46	1.70	1.77	1.29	0.48	0.69
Tm (ppm)	0.06	0.26	0.19	0.22	0.25	0.19	0.06	0.10
Yb (ppm)	0.41	1.71	1.22	1.55	1.61	1.30	0.36	0.56
Lu (ppm)	0.07	0.26	0.19	0.22	0.24	0.19	0.03	0.07
Hf (ppm)	5.6	3.2	4.4	5.4	5.3	4.6	5.6	6.5
Ta (ppm)	0.3	1.9	1.0	1.4	1.4	1.4	1.1	0.2
Pb (ppm)	12.3	5.2	8.7	13.7	10.9	14.6	11.3	12.6
Th (ppm)	22.1	14.1	14.9	18.8	17.5	20.4	41.7	36.3
U (ppm)	1.4	5.4	3.9	5.5	7.7	21.5	7.1	5.5
Li (wt-%)	0.001	0.006	0.008	0.009	0.008	0.008	0.001	0.003
V (ppm)	15.0	23.0	27.0	39.0	41.0	26.0	8.0	16.0
As (ppm)	0.5	2.0	0.9	0.9	0.5	0.5	0.5	0.5
Ag (ppm)	0.1	0.1	0.1	0.1	0.1	0.1	0.1	0.1
Sn (ppm)	1.0	16.0	9.0	9.0	12.0	10.0	6.0	4.0
Sb (ppm)	0.1	0.1	0.1	0.1	0.1	0.1	0.1	0.1
W (ppm)	0.5	1.3	0.8	1.1	0.5	1.2	0.8	1.1
Bi (ppm)	0.1	2.7	0.8	0.8	0.7	0.6	0.4	0.2
Cd (ppm)	0.1	0.1	0.1	0.1	0.1	0.1	0.1	0.1
Au (p.p.b.)	0.5	0.5	0.8	0.5	0.6	0.9	0.5	0.5
Se (ppm)	0.5	0.5	0.5	0.5	0.5	0.5	0.5	0.5
Hg (ppm)	0.0	0.0	0.0	0.0	0.0	0.0	0.0	0.0
Be (ppm)	1.0	8.0	6.0	5.0	4.0	8.0	6.0	2.0

Sample	567278	567279	567280	582725	585707	585717	585727	585728
Group name	Caledonian granite	Caledonian granite	Caledonian granite	Caledonian granite	Caledonian granite	Caledonian granite	Caledonian granite	Caledonian granite
Rock name *	granite	granite	quartz monzonite	granite	granite	granite	granite	granite
Collector §	TFK	TFK	TFK	PGUA	NJB	NJB	NJB	NJB
Year	2022	2022	2022	2022	2022	2022	2022	2022
Latitude (N)	73.6377	73.6279	73.6590	73.7809	73.9402	73.7805	73.7758	73.8688
Longitude (W)	-22.3164	-22.4109	-22.3821	-22.5185	-22.7564	-22.6527	-22.4944	-22.8247
Locality	Storelv S	Storelv S	Storelv S	Dybendal E	Stordal	Parkinson Bjerg	Stordal	Aravis
Major elements:								
SiO2 (wt-%)	73.59	68.81	67.44	75.34	72.50	74.65	75.02	74.27
TiO2 (wt-%)	0.14	0.54	0.55	0.09	0.25	0.09	0.08	0.07
Al2O3 (wt-%)	15.04	15.03	15.69	13.77	14.69	14.40	14.48	14.44
Fe2O3T (wt-%)	1.43	3.51	3.42	1.06	1.89	1.12	1.02	0.99
FeO (wt-%) #	1.04	2.84	2.76					
MnO (wt-%)	0.02	0.05	0.04	0.02	0.03	0.03	0.02	0.03
MgO (wt-%)	0.22	1.12	1.09	0.11	0.45	0.20	0.12	0.10
CaO (wt-%)	0.52	1.46	1.90	0.71	0.95	0.43	0.64	0.55
Na2O (wt-%)	3.86	3.85	3.56	3.72	3.43	4.57	4.85	4.59
K2O (wt-%)	4.89	3.90	4.83	4.65	4.96	4.53	2.93	4.11
P2O5 (wt-%)	0.20	0.23	0.23	0.14	0.13	0.11	0.10	0.09
LOI (wt-%)	0.66	1.58	1.03	0.84	1.09	0.49	0.78	0.37
Total	100.57	100.08	99.78	100.45	100.37	100.62	100.04	99.61
Trace elements:								
Co (ppm)	1.4	6.8	7.3	0.9	2.8	1.8	1.0	0.8
Ni (ppm)	1.6	8.1	8.4	1.4	4.0	2.1	1.7	1.5
Cu (ppm)	2.8	8.9	9.1	5.0	4.3	4.6	17.9	10.2
Zn (ppm)	26.0	70.0	69.0	31.0	36.0	26.0	20.0	31.0
Ga (ppm)	24.9	22.7	23.7	20.5	16.5	22.0	19.7	22.0
Rb (ppm)	390.6	196.6	245.6	249.4	132.5	244.4	139.4	249.3
Sr (ppm)	42.7	230.0	228.0	75.8	207.7	64.2	100.9	40.5
Y (ppm)	17.4	20.0	16.5	6.3	5.8	9.8	5.1	8.9
Zr (ppm)	66.2	179.0	208.2	44.5	111.1	43.1	21.6	35.3
Nb (ppm)	12.4	14.5	12.0	4.8	4.9	6.7	3.5	8.3
Mo (ppm)	0.3	1.5	0.6	0.3	0.3	0.9	1.3	0.4
Cs (ppm)	24.4	7.4	7.5	3.6	2.4	1.7	4.8	4.2
Ba (ppm)	165.0	378.0	547.0	177.0	526.0	176.0	203.0	100.0
La (ppm)	13.90	42.70	47.20	11.10	30.70	10.40	6.10	9.20
Ce (ppm)	30.90	90.60	97.80	23.20	66.40	18.00	12.70	17.50
Pr (ppm)	3.39	9.90	10.80	2.48	7.24	2.09	1.32	1.93
Nd (ppm)	12.00	35.80	39.70	8.50	25.60	8.20	4.50	6.20
Sm (ppm)	3.43	6.71	7.41	2.14	4.31	1.89	0.94	1.59
Eu (ppm)	0.36	0.98	1.23	0.37	0.96	0.20	0.50	0.23
Gd (ppm)	3.77	5.20	5.52	1.66	3.01	1.72	0.81	1.50
Tb (ppm)	0.69	0.79	0.76	0.25	0.33	0.30	0.12	0.25
Dy (ppm)	3.46	4.03	3.76	1.29	1.61	1.99	0.85	1.46
Ho (ppm)	0.55	0.76	0.67	0.24	0.22	0.35	0.19	0.23
Er (ppm)	1.25	1.93	1.72	0.65	0.49	1.22	0.57	0.83
Tm (ppm)	0.15	0.26	0.22	0.10	0.05	0.17	0.09	0.10
Yb (ppm)	0.92	1.70	1.38	0.62	0.40	1.24	0.73	0.65
Lu (ppm)	0.11	0.27	0.19	0.09	0.04	0.19	0.12	0.09
Hf (ppm)	2.4	5.2	5.9	1.6	3.2	1.9	0.7	1.4
Ta (ppm)	2.2	2.0	1.0	0.5	0.3	0.5	0.6	0.5
Pb (ppm)	10.6	10.4	9.8	15.3	17.7	10.4	16.8	7.5
Th (ppm)	10.3	19.7	19.8	6.7	14.7	4.5	2.4	3.6
U (ppm)	25.0	6.7	5.2	12.0	3.2	5.3	8.3	7.5
Li (wt-%)	0.008	0.010	0.006	0.001	0.001	<0.001	0.002	0.002
V (ppm)	24.0	53.0	50.0	<8	18.0	<8	<8	<8
As (ppm)	1.8	0.6	1.4	<0.5	<0.5	0.7	0.7	<0.5
Ag (ppm)	0.1	0.1	0.1	<0.1	<0.1	0.1	<0,1	<0.1
Sn (ppm)	35.0	12.0	8.0	9.0	3.0	8.0	6.0	14.0
Sb (ppm)	0.1	0.1	0.1	<0.1	<0.1	<0.1	<0,1	<0.1
W (ppm)	5.9	0.8	0.7	1.3	0.6	0.7	1.1	1.1
Bi (ppm)	5.0	2.2	0.3	2.5	<0.1	0.7	13.8	2.7
Cd (ppm)	0.1	0.1	0.1	<0.1	<0.1	<0.1	<0,1	<0.1
Au (p.p.b.)	0.5	0.5	0.8	<0.5	<0.5	<0.5	<0,5	<0.5
Se (ppm)	0.5	0.5	0.5	<0.5	<0.5	<0.5	<0,5	<0.5
Hg (ppm)	0.0	0.0	0.0	<0.01	<0.01	<0.01	<0,01	<0.01
Be (ppm)	19.0	12.0	4.0	6.0	7.0	9.0	9.0	6.0

Sample	587001	587005	587006	587008	587010	587016	587017	587018
Group name	Caledonian granite	Caledonian granite	Caledonian granite	Caledonian granite	Caledonian granite	Caledonian granite	Caledonian granite	Caledonian granite
Rock name *	granite	granite	granite	granite	granite	granite	granite	quartz monzonite
Collector [§]	DRO+TFK	DRO+TFK	DRO+TFK	DRO+TFK	DRO+TFK	DRO+TFK	DRO+TFK	DRO+TFK
Year	2022	2022	2022	2022	2022	2022	2022	2022
Latitude (N)	73.9383	73.9322	73.9309	73.9373	73.9458	73.9507	73.9534	73.9544
Longitude (W)	-22.4640	-22.4329	-22.4482	-22.4375	-22.3956	-22.3562	-22.3520	-22.3522
Locality	Passagedal W	Passagedal W	Passagedal W	Passagedal W	Passagedal E	Passagedal E	Passagedal E	Passagedal E
Major elements:								
SiO2 (wt-%)	72.15	70.25	74.82	74.81	71.12	71.71	76.12	66.25
TiO2 (wt-%)	0.30	0.37	0.14	0.09	0.37	0.29	0.15	0.44
Al2O3 (wt-%)	14.93	16.38	14.50	14.36	15.08	15.12	13.52	17.47
Fe2O3T (wt-%)	1.95	3.07	0.78	0.85	2.14	2.29	1.36	3.92
FeO (wt-%) [#]	1.47	2.09	0.64	0.65	1.50	1.74	0.89	1.84
MnO (wt-%)	0.04	0.06	0.04	0.04	0.04	0.05	0.03	0.04
MgO (wt-%)	0.46	0.73	0.17	0.19	0.51	0.68	0.19	1.24
CaO (wt-%)	0.69	0.34	1.12	1.01	0.83	0.78	0.27	1.81
Na2O (wt-%)	3.74	3.79	3.66	4.20	3.37	3.49	3.58	5.54
K2O (wt-%)	5.02	2.91	4.66	4.32	5.14	5.23	4.00	2.82
P2O5 (wt-%)	0.20	0.15	0.11	0.10	0.26	0.15	0.09	0.12
LOI (wt-%)	0.70	1.70	0.44	0.47	0.96	0.93	0.89	1.35
Total	100.18	99.75	100.44	100.44	99.82	100.72	100.20	101.00
Trace elements:								
Co (ppm)	2.6	4.8	0.9	1.4	3.5	4.8	0.7	2.6
Ni (ppm)	3.5	8.3	1.8	2.4	5.0	8.5	1.5	3.4
Cu (ppm)	4.4	45.4	4.6	4.7	9.0	4.4	3.1	2.0
Zn (ppm)	54.0	24.0	12.0	13.0	91.0	38.0	46.0	19.0
Ga (ppm)	24.1	20.9	14.3	13.0	27.7	13.6	17.9	27.0
Rb (ppm)	292.5	159.9	167.3	143.7	351.1	148.5	180.8	74.3
Sr (ppm)	84.4	65.5	116.3	157.3	74.9	337.8	179.7	611.4
Y (ppm)	8.2	14.5	4.9	11.0	8.9	15.4	8.7	13.7
Zr (ppm)	158.2	106.5	42.1	87.0	170.1	252.2	80.9	372.5
Nb (ppm)	7.7	8.9	3.5	2.7	4.6	5.5	5.8	5.5
Mo (ppm)	0.8	1.1	0.3	0.7	0.7	0.7	0.4	0.6
Cs (ppm)	4.9	4.4	5.0	4.6	6.2	2.0	2.7	1.4
Ba (ppm)	330.0	482.0	387.0	432.0	304.0	1197.0	406.0	931.0
La (ppm)	45.20	41.20	14.10	17.00	51.00	96.40	22.10	334.40
Ce (ppm)	99.70	84.60	26.40	35.30	118.10	201.90	43.60	489.60
Pr (ppm)	11.07	9.43	3.06	4.02	14.92	23.88	5.32	47.28
Nd (ppm)	40.60	34.30	11.20	14.10	55.10	87.50	20.90	145.00
Sm (ppm)	6.53	5.95	2.25	3.01	9.78	15.06	4.29	15.07
Eu (ppm)	0.63	1.05	0.76	1.00	0.66	2.12	0.43	3.40
Gd (ppm)	3.97	3.94	1.66	2.31	5.15	9.08	3.29	7.42
Tb (ppm)	0.44	0.57	0.22	0.37	0.53	1.07	0.39	0.70
Dy (ppm)	1.97	2.96	1.19	1.95	2.07	4.25	1.84	2.95
Ho (ppm)	0.29	0.58	0.18	0.39	0.28	0.53	0.28	0.41
Er (ppm)	0.62	1.83	0.47	1.04	0.70	1.10	0.69	1.00
Tm (ppm)	0.11	0.27	0.06	0.15	0.10	0.14	0.10	0.14
Yb (ppm)	0.68	1.96	0.53	1.06	0.70	0.82	0.61	0.96
Lu (ppm)	0.09	0.34	0.07	0.14	0.09	0.13	0.09	0.13
Hf (ppm)	4.6	3.2	1.6	3.0	5.4	7.5	2.8	7.9
Ta (ppm)	0.8	0.9	0.5	0.3	0.4	0.5	0.3	0.3
Pb (ppm)	6.9	3.9	9.8	13.2	5.5	13.6	20.8	1.7
Th (ppm)	29.7	17.5	6.9	8.2	37.8	52.3	8.1	16.1
U (ppm)	14.0	4.6	1.8	2.0	15.8	5.6	3.3	1.8
Li (wt-%)	0.004	0.002	0.001	0.001	0.007	0.002	0.001	0.003
V (ppm)	16.0	29.0	14.0	8.0	18.0	25.0	8.0	48.0
As (ppm)	0.5	0.5	0.5	0.5	0.8	0.5	0.5	0.5
Ag (ppm)	0.1	0.1	0.1	0.1	0.1	0.1	0.1	0.1
Sn (ppm)	7.0	9.0	5.0	5.0	8.0	4.0	3.0	1.0
Sb (ppm)	0.1	0.1	0.1	0.1	0.1	0.1	0.1	0.1
W (ppm)	1.0	3.6	0.6	0.5	1.2	0.6	0.5	0.5
Bi (ppm)	0.7	0.1	0.4	0.2	0.3	0.1	0.1	0.1
Cd (ppm)	0.1	0.1	0.1	0.1	0.1	0.1	0.1	0.1
Au (p.p.b.)	0.5	0.5	0.5	0.5	0.5	0.5	0.5	0.5
Se (ppm)	0.5	0.5	0.5	0.5	0.5	0.5	0.5	0.5
Hg (ppm)	0.0	0.0	0.0	0.0	0.0	0.0	0.0	0.0
Be (ppm)	7.0	2.0	5.0	4.0	10.0	3.0	5.0	2.0

Sample	587020	587023	587025	587028	587029	587032	587033	587038
Group name	Caledonian granite	Caledonian granite	Caledonian granite	Caledonian granite	Caledonian granite	Caledonian granite	Caledonian granite	Caledonian granite
Rock name *	granite	granite	granite	granite	granite	granite	granite	granite
Collector [§]	DRO+TFK	DRO+TFK	DRO+TFK	DRO+TFK	DRO+TFK	DRO+TFK	DRO+TFK	DRO+TFK
Year	2022	2022	2022	2022	2022	2022	2022	2022
Latitude (N)	73.9296	73.9268	73.9232	73.7747	73.7747	74.0435	74.0435	73.9907
Longitude (W)	-22.3899	-22.3923	-22.3916	-22.4100	-22.4100	-22.5142	-22.5142	-22.5344
Locality	Passagedal E	Passagedal E	Passagedal E	Passagedal E	Passagedal E	Nørlund Alper	Nørlund Alper	Nørlund Alper
Major elements:								
SiO2 (wt-%)	73.99	70.66	71.59	71.08	72.87	70.74	72.58	74.20
TiO2 (wt-%)	0.19	0.35	0.36	0.49	0.03	0.48	0.37	0.10
Al2O3 (wt-%)	14.00	14.90	15.15	15.29	14.54	15.03	13.85	15.28
Fe2O3T (wt-%)	1.30	2.10	2.24	2.76	0.74	2.17	2.33	1.06
FeO (wt-%) [#]	0.99	1.63	1.71	2.01	0.58	1.65	1.88	0.83
MnO (wt-%)	0.04	0.05	0.04	0.04	0.05	0.05	0.05	0.02
MgO (wt-%)	0.29	0.49	0.51	0.70	0.09	0.48	0.55	0.20
CaO (wt-%)	0.90	1.31	0.86	0.67	1.06	0.88	0.58	1.23
Na2O (wt-%)	3.52	3.42	3.49	3.10	5.28	3.11	3.23	3.57
K2O (wt-%)	4.89	5.09	5.19	5.70	4.33	5.95	4.85	4.86
P2O5 (wt-%)	0.14	0.26	0.26	0.29	0.20	0.30	0.08	0.09
LOI (wt-%)	1.17	1.56	1.15	1.02	0.81	1.01	0.93	0.54
Total	100.43	100.19	100.84	101.14	100.00	100.20	99.40	101.15
Trace elements:								
Co (ppm)	1.7	3.3	2.9	4.5	0.4	3.8	3.6	1.0
Ni (ppm)	2.2	4.5	5.2	6.5	1.1	2.4	6.0	1.6
Cu (ppm)	3.4	8.5	12.0	7.8	62.5	2.1	3.6	2.3
Zn (ppm)	32.0	95.0	100.0	80.0	13.0	35.0	43.0	12.0
Ga (ppm)	17.5	26.5	26.3	26.4	15.6	19.3	15.1	16.7
Rb (ppm)	212.6	339.8	351.3	319.7	241.7	198.7	174.9	116.3
Sr (ppm)	147.0	72.1	67.4	97.9	29.4	138.6	141.5	143.3
Y (ppm)	5.9	8.8	9.5	12.6	2.3	23.9	21.9	14.3
Zr (ppm)	89.5	163.4	171.5	243.4	6.5	310.3	194.3	59.9
Nb (ppm)	4.9	4.5	4.3	4.7	5.3	7.3	7.6	2.5
Mo (ppm)	0.9	0.9	1.3	1.1	0.3	1.0	0.3	0.9
Cs (ppm)	4.6	4.7	3.3	10.9	8.1	2.6	3.6	1.3
Ba (ppm)	422.0	291.0	294.0	456.0	65.0	822.0	783.0	441.0
La (ppm)	26.10	47.10	50.70	74.80	3.90	115.50	27.40	12.20
Ce (ppm)	47.80	107.00	116.70	172.50	7.20	245.40	55.10	24.60
Pr (ppm)	5.59	13.54	14.39	21.66	0.71	29.37	6.27	2.85
Nd (ppm)	19.60	50.00	54.10	77.30	3.10	104.70	23.40	10.90
Sm (ppm)	3.46	9.11	9.48	13.70	0.63	16.34	4.37	2.29
Eu (ppm)	0.66	0.62	0.62	0.88	0.18	1.35	1.12	1.05
Gd (ppm)	2.17	4.61	4.97	7.16	0.48	9.08	3.73	2.64
Tb (ppm)	0.26	0.48	0.49	0.72	0.06	0.98	0.60	0.46
Dy (ppm)	1.20	2.06	2.01	2.92	0.33	4.62	3.69	2.80
Ho (ppm)	0.19	0.28	0.28	0.39	0.06	0.81	0.77	0.48
Er (ppm)	0.55	0.72	0.76	1.02	0.20	2.20	2.26	1.35
Tm (ppm)	0.07	0.11	0.11	0.14	0.03	0.29	0.32	0.20
Yb (ppm)	0.58	0.69	0.68	0.94	0.23	1.80	2.10	1.18
Lu (ppm)	0.07	0.10	0.11	0.13	0.03	0.23	0.31	0.19
Hf (ppm)	2.7	5.0	5.2	6.9	0.3	9.1	5.5	1.9
Ta (ppm)	0.5	0.4	0.5	0.3	2.3	0.7	0.7	0.2
Pb (ppm)	13.0	9.5	10.4	9.6	6.7	10.2	9.5	6.4
Th (ppm)	15.3	35.2	37.0	53.7	0.5	78.6	9.6	4.2
U (ppm)	4.7	16.2	14.3	8.1	2.3	9.1	3.5	3.0
Li (wt-%)	0.002	0.006	0.005	0.008	0.001	0.002	0.003	0.002
V (ppm)	8.0	16.0	17.0	28.0	8.0	23.0	25.0	28.0
As (ppm)	0.5	0.5	0.5	0.5	0.5	0.5	0.5	0.5
Ag (ppm)	0.1	0.1	0.1	0.1	0.1	0.1	0.1	0.1
Sn (ppm)	9.0	8.0	6.0	4.0	8.0	5.0	8.0	2.0
Sb (ppm)	0.1	0.1	0.1	0.1	0.1	0.1	0.1	0.1
W (ppm)	1.7	0.8	0.7	1.7	0.6	1.1	1.5	0.5
Bi (ppm)	0.7	0.4	0.6	0.3	0.2	0.1	0.3	0.1
Cd (ppm)	0.1	0.1	0.1	0.1	0.1	0.1	0.1	0.1
Au (p.p.b.)	0.5	0.5	0.5	0.5	0.5	0.5	0.5	0.9
Se (ppm)	0.5	0.5	0.5	0.5	0.5	0.5	0.5	0.5
Hg (ppm)	0.0	0.0	0.0	0.0	0.0	0.0	0.0	0.0
Be (ppm)	4.0	6.0	1.0	7.0	26.0	2.0	4.0	6.0

Sample	587039	587044	587047	587054	587062	587063	587070	587073
Group name	Caledonian granite	Caledonian granite	Caledonian granite	Caledonian granite	Caledonian granite	Caledonian granite	Caledonian granite	Caledonian granite
Rock name *	granite	granite	granite	granite	granite	granite	granite	granite
Collector [§]	DRO+TFK	DRO+TFK	DRO+TFK	DRO	DRO	DRO	DRO	DRO
Year	2022	2022	2022	2022	2022	2022	2022	2022
Latitude (N)	73.9689	73.9399	73.9433	73.6917	73.7103	73.7074	73.7389	73.7389
Longitude (W)	-22.6420	-22.4087	-22.4164	-22.5765	-22.5640	-22.5534	-22.6417	-22.6417
Locality	Nørlund Alper	Passagedal E	Passagedal E	Fuchs Bjerg	Fuchs Bjerg	Fuchs Bjerg	Blokadedal	Blokadedal
Major elements:								
SiO2 (wt-%)	74.07	68.79	77.43	72.18	71.26	71.37	71.46	72.66
TiO2 (wt-%)	0.20	0.49	0.06	0.40	0.36	0.33	0.31	0.27
Al2O3 (wt-%)	14.86	14.53	13.04	14.94	14.86	14.87	14.42	14.56
Fe2O3T (wt-%)	1.40	2.68	0.76	1.64	2.13	2.04	2.49	1.90
FeO (wt-%) [#]	1.05	2.01	0.59	0.64	1.61	1.55	1.39	0.46
MnO (wt-%)	0.02	0.03	0.02	0.02	0.02	0.03	0.03	0.02
MgO (wt-%)	0.31	0.65	0.11	0.47	0.50	0.45	0.55	0.28
CaO (wt-%)	0.54	3.16	0.29	0.78	0.96	1.02	0.82	0.41
Na2O (wt-%)	3.57	3.03	3.64	3.32	3.31	3.48	2.77	2.78
K2O (wt-%)	5.13	4.92	5.13	5.29	5.31	5.06	5.68	5.95
P2O5 (wt-%)	0.08	0.31	0.09	0.26	0.26	0.25	0.13	0.19
LOI (wt-%)	0.76	2.01	0.37	1.06	1.17	1.10	1.39	0.97
Total	100.94	100.60	100.94	100.36	100.14	100.00	100.05	99.99
Trace elements:								
Co (ppm)	2.1	5.3	0.5	3.4	3.5	3.0	3.7	1.7
Ni (ppm)	2.3	6.3	1.2	4.3	5.0	4.1	4.8	1.7
Cu (ppm)	2.2	14.9	7.3	5.1	5.7	11.7	6.9	9.5
Zn (ppm)	25.0	106.0	9.0	75.0	72.0	83.0	57.0	28.0
Ga (ppm)	18.0	26.7	12.8	27.2	27.8	28.5	21.3	28.8
Rb (ppm)	205.1	260.2	180.0	381.9	370.5	380.3	404.4	500.2
Sr (ppm)	160.4	97.7	136.8	68.1	71.5	79.0	102.5	65.7
Y (ppm)	7.4	17.0	2.9	8.7	9.7	9.7	17.5	11.8
Zr (ppm)	99.1	240.0	32.5	218.3	188.6	176.4	110.4	162.6
Nb (ppm)	4.4	6.4	3.5	8.6	4.2	4.3	12.6	10.2
Mo (ppm)	0.3	1.0	0.3	0.5	1.1	0.4	1.9	1.6
Cs (ppm)	7.9	5.5	5.6	9.1	4.8	6.7	12.5	20.1
Ba (ppm)	387.0	366.0	360.0	268.0	305.0	276.0	308.0	328.0
La (ppm)	34.60	75.20	3.50	52.70	56.90	54.10	24.60	54.40
Ce (ppm)	70.60	178.80	6.10	126.00	138.10	130.20	52.40	122.10
Pr (ppm)	7.84	21.33	0.68	15.12	16.45	15.18	5.93	13.06
Nd (ppm)	27.50	78.30	2.50	55.20	61.50	54.80	21.40	45.60
Sm (ppm)	5.46	14.35	0.54	9.79	11.13	9.93	4.27	7.95
Eu (ppm)	0.80	0.86	0.54	0.65	0.65	0.66	0.64	0.62
Gd (ppm)	3.71	8.14	0.36	5.46	5.83	5.39	3.64	4.48
Tb (ppm)	0.46	0.84	0.07	0.53	0.61	0.56	0.56	0.54
Dy (ppm)	1.85	3.47	0.39	2.31	2.40	2.18	3.12	2.28
Ho (ppm)	0.27	0.53	0.08	0.33	0.30	0.27	0.57	0.35
Er (ppm)	0.60	1.47	0.24	0.93	0.96	0.88	1.75	1.01
Tm (ppm)	0.05	0.20	0.04	0.12	0.10	0.11	0.23	0.13
Yb (ppm)	0.45	1.14	0.26	0.84	0.84	0.80	1.50	0.95
Lu (ppm)	0.07	0.17	0.05	0.11	0.10	0.09	0.21	0.13
Hf (ppm)	3.1	7.3	1.0	5.9	5.7	5.2	3.3	4.6
Ta (ppm)	0.3	0.4	0.6	0.5	0.4	0.4	2.5	1.1
Pb (ppm)	13.1	11.7	7.1	4.3	8.6	8.1	15.6	18.8
Th (ppm)	19.5	55.9	1.2	37.8	38.5	38.3	12.8	37.6
U (ppm)	3.9	14.8	8.9	4.6	8.2	14.5	4.1	5.0
Li (wt-%)	0.002	0.007	0.001	0.005	0.005	0.006	0.004	0.002
V (ppm)	19.0	40.0	17.0	18.0	19.0	17.0	21.0	18.0
As (ppm)	0.5	0.5	1.2	<0.5	<0.5	0.8	3.1	5.3
Ag (ppm)	0.1	0.1	0.1	<0.1	<0.1	<0.1	<0.1	<0.1
Sn (ppm)	8.0	5.0	9.0	8.0	7.0	9.0	12.0	17.0
Sb (ppm)	0.1	0.1	0.1	<0.1	<0.1	<0.1	0.2	0.2
W (ppm)	0.8	1.1	3.1	1.2	1.2	0.8	2.0	5.1
Bi (ppm)	0.1	0.3	0.4	0.3	0.3	0.4	9.1	1.6
Cd (ppm)	0.2	0.1	0.1	<0.1	<0.1	<0.1	<0.1	<0.1
Au (p.p.b.)	0.5	0.5	0.5	<0.5	<0.5	<0.5	0.5	<0.5
Se (ppm)	0.5	0.5	0.5	<0.5	<0.5	<0.5	<0.5	<0.5
Hg (ppm)	0.0	0.0	0.0	<0.01	<0.01	<0.01	<0.01	<0.01
Be (ppm)	4.0	7.0	6.0	14.0	7.0	5.0	8.0	4.0

Sample	587078	592011
Group name	Caledonian granite	Caledonian granite
Rock name *	granite	granite
Collector §	DRO	MBJ
Year	2022	2022
Latitude (N)	73.7556	73.8481
Longitude (W)	-22.6011	-22.9187
Locality	Blokadedal	Dybendal
Major elements:		
SiO2 (wt-%)	73.60	74.35
TiO2 (wt-%)	0.18	0.02
Al2O3 (wt-%)	14.43	14.15
Fe2O3T (wt-%)	1.37	0.57
FeO (wt-%) #	1.01	
MnO (wt-%)	0.03	0.03
MgO (wt-%)	0.22	0.09
CaO (wt-%)	0.86	0.78
Na2O (wt-%)	3.60	4.19
K2O (wt-%)	5.90	5.63
P2O5 (wt-%)	0.15	0.10
LOI (wt-%)	0.47	0.74
Total	100.81	100.65
Trace elements:		
Co (ppm)	1.4	0.6
Ni (ppm)	1.9	1.7
Cu (ppm)	43.8	3.1
Zn (ppm)	28.0	4.0
Ga (ppm)	24.5	13.4
Rb (ppm)	284.5	304.7
Sr (ppm)	196.3	63.1
Y (ppm)	11.0	3.9
Zr (ppm)	103.0	17.9
Nb (ppm)	12.2	4.6
Mo (ppm)	0.5	1.0
Cs (ppm)	6.1	8.1
Ba (ppm)	424.0	359.0
La (ppm)	28.80	0.70
Ce (ppm)	60.10	0.80
Pr (ppm)	6.50	0.07
Nd (ppm)	23.60	0.40
Sm (ppm)	4.00	0.20
Eu (ppm)	0.65	0.20
Gd (ppm)	2.80	0.28
Tb (ppm)	0.41	0.07
Dy (ppm)	2.22	0.59
Ho (ppm)	0.38	0.11
Er (ppm)	1.08	0.42
Tm (ppm)	0.15	0.07
Yb (ppm)	0.93	0.66
Lu (ppm)	0.17	0.12
Hf (ppm)	3.9	1.1
Ta (ppm)	1.4	1.7
Pb (ppm)	21.0	10.8
Th (ppm)	12.3	1.4
U (ppm)	10.8	2.2
Li (wt-%)	0.003	<0.001
V (ppm)	9.0	<8
As (ppm)	0.6	<0.5
Ag (ppm)	<0.1	<0.1
Sn (ppm)	4.0	6.0
Sb (ppm)	<0.1	<0.1
W (ppm)	<0.5	0.5
Bi (ppm)	0.1	0.4
Cd (ppm)	0.1	<0.1
Au (p.p.b.)	<0.5	1.0
Se (ppm)	<0.5	<0.5
Hg (ppm)	<0.01	<0.01
Be (ppm)	6.0	36.0

* Plutonic rocks classified after Middlemost (1985); volcanic rocks classified after Pearce et al. (1996)
§ TFK = T.F. Kokfelt; DRO = Diogo Rosa; NJB = N.J. Baker; PGUA = P. Guarnieri; MBJ = M. Bjerager
# FeO determined by titration

Discussion based on total geochemical dataset

All the figures in the following section depict the new analyses together with the analyses presented in Thrane et al. (2021) and are here referred to as 'the total geochemical dataset'. In general, the same plot symbology is used as in Thrane et al. (2021), except for one new plot group of Devonian rhyolites that are identified as being altered (see below). These altered rhyolites are shown as green open triangles and are shown by a light green color in Table 1.

Rock alteration

The possibility of metasomatic alteration, which would affect the mobile element systematics, was briefly assessed using the Hughes (1973) diagram (Figure 3) which plots K_2O+Na_2O vs. $K_2O/(K_2O+Na_2O)$. This shows that the majority of the analysed samples falls within the igneous spectrum and can therefore be considered unaltered or weakly altered. However, the Caledonian monzonites and Devonian rhyolites plot in the field of potassic alteration. As a result, further petrography is warranted to evaluate whether the high potassium contents of these rocks are primary or secondary, and their characterisation using mobile major element plots needs to be done cautiously and supplemented with information from immobile trace elements. Several of the granitic and rhyolitic rock samples were collected where the radioactivity was high due to uranium mineralisation in fractures and hydrothermally altered rocks. A group of Devonian rhyolites from 'OK-fjeld' in Moskusokselandet are also seen to be potassic altered plotting in the lower right-hand corner of the diagram.

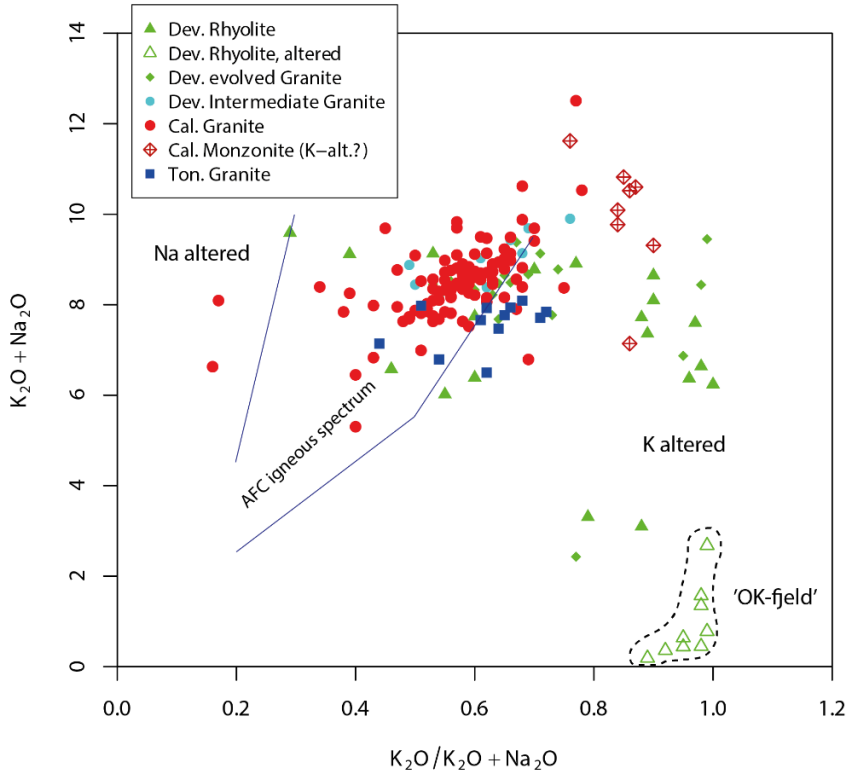

Figure 3: *Alteration diagram after Hughes (1973) plotting K_2O+Na_2O vs. $K_2O/(K_2O+Na_2O)$.*

Rock classification and tectonic setting

Major elements

Major element geochemistry of granitic rocks from Hudson Land, Gauss Halvø and Clavering Ø has been arranged according to the classification scheme of Frost et al. (2001). This scheme is based on three variables: Fe-number, modified alkali-lime index (MALI) and aluminum saturation (Figure 4a-c). The Caledonian monzonite samples stand out by being intermediate (SiO_2 = 53-61 wt.%), metaluminous, magnesian and alkalic in composition. According to Frost et al. (2001), granitoids with these characteristics are formed in plutons inboard from Cordilleran batholiths, with the Yamato Mountains, in Antarctica, as a possible analogue (Zhao et al., 1995). As such, these monzonites are interpreted to reflect a magmatic arc stage. This contrasts with the remaining samples (Tonian and Caledonian granites, and Devonian granitoids), which are more evolved (SiO_2 > 67 wt. %), particularly some of the Devonian granitoids that stand aside by being peraluminous (Figure 4c), magnesian to ferroan (Figure 4a) and calc-alkalic to alkali-calcic compositions (Figure 4b) with only a few outliers in the calcic or alkalic fields.

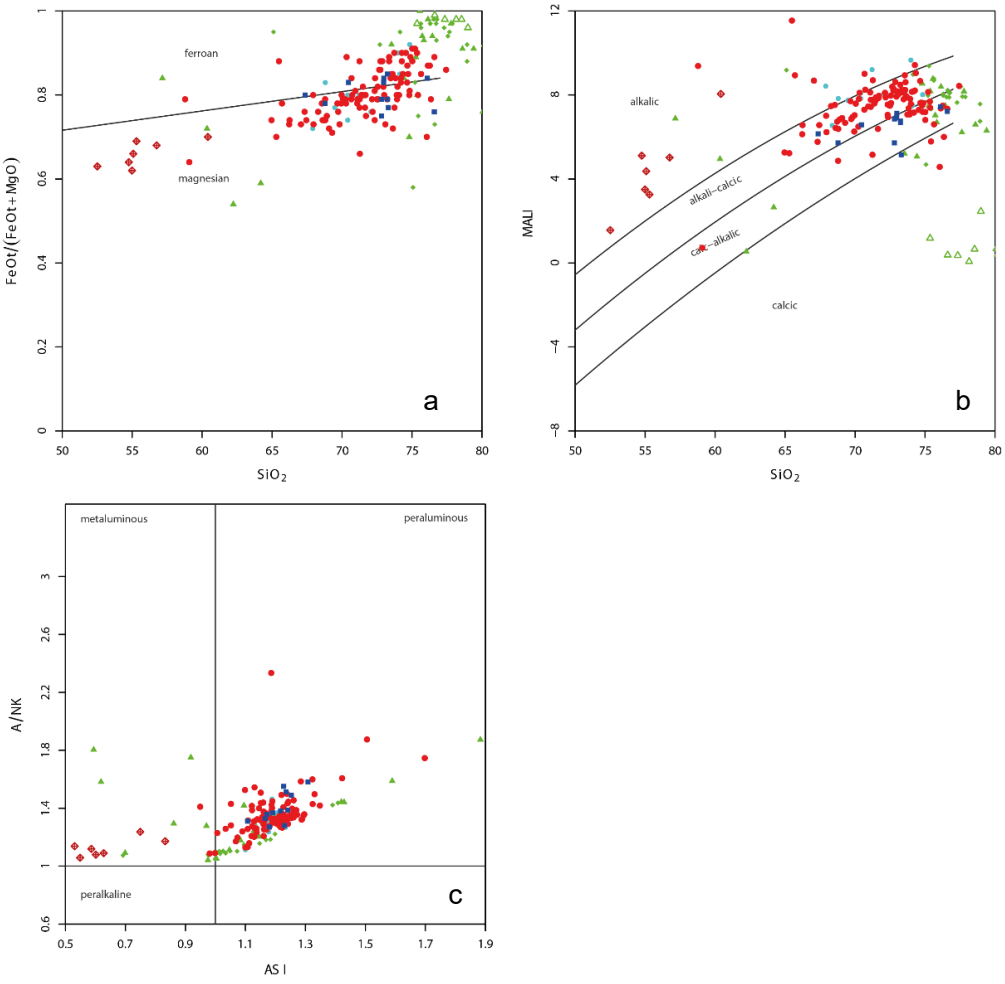

Figure 4: *Classification scheme after Frost et al. (2001) using (a) the three parameters Fe-number, (b) modified alkali-lime index (MALI) and (c) aluminium saturation index. Symbols as in Figure 3.*

Furthermore, the Tonian granites appear to be more calcic than the Caledonian granites. It is presently unclear whether intermediate compositions of Caledonian age are missing in the study area or whether this merely reflects a sampling bias in our compilation. If intermediate compositions indeed are lacking, the remaining samples can be grouped as peraluminous leucogranites that are typical of a syn-collisional stage (Frost et al. 2001). In terms of the classification by Chappel & White (1974), the Caledonian monzonite would classify as I-type, inferred to have formed from a meta-igneous source, in contrast with remaining analysed samples which would classify as S-type, inferred to have formed from melting of metasedimentary rocks.

Further insights into the major element geochemistry can be obtained using the Grebennikov (2014) ternary diagram (Figure 5). This diagram is used for samples with >67% SiO_2 and therefore does not include any of the Caledonian monzonite samples. The diagram suggests a distinction between Caledonian and Devonian granitoid samples, particularly the more evolved ones. The Caledonian granites plot mostly outside the A-type granitoid fields, which is typical of arc and syn-collisional granites, while the Devonian granitoids are centered within the A2 field. According to Grebennikov (2014), rocks plotting in the latter field are formed during post-collisional rifting caused by extension and thinning of continental crust, namely as a result of oblique convergence. The Tonian granite is not clearly classified in this diagram but could also be post-collisional (Figure 5).

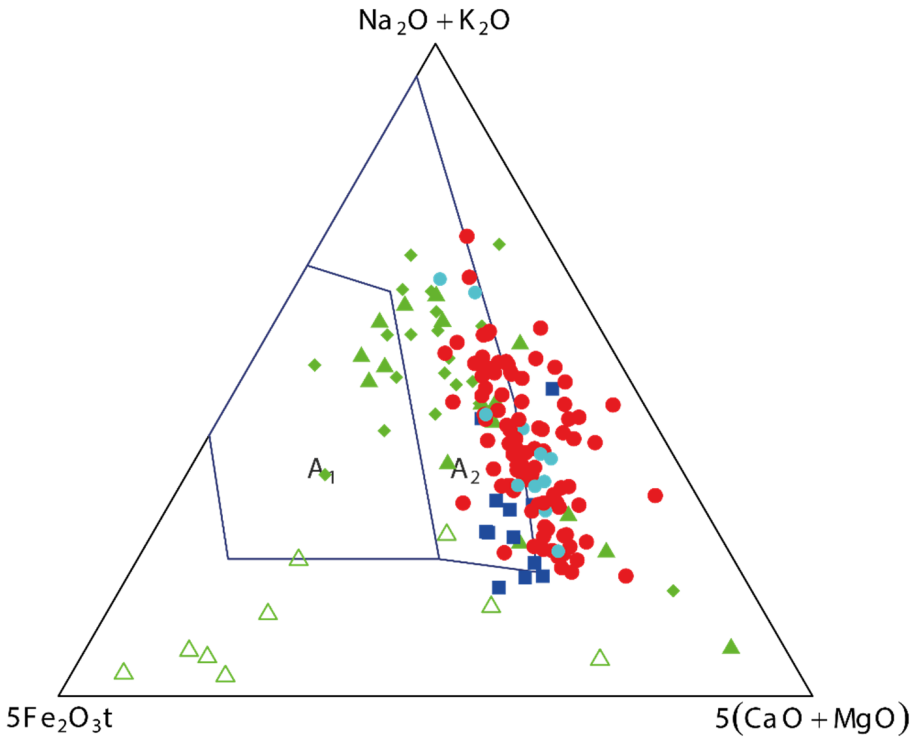

Figure 5: *Ternary diagram of Grebennikov (2014) plotting Fe_2O_3x5 – Na_2O+K_2O – (CaO+MgO)x5 to distinguish different A-type magmas (only SiO_2 > 67 wt% plotted). A1: within-plate geodynamic setting, oceanic islands, and continental rifts. A2: local extension zones of intracontinental and continental marginal areas. Symbols as in Figure 3.*

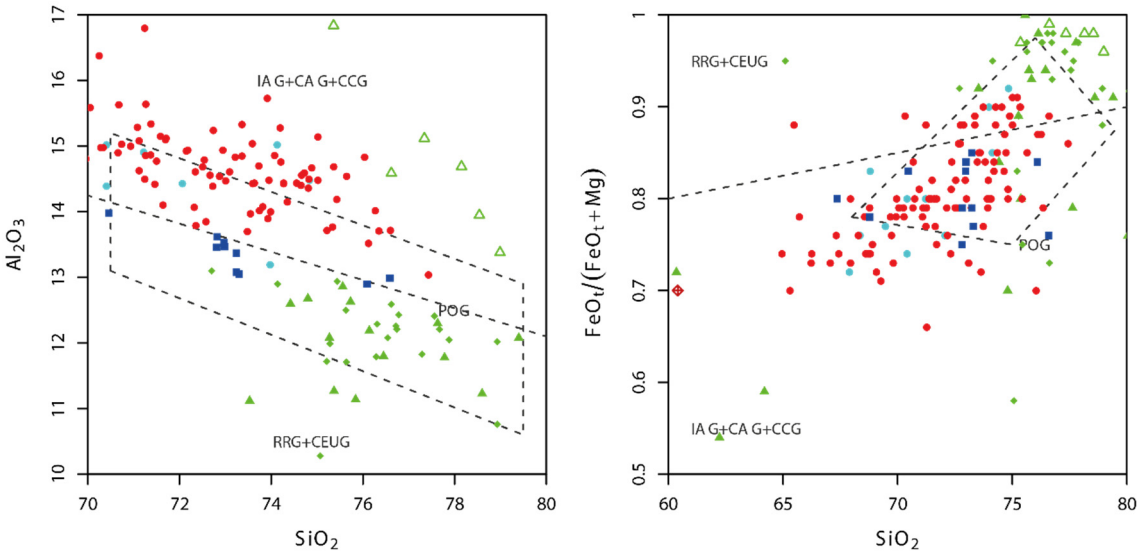

Figure 6: *Geotectonic scheme of Maniar & Piccoli (1989) plotting SiO_2 – Al_2O_3 and SiO_2 – $FeOt/(FeOt+MgO)$. IAG: island arc granitoids, CAG: continental arc granitoids, CCG: continental collision granitoids, POG: postorogenic granitoids, RRG: rift-related granitoids, and CEUG: continental epeirogenic uplift granitoids. Symbols as in Figure 3.*

The SiO_2-Al_2O_3 and SiO_2-$FeO_t/(FeO_t+MgO)$ diagrams of Maniar & Piccoli (1989) highlight both the Tonian and Devonian evolved granitoids as post-orogenic (Figure 6a,b) e.g. from two different events.

Trace elements

The distinct geochemistry of the more evolved Devonian rocks is also apparent on the Whalen et al. (1987) and Pearce et al. (1984) diagrams using trace elements that are considered fluid-immobile and therefore robust with respect to seeing through alteration processes.

On the Whalen et al. (1987) diagrams, utilising trace elements Nb, Y and Ce vs. Ga/Al (Figure 7a,b), the Devonian evolved granites have high Ga/Al ratios and high Nb, Y (especially), but also Ce concentrations, that distinguish them from all of the other analysed rocks, and are characteristic of A-type granitoids. As further defined by Grebennikov (2014), A-type granitoids can be subdivided into peralkaline (A1) and peraluminous (A2), reflecting distinct geotectonic settings, and the studied Devonian evolved granite belongs to the latter group (Figure 7).

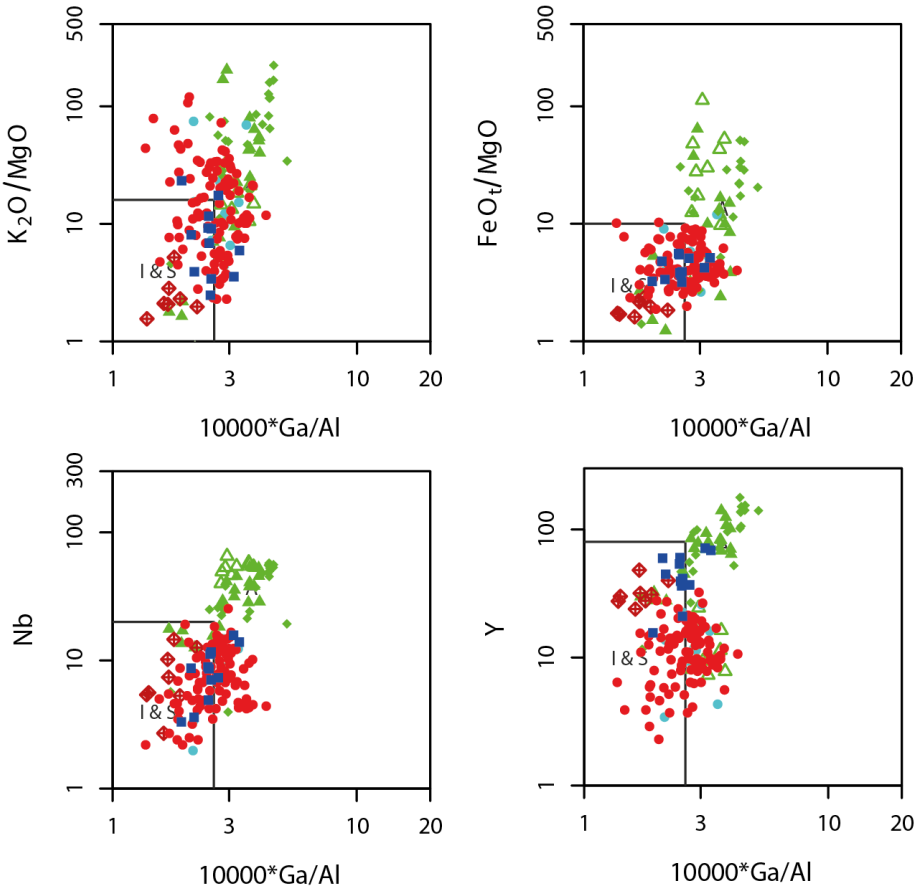

Figure 7: *Whalen et al. (1987) diagrams plotting K2O/MgO, FeOt/MgO, Y and Nb vs. Ga/Al. The boxed field marked 'I & S' represents the compositional field of I- and S-type granitoids according to the definition of White & Chappell (1977), while A-type granitoids occupy the area outside the box. Symbols as in Figure 3.*

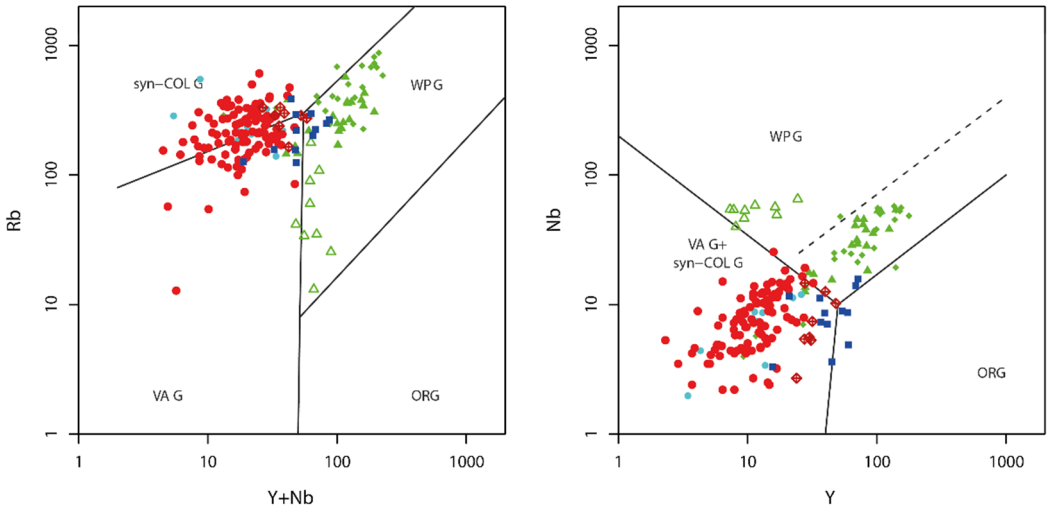

Figure 8: *Geotectonic discrimination diagrams after Pearce (1984) plotting Rb vs. Y+Nb and Nb vs. Y. Symbols as in Figure 3.*

On the Pearce et al. (1984) diagrams (Figure 8), the Devonian evolved granites clearly plot in the within-plate field. The remaining analysed rocks tend to plot in the volcanic arc and/or syn-collisional fields, the Caledonian monzonites tendentially in the volcanic arc field, while the Caledonian granites are straddling the volcanic arc - syn-collisional boundary. The Tonian granites plot across different fields, which possibly reflects the influence of a variety of sources typical of post-collisional granitoids.

Figure 9 & 10 present chondrite-normalised rare earth element (REE) and extended primitive mantle-normalised trace element plots, respectively. In the REE-diagrams (Figure 9) the evolved Devonian group stands out as by a moderate LREE enrichment, relatively flat, elevated heavy (H)REE patterns, and deep negative Eu-anomalies, the latter signifying extensive plagioclase fractionation to have played a role. The group of Devonian volcanic rocks from 'OK-fjeld' that were identified in Figure 3 as being K altered have also unusually low MREE concentrations. This 'depressed' REE pattern is interpreted to reflect preferential loss of MREE during intense alteration that these rocks underwent. The Caledonian granites show comparatively more variation and have steeper LREE/HREE slopes and less distinct negative Eu-anomalies, occasionally positive in a few samples. The intermediate Devonian granites overlap completely with the Caledonian granites. The Tonian granites have intermediate patterns relative to the Caledonian and Devonian granites.

In the multi-element diagrams (Figure 10) the three main groups also stand apart. Again, the evolved Devonian granites show the most extreme 'saw-tooth' patterns with strong negative anomalies for Ba, Sr, P, and elevated contents of Nb + HREE+Y. The Caledonian granites + intermediate Devonian granites show a relatively wide and scattered range with generally higher Ba and Sr and lower HREE+Y. The identifiably altered rhyolites show comparative depletions in LILE (Cs, Rb, Ba) + MREE. The Tonian granites show a comparatively restricted intermediate range between the other two groups.

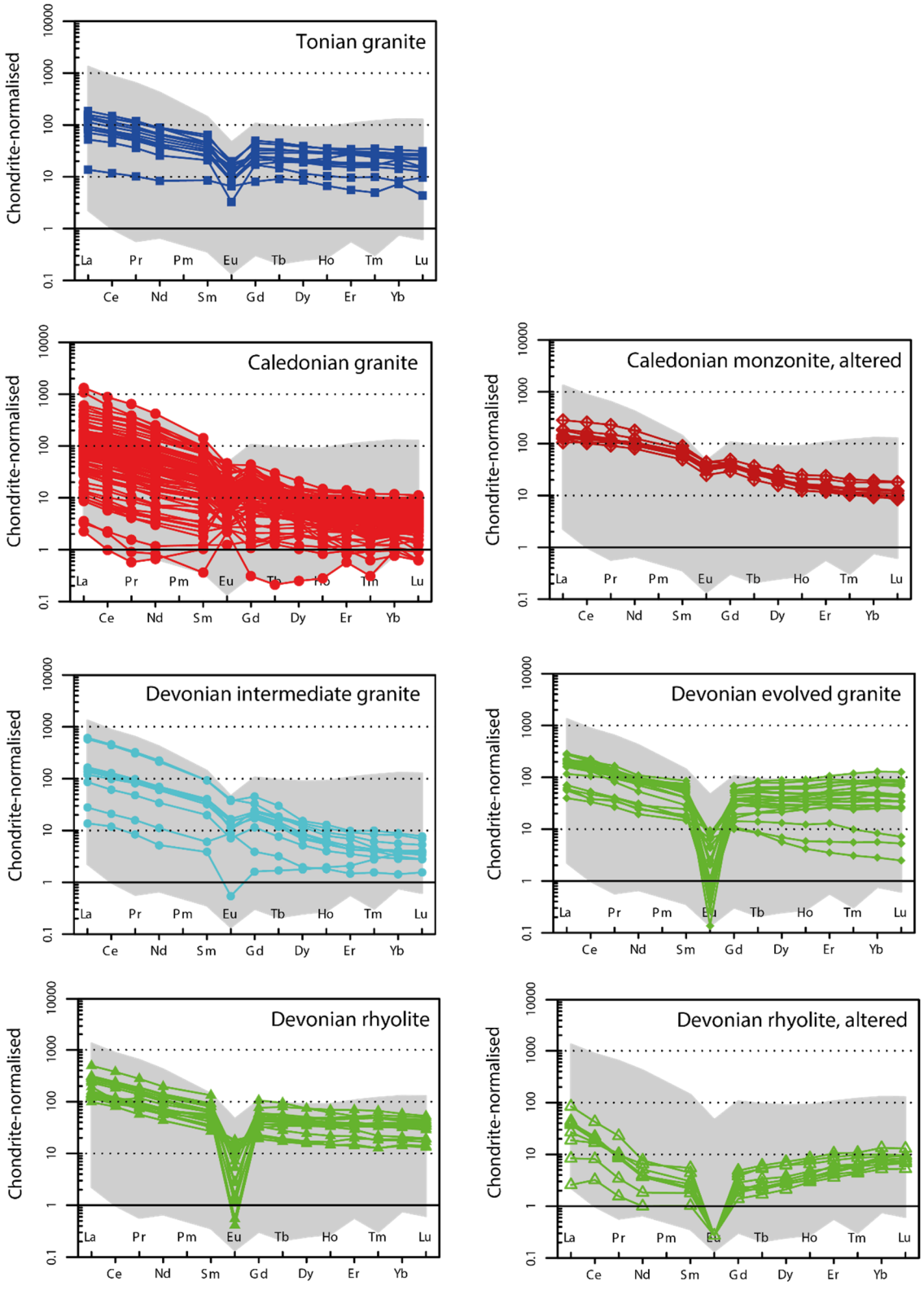

Figure 9: *'Spider' diagrams for the East Greenland granitoid samples showing concentrations of rare earth elements (REE) normalised to chondrite (Boynton 1984). Symbols as in Figure 3.*

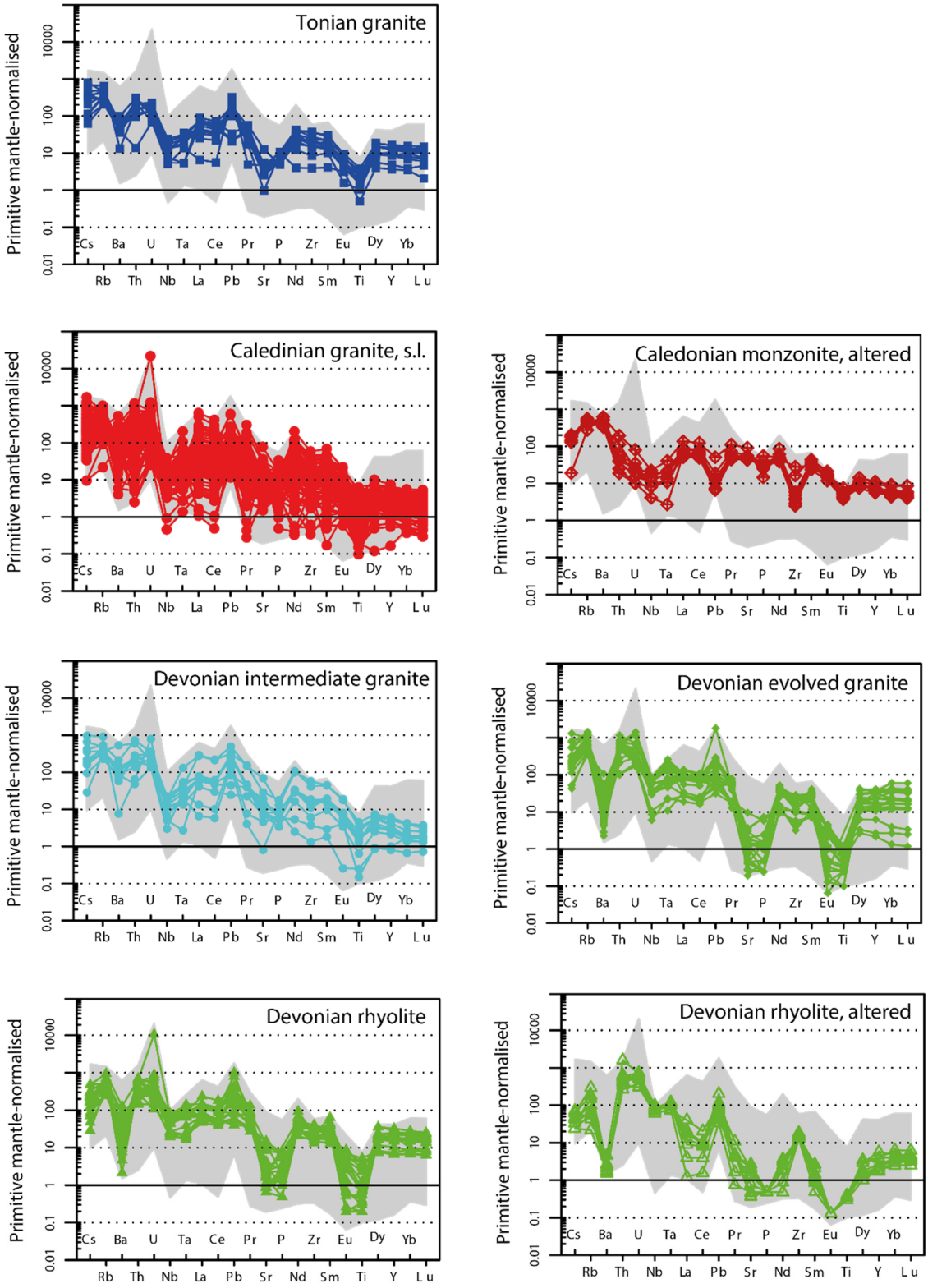

Figure 10: *'Spider' diagrams for the East Greenland granitoid samples showing multi-element concentrations normalised to primitive mantle (McDonough & Sun 1995). Symbols as in Figure 3.*

In summary, the studied rocks appear on geochemical grounds to record different geotectonic settings. The geochemical signature of the Tonian granites is generally similar to that of the Caledonian granites, with the noticeable exception of the Tonian granites having consistently higher FeOt and lower Al_2O_3 compared to the Caledonian granites (Figure 6 and 7a), which suggests different sources for these two rock groups. Despite the limited number of Tonian granites analysed, they do form a rather tight group that seems to be consistent with a post-collisional setting in an Early Neoproterozoic (Grenvillian) orogeny (Figure 7). For the Caledonian orogeny, it is suggested that the Caledonian monzonites formed during the magmatic arc stage, that the Caledonian granites mainly formed during the syn-collisional stage and, finally, the Devonian evolved granitoids already reflect a post-collisional rift stage. The Devonian intermediate granites consistently plot together with the Caledonian granites, and it is therefore suggested that the former should potentially be considered part of the latter, and the classification used in the Haller (1971) map should be reevaluated. Alternatively, the indicated change of tectonic setting took place during the Devonian. In the latter option, it is hypothesised that the Devonian intermediate granite could be Early Devonian, formed during the syn-collisional stage, while the Devonian evolved granitoids could be Late Devonian, formed during the subsequent post-collisional stage.

Magma fertility

Empirical and theoretical evidence support a strong correlation may exist between the granites composition and metal association in related mineralisation (Blevin & Chappell 1992, 1995; Meinert 1992). According to these authors, the parameters that control fertility of a granite magma (i.e., its mineralization potential), include magma geochemistry (e.g., S-, I- or A-type), evolutionary stage and oxidation state. Figure 11 plots K/Rb vs. SiO_2 and shows that the studied granitoids range from moderately to strongly differentiated, with some of the Devonian granitoids being particularly fractionated with SiO_2 >75 wt% and low K/Rb ratios (<250). This suggests that these rocks can be associated with Mo-W-Sn mineralisation. Which of these metals that will dominate depends on the magma oxidation state, which is essentially inherited from its source, although the effects of wall rock interaction can be locally important. In reduced S-type magmas, such as the studied Caledonian and Devonian granitoids, Sn and (to a lesser degree) W both behave incompatibly and build up in the magma during differentiation.

Figure 12 plots Fe_2O_3/FeO vs. Rb/Sr and shows that Tonian and Caledonian granites are indeed relatively reduced and would be favorable to host W and Sn-W mineralisation. These would be core element associations, i.e., the most intrusion-proximal element association, but base metal, precious metal and U-F mineralisation can be expected to be found more distally to the intrusion.

In contrast, Devonian rhyolites and some evolved Devonian granites (sample 567203 and 567235 from Högboms Bjerg) display high oxidation states (Figure 12). This is interpreted to reflect magma oxidation during shallow emplacement within oxidising wall rocks and/or subsequent rock oxidation due to alteration or weathering. This is supported by the fact that possible secondary processes were already highlighted (Figure 3) to have been potentially important for these rocks.

When plotted on a diagram of Ba/Th vs. La/Sm by Li et al. (2017) (Figure 13), the Devonian evolved granitoids plot in the field of the Yanshanian granite related to Sn and W deposits, while the Caledonian granites and Devonian intermediate granites plot in the field of the Yanshanian granite related to W and base metal deposits, which these authors interpret to reflect relatively lower and higher magma oxidation, respectively.

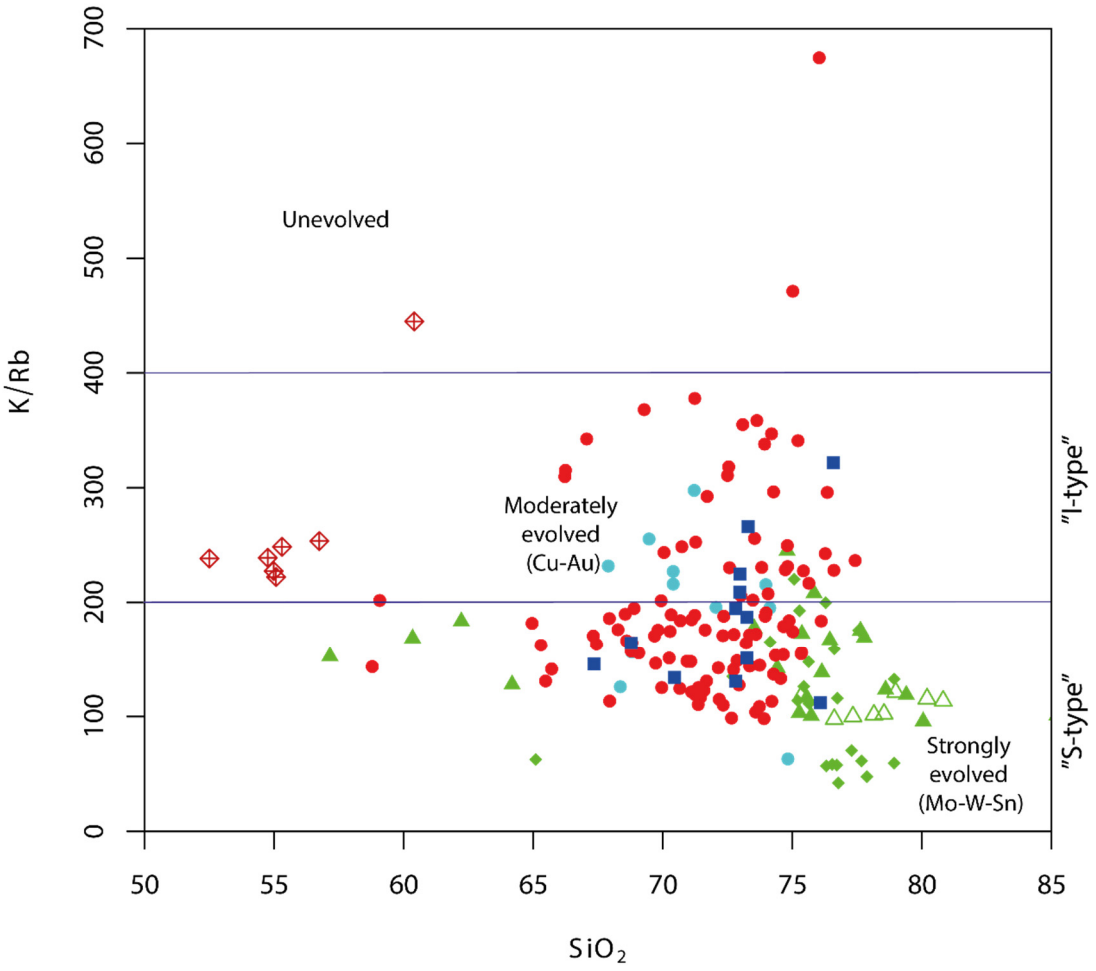

Figure 11: *K/Rb – SiO_2 after Blevin & Chappell (1992, 1995) showing granite types and their typical associated mineralisation. Symbols as in Figure 3.*

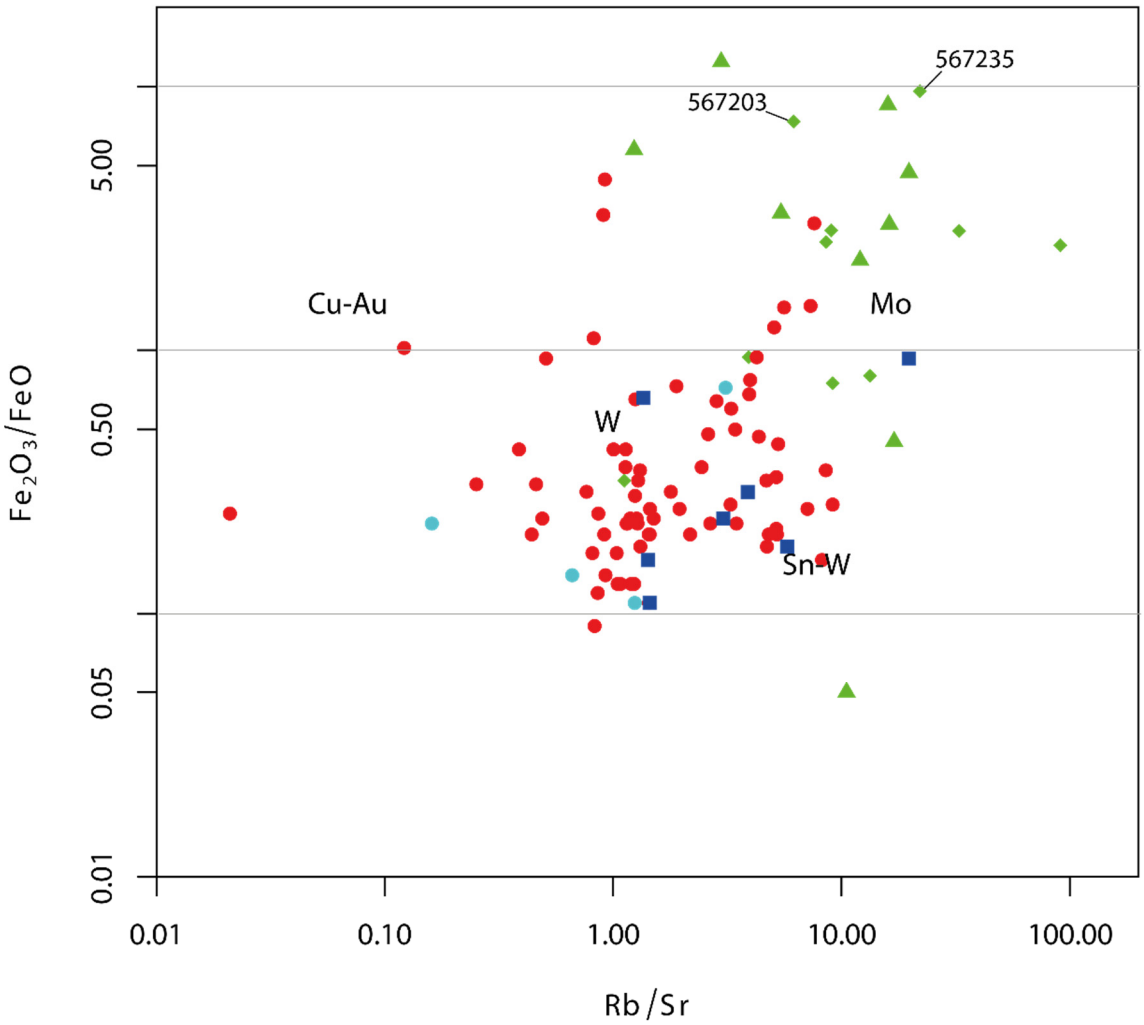

Figure 12: *Fe_2O_3/FeO – Rb/Sr after Blevin & Chappell (1992, 1995) with fields for associated mineralisation type. Note high Fe_2O_3/FeO in Devonian granite samples (567203 and 567235) from Högboms Bjerg. Symbols as in Figure 3.*

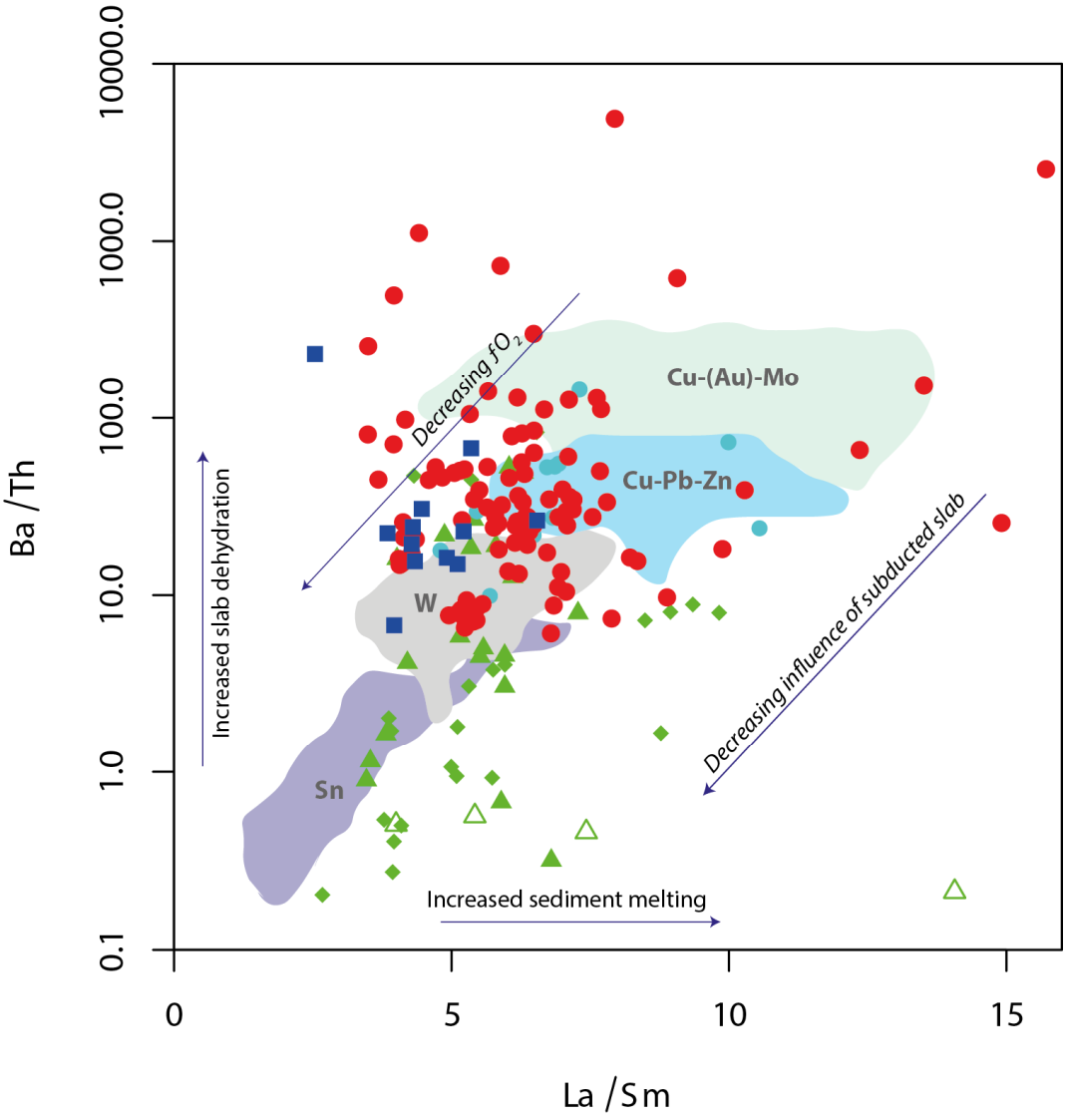

Figure 13: *Ba/Th - La/Sm after Li et al. (2017) used to discriminate the mineralisation potential of granite magmas as function of oxidation state and slab contribution. The coloured fields reflect Yanshanian granite samples hosting Sn, W and base metal deposits. Symbols as in Figure 3.*

It should be noted that magma fertility, *per se*, does not predict whether a given granitoid is mineralised. In addition to the magma fertility, assessed through the geochemistry, physical parameters such as the level of magma emplacement, erosional level and volatile content need to be considered for a more complete evaluation. In any case, the Caledonian and Devonian granitoids studied can be considered favourable for W and Sn mineralisation. The Devonian evolved granitoids, in particular, have undergone extensive fractionation during which Sn, W and other metals could have built up in the relatively reduced magma. Moreover, the occurrence of cassiterite and W-mineralisation associated with several Devonian granites in Central East Greenland (see Keulen et al. 2023, and references therein) verifies that this process indeed was operating.

Geochronology results

523813 – Augen granite (Tonian)

Clavering Ø: 74.35826 N, 21.03908 W

Description: Large outcrop of very coarse-grained augen granite, intruded into the Krummedal Supracrustal Sequence and forming a mountain top to the west of Skille Gletsjer. Individual K-feldspar augens are up to 7 cm long (Figure 14).

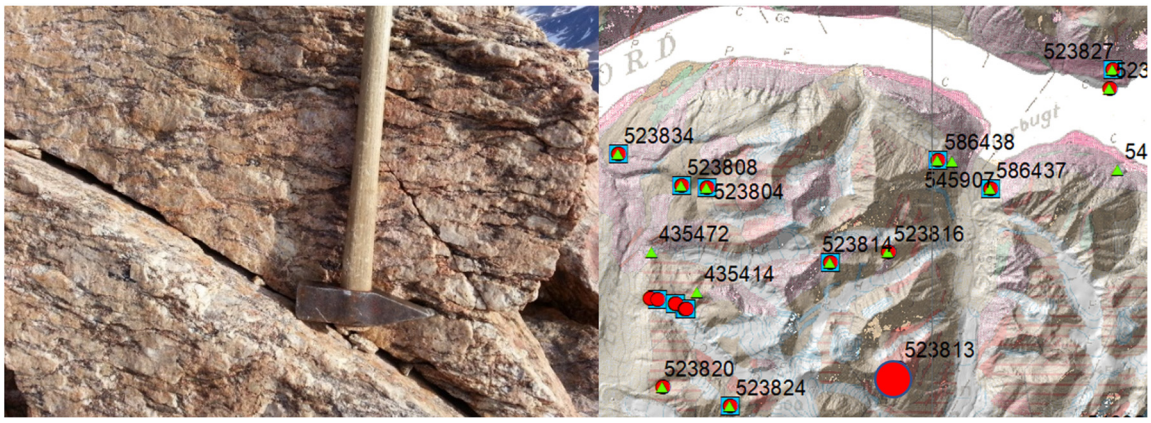

Figure 14: *Outcrop of very coarse-grained granitic gneiss, sample 523813, from Northern Clavering Ø.*

Zircon morphology: The zircons are subhedral and elongated. They generally range from 100-200 µm, a few grains are larger. Most zircons show oscillatory zonation and have what looks like several generations of zonation. The zircons are generally well preserved, but some grains do show irregular zonation in the cores, possibly reflecting recrystallisation.

Zircon data: 38 analyses were carried out. The ages cluster around c. 430 and 950 Ma, and a few older ages are also present. A discordia line through the main cluster yield an upper intercept age of 963 ± 16 Ma and a lower intercept age of 432 ± 27 Ma (MSWD = 3.2, n= 31) (Figure 15). The ages are interpreted as crystallisation and metamorphic overprint ages, respectively.

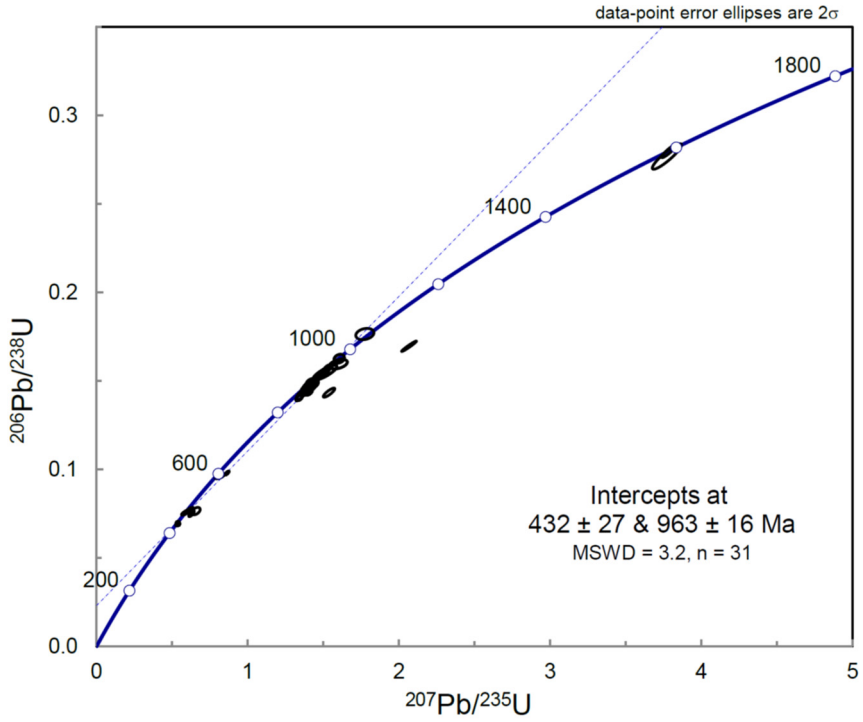

Figure 15: *Sample 523813, very coarse-grained augen granite, giving a upper intercept age of 963 ± 16 Ma (Tonian) and a lower intercept of 432 ± 27 Ma (Silurian) (MSWD = 3.2, n = 31/54), corresponding to time of crystallisation and metamorphism, respectively.*

521688 – Augen granite (Tonian)

Clavering Ø: 74.2546 N, 20.8377 W

Locality: Eastern side of central Clavering Ø, west end of E-W valley west of Camp 3 (Kokfelt 2019).

Description: Strongly deformed Kfsp augen granite (gneiss) with up to very large (<7 cm), often deformed K-feldspar megacrysts in a coarse-grained granitic matrix (Figure 16).

Zircon morphology: Subhedral to anhedral rounded, stubby or prismatic grains, usually about 70-120 µm with aspect ratios of 1:2 - 1:3. Most grains show remnant complex oscillatory zoning, often with more diffuse patchy domains. Some grains show distinct CL-bright cores.

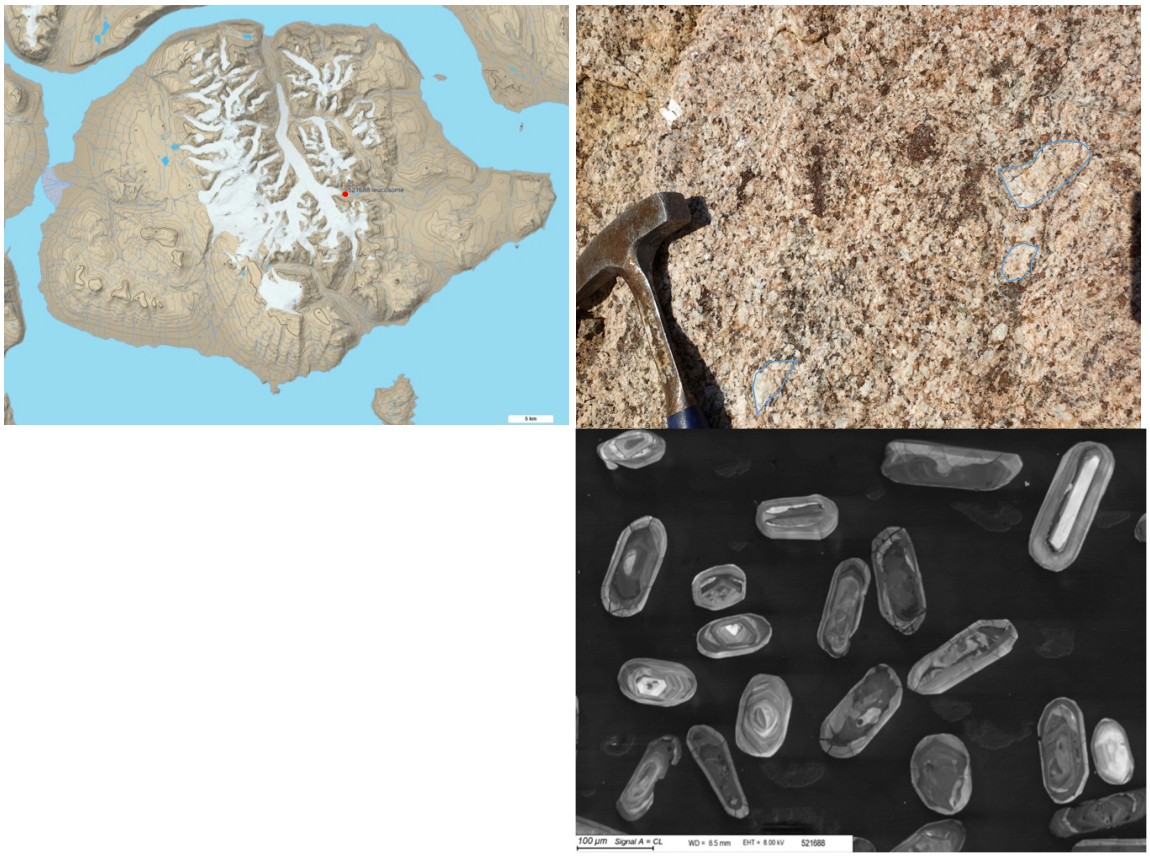

Figure 16: *Sample 521688 of a very coarse-grained augen granite. Notice the deformed megacrystic K-feldspar augens (annotated on photo). CL-image: Zircons are rounded, stubby or prismatic, occasionally showing oscillatory zoning, or more diffuse or patchy zoning.*

Zircon data: A total of 144 spots were analysed of which 60 returned acceptable data, the remaining 84 represented poor analyses or had issues with cPb. A main population of zircon have ages of around 900-930 Ma, among these a subset of 95-105% concordant grains yields a plateau $^{238}U/^{206}Pb$ age of 915 ± 7 Ma (MSWD = 1.6, n = 23) (Figure 17). This age is interpreted as the crystallisation age of the gneiss protolith. Three younger discordant grains are likely to record Pb-loss, likely reflecting overprinting during Caledonian metamorphism (not possible to constrain further). Seven older partially discordant grains record ages from ca. 1260 to 1740 Ma interpreted to reflect crustal inheritance.

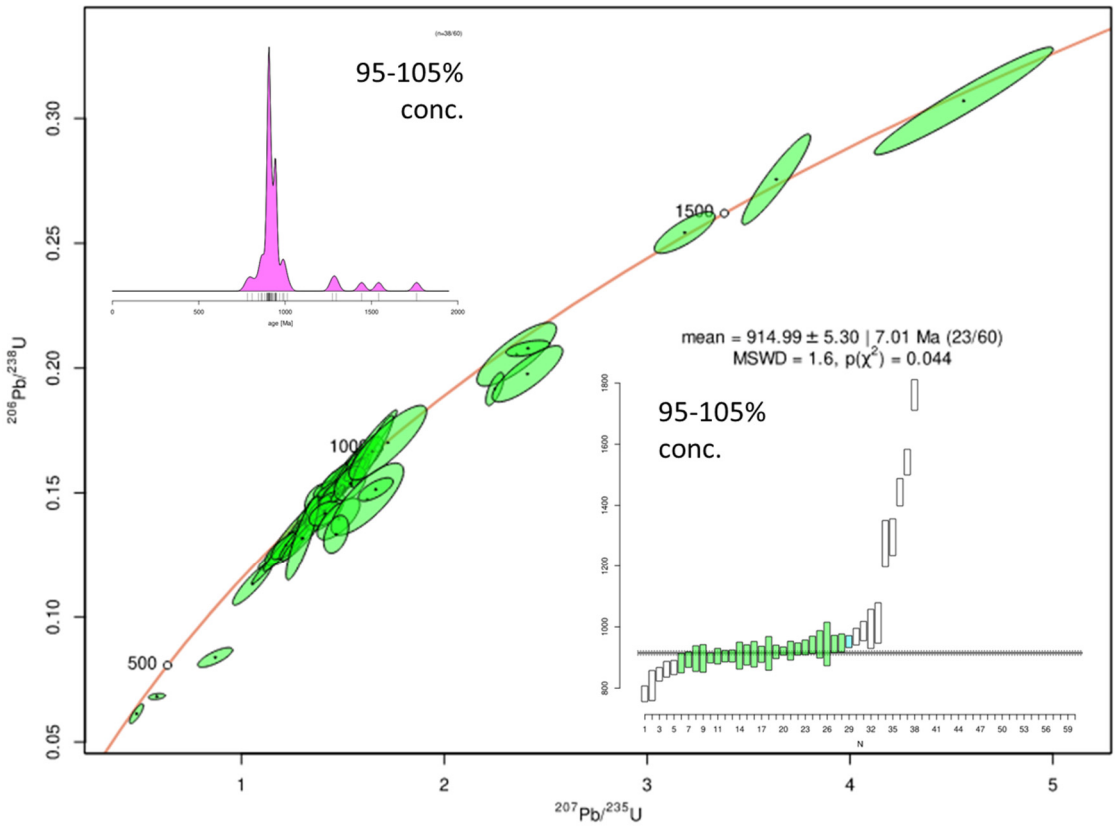

Figure 17: *Wetherill-Concordia plot for sample 521688. Insert diagrams for 95-105% concordant grains of adaptive KDE and weighted average plots. The main population gives an average plateau $^{238}U/^{206}Pb$ age of 915 ± 7 Ma (MSWD = 1.6, n = 23), interpreted as the crystallisation age of the gneiss protolith.*

521649 – Monzonite (Caledonian)

Clavering Ø: 74.3021 N, 21.4653 W
Locality: Western side of central Clavering Ø, ridge west of Camp 2 (Kokfelt, 2019).

Description: The rock is a medium-grained monzonite with ca 20% mafic minerals showing a clear foliation with a planar fabric underlined by alignment of the tabular Kfsp megacrysts and interstitial mafic aggregates of mainly amphibole crystals. The rock shows a distinct red colouring in the field and feldspars are generally quite turbid, which together with the abnormally high K whole-rock contents suggest significant deuteric alteration (K-alteration) (Figure 18). The intrusion was mapped as post-orogenic granite by Koch & Haller (1971). However, the distinct fabric indicates that the rock unit is clearly not post-orogenic but experienced orogenic deformation. The monzonite is associated with enclaves of more mafic (monzodioritic), or even ultramafic rocks, likewise deformed. The unit is cut by relatively undeformed later granitic veins and pegmatites.

Zircon morphology: Small (<100µm) rounded anhedral grains, showing dissolution textures and complex (multi-stage) zoning patterns, typically with very thin CL-bright rims (beyond targeting), interpreted reflecting metamorphic overprinting.

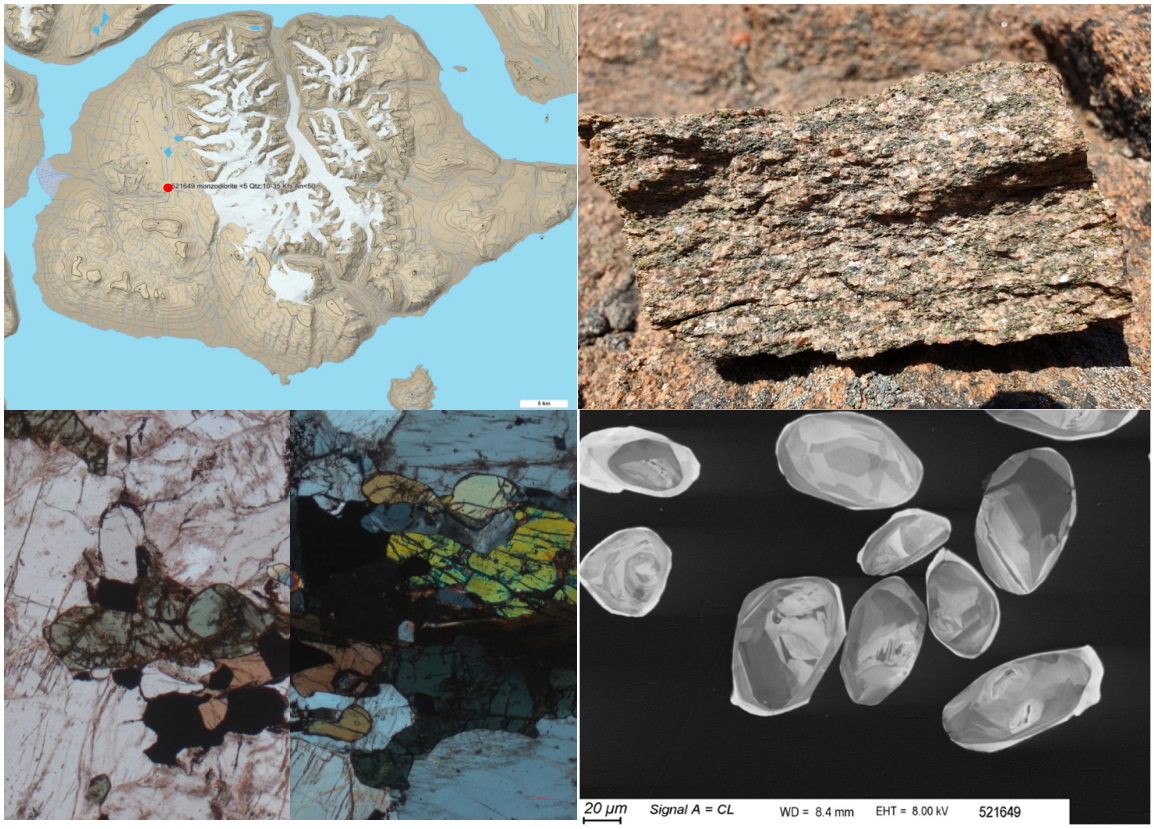

Figure 18: *Sample 521649 of coarse-grained monzonite from the western part of Central Clavering Ø. The rock shows a distinct red colouring in the field and feldspars are always turbid, which along with unusually high K whole-rock contents suggest significant deuteric alteration (K-alteration) of the rock.*

Zircon data: A total of 35 spots were analysed of which 27 returned acceptable data, three had some influence of cPb and five were bad. All accepted data are within 95-105 % concordant. A single population of 23 concordant zircons gives an isochron age of **446.3 ± 3.1 Ma** (MSWD = 0.42; n/N = 23/27) (Figure 19). A similar age within error is calculated as a weighted mean $^{238}U/^{206}Pb$ age of 446.9 ± 2.5 Ma (MSWD = 1.5; n/N = 23/27). This late Ordovician age is taken as the crystallisation age of the monzonite placing it before the main Caledonian metamorphism event at ca 430 Ma. The early Caledonian age agrees with the chemistry as an I-type granitoid, i.e., predating collision and crustal thickening. Noteworthy, there are no inherited grains, which is otherwise very common for typical Caledonian S-type granites.

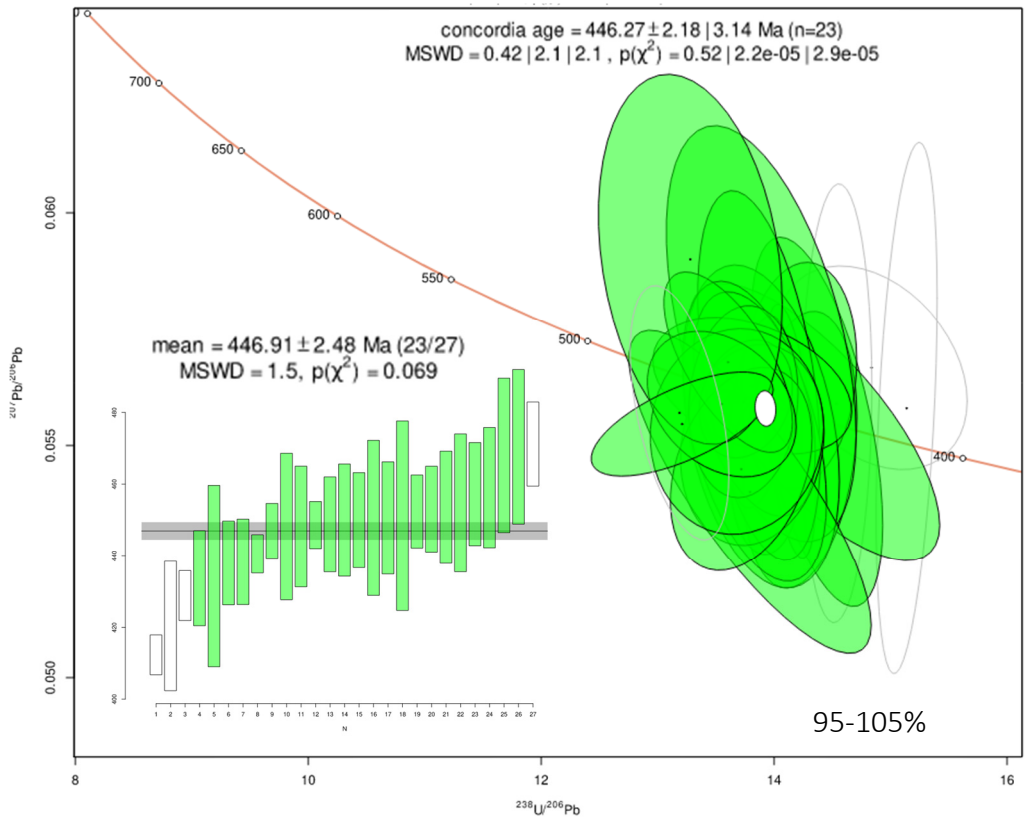

Figure 19: *Sample 521649. Terra-Wasserburg Concordia-diagram showing a preferred Concordia age of 446.3 ± 2.2 Ma (MSWD = 0.42; n/N = 23/27). The age is consistent with a weighted mean $^{238}U/^{206}Pb$ age of 446.9 ± 2.5 Ma (MSWD = 1.5; n/N = 23/27).*

523808 – Monzonite (Caledonian)

Clavering Ø: 74.41691 N, 21.30040 W

Description: The intrusion was mapped as post-orogenic granite by Koch & Haller (1971). Magmatic rock, relationship to the surrounding metasedimentary rocks is unclear, but the foliation is typically much less well developed in this rock type than in the surrounding metasedimentary rocks (Figure 20). Thin pink pegmatite veins intrude the monzonite, and it also contains lenses of deformed amphibolite. The sample contains 56.8 % SiO_2, 9.2 % K_2O and 1.6 % Na_2O and is classified as a monzonite in the alkali-silica diagram by Middlemost (1994) (Table 1).

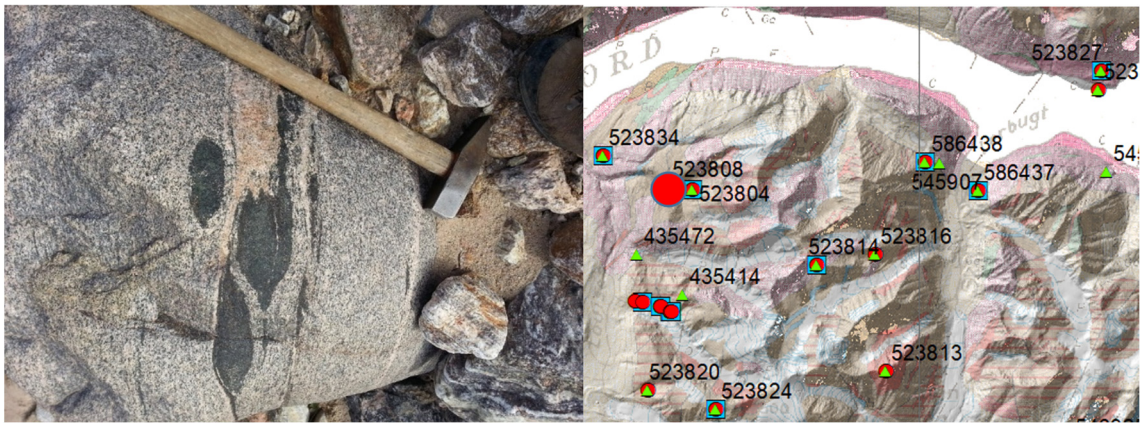

Figure 20: *Outcrop of foliated monzonite (grey), sample 523808, with amphibolitic inclusions, Northern Clavering Ø.*

Zircon morphology: The zircons are mostly stubby and subhedral. Most grains are from c. 75-150 µm long with a few larger grains. Some zircons show an oscillatory zonation, but most show a more disturbed pattern in the core, probably do to recrystallisation. In some cases, the grains have a homogenous rim with variable thickness.

Zircon data: 80 analyses were carried out. The ages range from 1637 to 398 Ma, with most ages between 500 and 400 Ma, with the main cluster at c. 450-410 Ma. A few older ages (>550 Ma) are interpreted as inherited. It is difficult to determine an exact crystallisation age, as the analyses all fall along the Concordia line, but we interpret the younger ages to be a consequence of Pb-loss, and it is therefore possible to retrieve an intercept age of **456 ± 9 Ma** (MSWD = 4.4, n = 68) when anchoring the lower intercept at 1 ± 10 Ma (Figure 21). The mean $^{238}U/^{206}Pb$ age yields a significant younger age of 426 ± 4 Ma (MSWD = 54), but has less statistical significance, due to the large scatter of $^{238}U/^{206}Pb$ ages. Due to the statistics and because the sample is deformed, the older ages seem more plausible. The age is within error the same as for monzonite sample 521649, which is from the same map unit, collected further to the south in Clavering Ø.

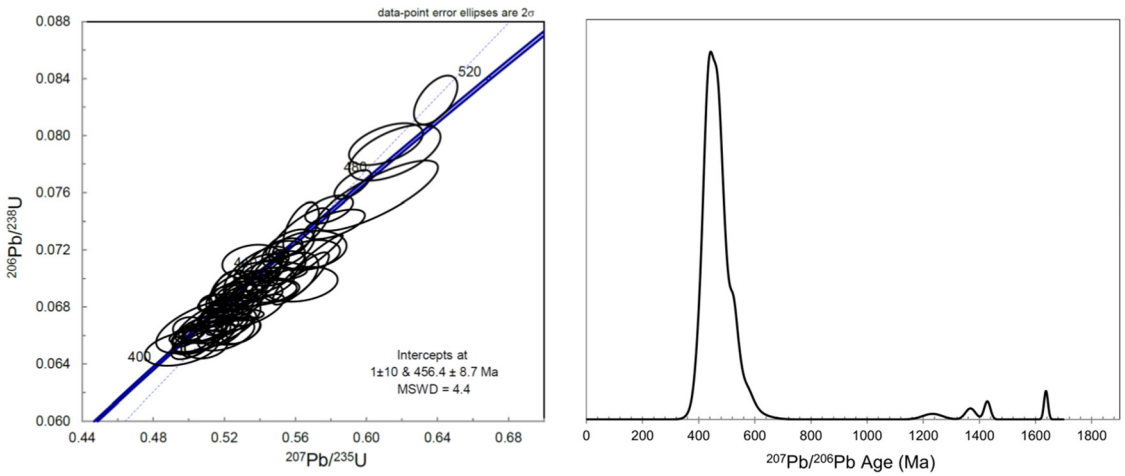

Figure 21: *Sample 523808, foliated monzonite, giving a rough upper Concordia intercept age of 456 ± 8.7 Ma (MSWD = 4.4). The sample contains a few inherited grains at 1250-1650 Ma.*

567268 – Porphyritic granite (Caledonian)

Storelv S: 73.66989 N, 22.32271 W

Description: Coarse-grained Kfsp porphyritic biotite-muscovite granite from the Storeelv area in SE Hudson Land (Figure 22). Geochemically the rock is classified as a quartz monzonite in the TAS-diagram. The porphyritic granite is locally cut by equigranular granite type. Both granite types are mappable units on the scale of mapping (1:100,000).

Zircon morphology: Subhedral to anhedral large prismatic or stubby grains (100-350 µm) with aspect ratios of 1:2 - 1:4, many showing oscillatory zoning, or complex multi-stage zoning with relict cores overgrown by magmatic zircon mantles and rims.

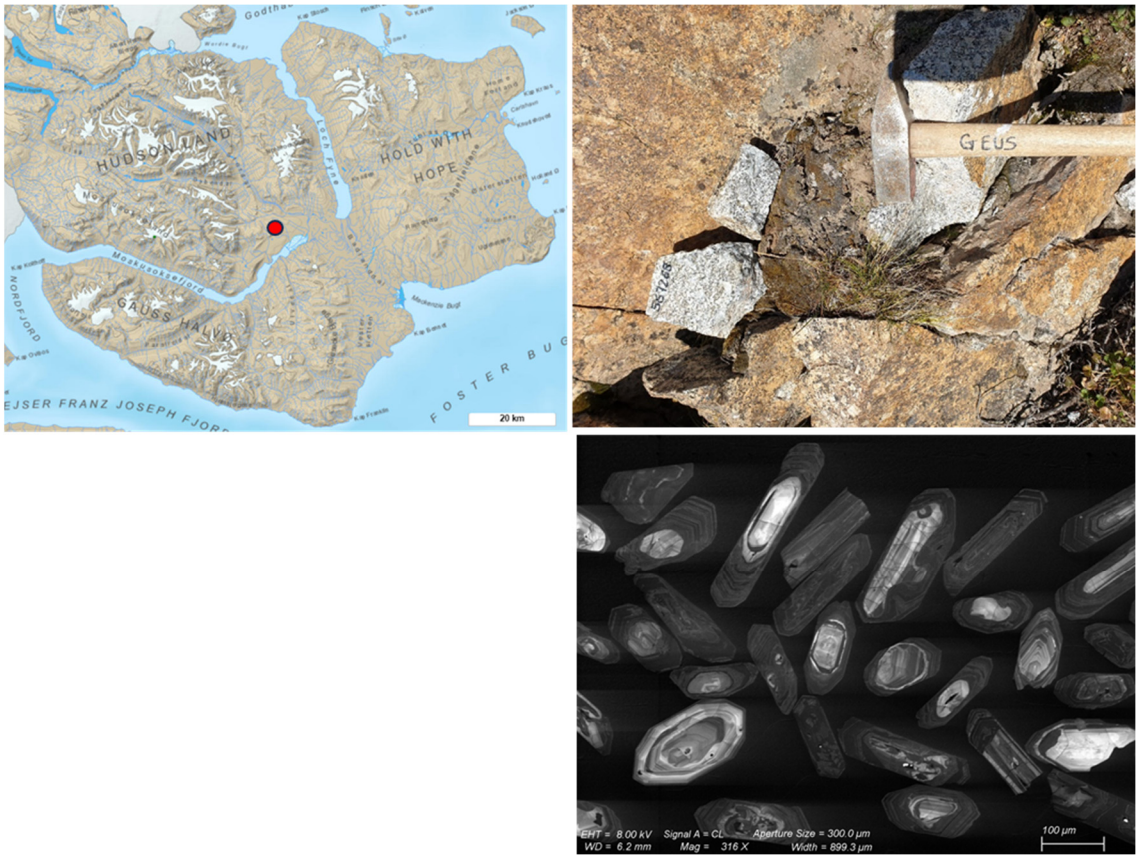

Figure 22: *Sample 567268 of coarse-grained granite Kfsp porphyritic granite from the south-eastern part of Hudson Land. The rock shows a weak to moderate foliation (lineation) with alignment of feldspar megacrysts. Zircons are large prismatic or stubby grains (100-350 µm) with aspect ratios of 1:2 - 1:4, many showing oscillatory or complex multi-stage zoning.*

Zircon data: A total of 120 grains were analysed out of which 59 were of acceptable quality and showing a high degree of concordancy (the rest representing bad analyses or data with significant cPb contents). The data are generally concordant and constitute a composite age distribution with a large proportion of grains falling in the age range of ca. 900 – 1800 Ma, and a single younger age peak at ca 450 Ma. Based on the most concordant grains (95-105%) a Concordia age of **455.4 ± 2.3 Ma** (n = 8) is calculated (Figure 23). A similar age of 445.4 ± 1.21 Ma (n = 19/57, MSWD = 2.7) can be derived based on a weighted average. The

Concordia age is taken as the crystallisation age of the granite. The older (900-1800 Ma) ages are interpreted as inherited.

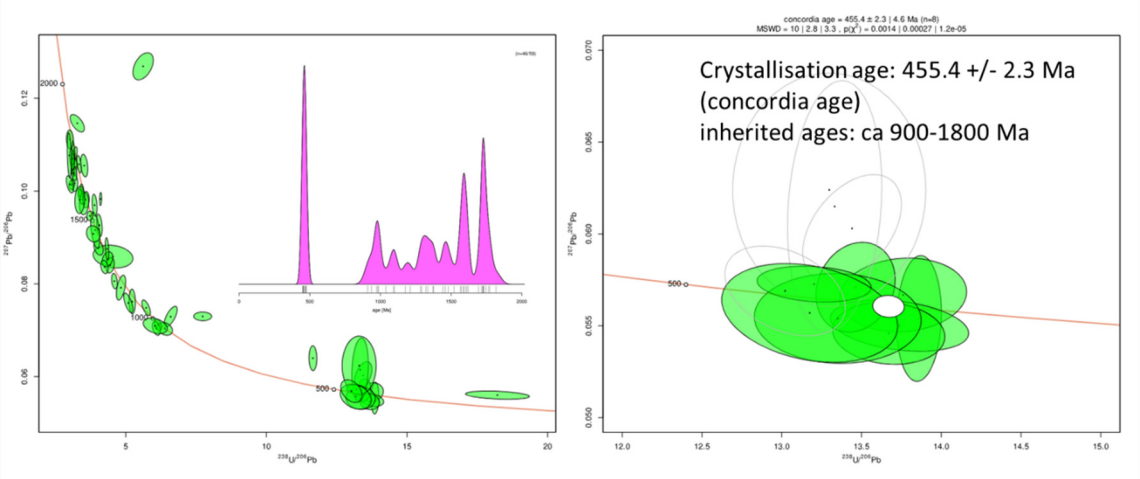

Figure 23: *Sample 567268 plotted in the Tera-Wasserburg diagram. A Concordia age of 455.4 ± 2.3 Ma (n = 8) is calculated based on the most concordant grains (95-105%). A similar age of 445.4 ± 1.21 Ma (n = 19/57, MSWD = 2.7) is derived based on a weighted average. A large proportion of inherited concordant zircons fall between ca. 900 and 1800 Ma.*

587001 – Medium-grained equigranular two-mica granite (Caledonian)

Passagedal W: 73.93831 N, 22.46401 W

Sample: The sample is a white/pale to grey, relatively homogenous equigranular biotite-muscovite granite (Figure 24). On the 1:500 000 scale map the granite (gm-label 'g6') is mapped as 'Caledonian granite with screens of metasediments (ca 430 Ma)'. The sample was collected several hundred meters within the granite intrusion exposed on the western side of Passagedal, away from the inclusion-rich marginal parts of the intrusion.

Zircon morphology: Subhedral to euhedral prismatic grains (100-150 µm) with aspect ratios mostly of 1:3 (1:2-1:4) with complex (multi-stage) oscillatory zoning in cores, sometimes with complex intersecting growth domains and rims.

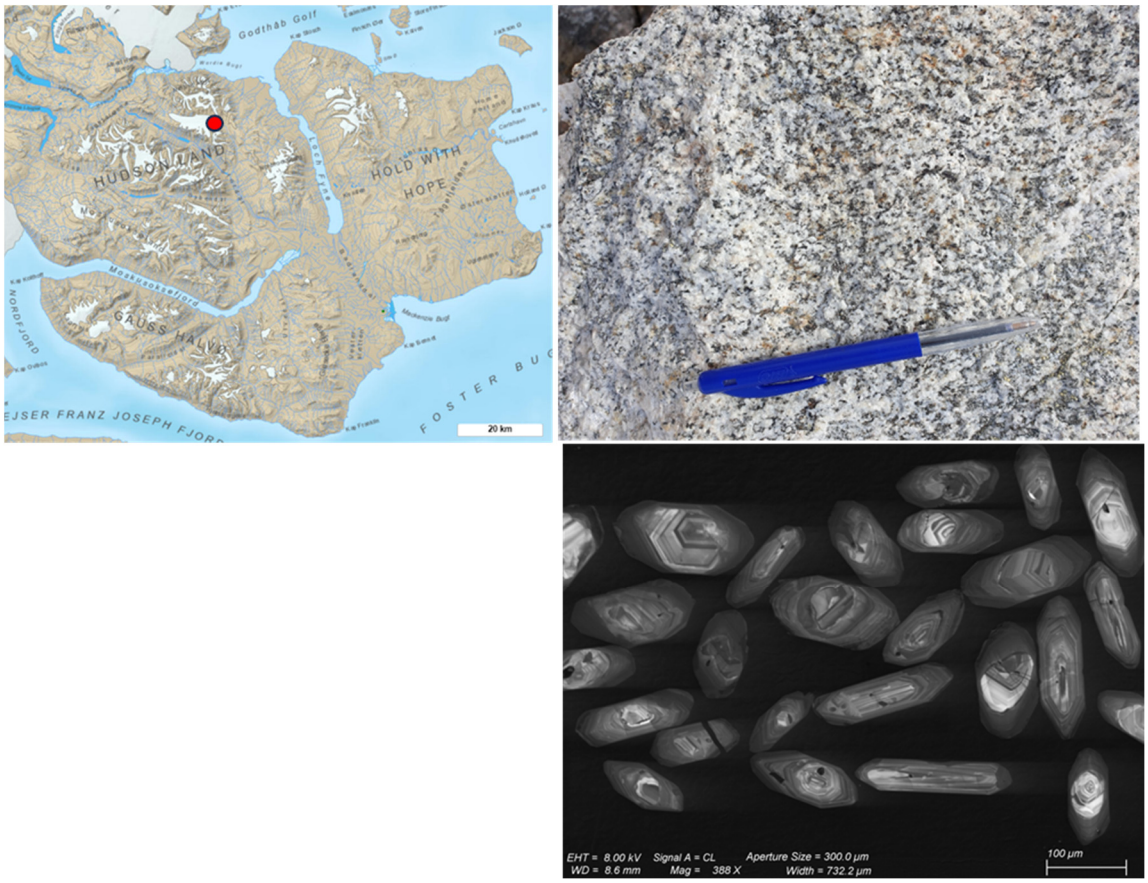

Figure 24: *Sample 587001 of medium-grained biotite-muscovite granite from the northern Hudson Land. CL-image: Zircons are stubby to prismatic (100-150µm) with aspect ratios around 1:3, with complex oscillatory and internal multi-stage zonation patterns.*

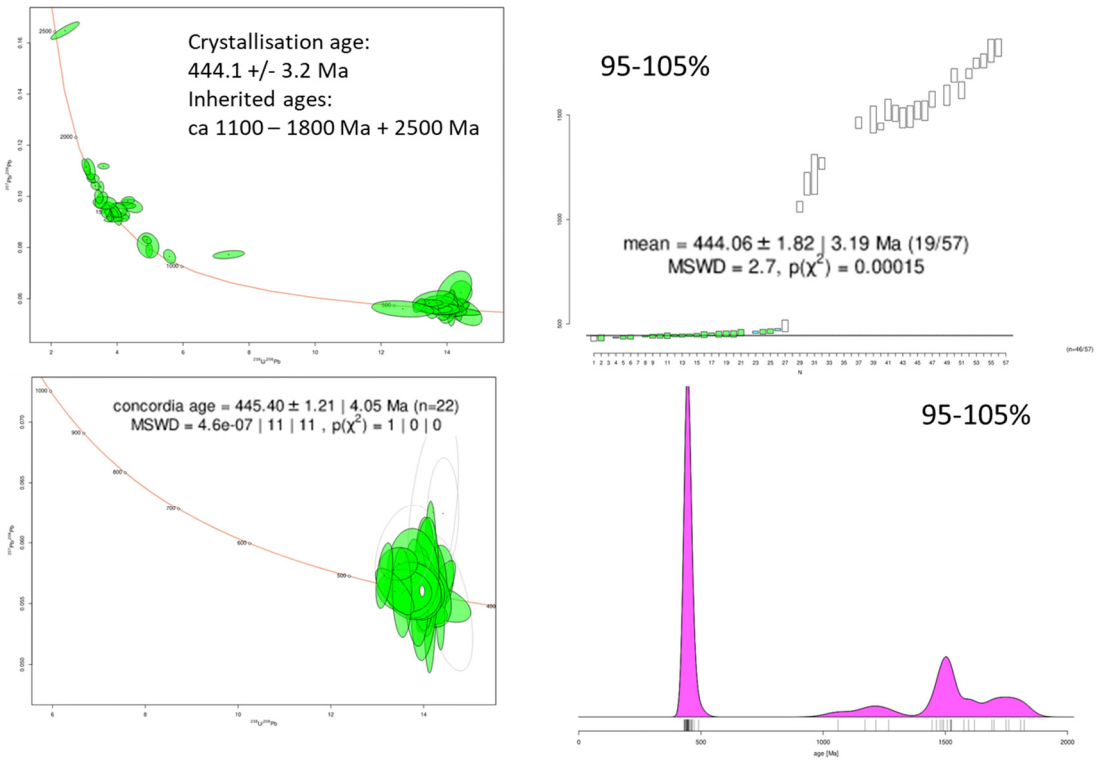

Figure 25: *Sample 587001 plotted in the Tera-Wasserburg diagram. A Concordia age of 445.4 +/- 1.21 Ma (n = 22) is calculated based on the most concordant grains (95-105%). A similar age of 445.4 +/- 1.21 Ma (n = 19/57, MSWD = 2.7) is derived based on a weighted average.*

Zircon data: A total of 127 spots were analysed of which 57 returned acceptable data, the remaining representing either poor analyses or data with significant influence of cPb. The filtered data are generally highly concordant, mostly within 95-105 % concordancy range. The ages show a wide distribution with a group of inherited grains at ca 1100 – 1800 Ma, with a single grain at 2500 Ma, and a main cluster at ca 450 Ma. A Concordia age based on 95-105% concordant grains of the lower age group yields **445.4 ± 1.2 Ma**, interpreted as the crystallisation age of the granite. A similar age of 444.1 ± 1.8 Ma (n = 19/57, MSWD = 2.7) is derived based on a weighted average (Figure 25).

523816 - Granitic vein (Caledonian)

Clavering Ø: 74.39570 N, 21.05184 W

Description: The metasedimentary rocks of the Krummedal Supracrustal Sequence are crosscut by numerous pegmatitic veins of granitic composition. The white veins stand clearly out in the brown host rock. The veins are up to tens of meters wide and can be followed for several 100 meters (Figure 26). This is a sample of a coarse-grained granitic vein. The age of the granite is expected to reflect the peak metamorphism in the area.

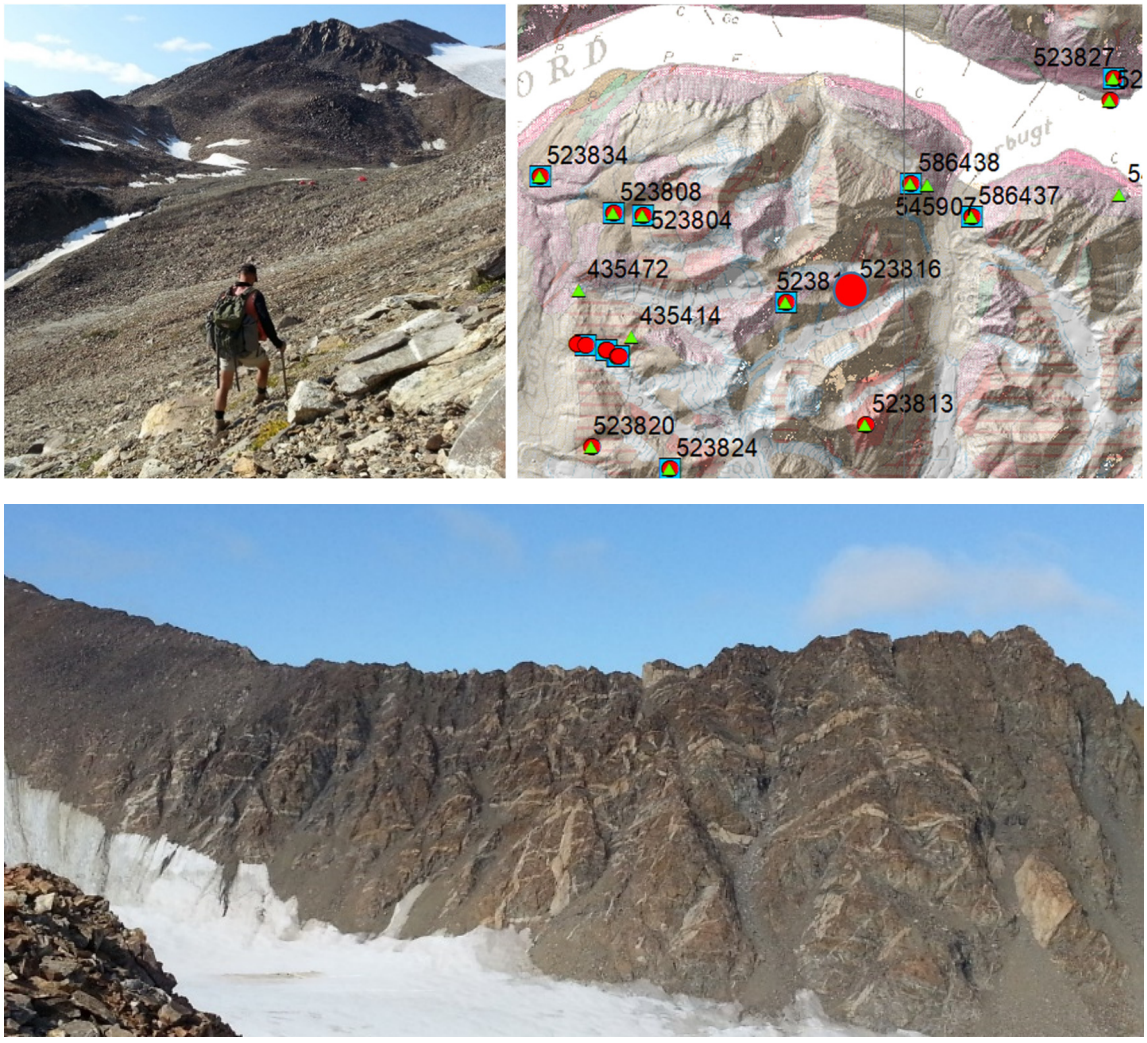

Figure 26: *Outcrop of granitic veins intruding metasediments of the Krummedal sequence in Northern Clavering Ø.*

Zircon morphology: The zircons are sub- to euhedral. Both elongated and stubby grains are present. Most grains are in poor condition, they are full of cracks, and broken into pieces. Most grains show no zonation and the few that does, mostly show an irregular, disturbed pattern.

Zircon data: This sample was analysed twice. In the first round 54 spots were analysed. The $^{207}Pb/^{206}Pb$ ages range from 477 to 401 Ma, with a cluster around 420 Ma.

Due to the scatter of ages, it is difficult to obtain a statistically significant age. An upper intercept age can be obtained at 437 ± 22 Ma (MSWD = 11) from all analyses, while a more statistically significant age of 430 ± 17 Ma (MSWD = 3.2, n = 31/54) is obtained if the outliers are filtered away (Figure 27).

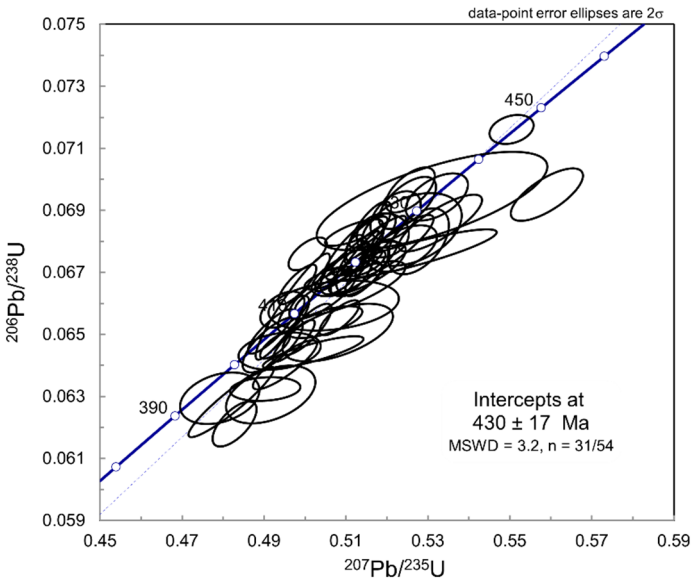

Figure 27: *Sample 523816. A rough Concordia upper intercept age of 430 ± 17 Ma (MSWD = 3.2, n = 31/54) may be calculated.*

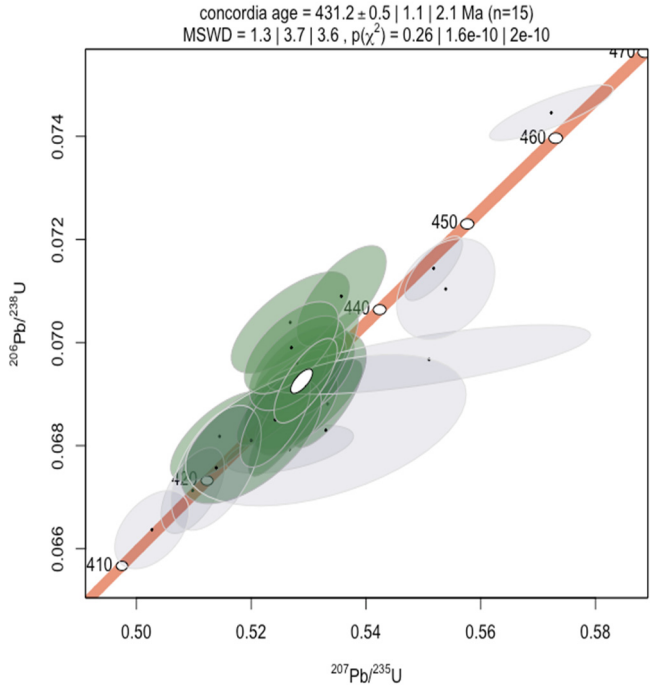

Figure 28: *Sample 523816. Treated data (annealed and acid leached) give a Concordia age of 431.2 ± 0.5 Ma (MSWD = 1.3, n =15/24), which is taken as the crystallisation age of the granite vein.*

In attempt to improve the precision of the age determination, a second analytical round was performed on extracted zircons that were annealed (heated) and acid leached prior analysis. The annealing and leaching process removes loosely bound Pb and therefore generally result in a reduced amount of scatter in the derived ages. The treated data shows less scatter and enables for a more precise Concordia age to be determined of **431.2 ± 0.5 Ma** (MSWD = 1.3, n =15/24) (Figure 28). This age is taken as best estimate of the crystallisation age of the granite.

546917 – Two-mica granite (Caledonian)

Clavering Ø: 74.3403 N, 20.7157 W

Locality: Djævlekløften, northeastern part of Clavering Ø (Camp 4). Pink homogeneous granite intrudes into a sequence of migmatitic metasedimentary rocks presumed to belong to the Krummedal sequence. The exposure extends in the northern valley side over a 300-400 m wide zone reaching ca 300 m above the valley floor (Figure 29).

Description: The rock is a medium-grained, pink, homogeneous leucocratic biotite-muscovite granite showing a weakly developed planar fabric. The granite contains euhedral quartz, suggesting quartz to be an early cumulus phase during crystallisation (possibly reflecting an enhanced F-contents in the magma).

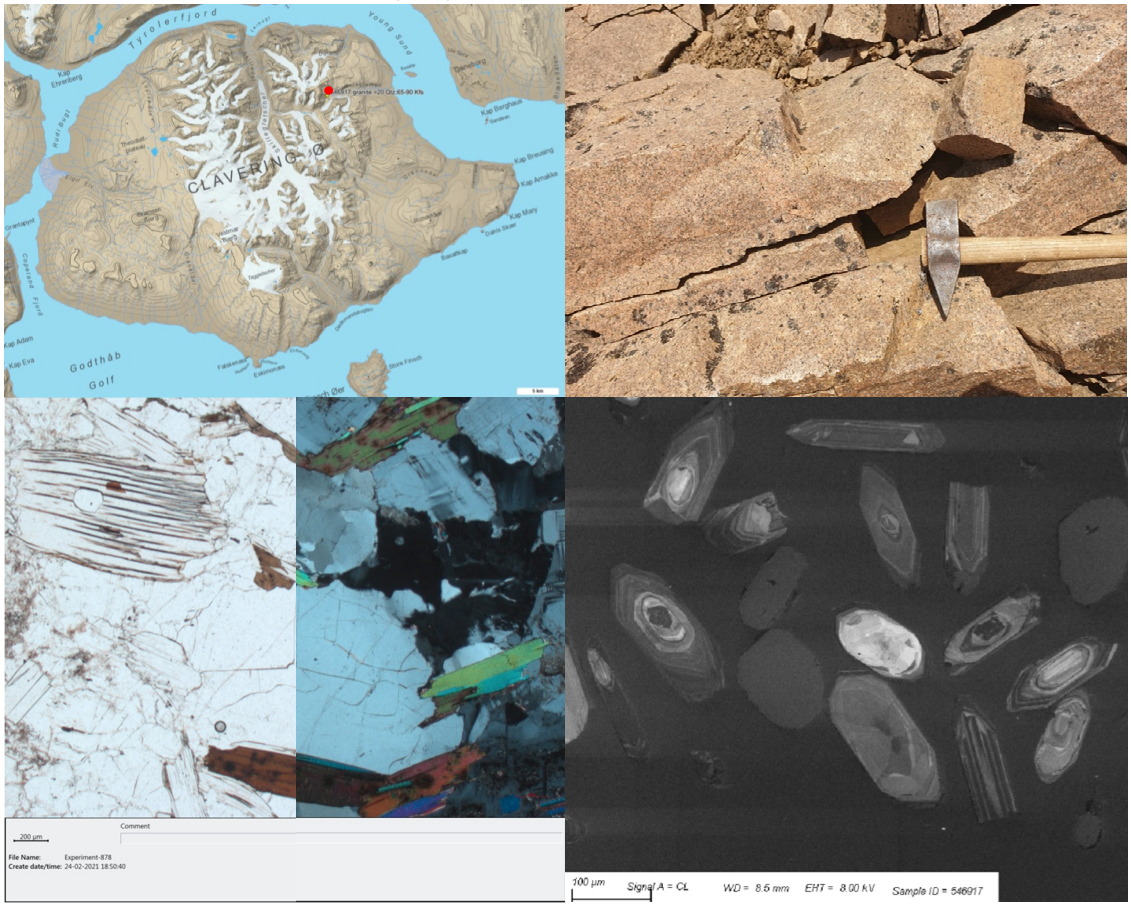

Figure 29: *Sample 546917, biotite-muscovite granite from 'Djævlekløften' in northeastern Clavering Ø. CL image: Zircons typically show oscillatory zonation, locally with irregular patchy zoning.*

Zircon morphology: Grains are stubby to prismatic sub- to euhedral grains with aspect ratios of 1:2 – 1:3, 100-150 µm long, typically oscillatory zoned, locally showing irregular patchy zoning suggesting metamorphic overprinting affected part of the grains (Figure 29).

Zircon data: In the first round of analyses without annealing experiments a total of 128 spots were analysed of which 35 returned acceptable data, 16 had some influence of cPb and 77 were bad. As a test a portion of zircons were selected for annealing experiment (to remove cPb) followed by acid leaching and mass spec analysis. A total of 55 zircons were analysed after treatment by annealing and acid leaching of which 14 returned acceptable data, 12 still had some influence of cPb and 29 were bad.

The combined data (untreated and treated) are plotted in Concordia diagram, distinguishing the untreated (red symbols) from the treated (green) data (Figure 30). Twelve grains lie in the range ca 1030 to 1780 Ma with two subgroups of each 4 grains yielding rough ages of 1060 ± 50 Ma and 1622 ± 57 Ma. The lower age group yields an average 8/6 age of 422.6 ± 4.5 Ma (MSDW = 8.1) for the 90-110% concordant grains, while a similar age is derived from taking only the most highly concordant grains 98-102%, namely 423.1 ± 3.1 Ma, but with much better statistics (MSDW = 2.1). Noteworthy, the annealed analyses remain after applying the 98-102% conc. filter suggesting that the annealing process indeed is getting rid of grains that are slightly disturbed. The annealed age data of **423.1 ± 3.1 Ma** is taken as the crystallisation age of the granite, while all older grains are inherited.
The sample was previously assigned to Devonian granite based on preliminary age dating. The annealed data show that the sample is upper Silurian rather than Devonian, so it is consequently reclassified as 'Caledonian'.

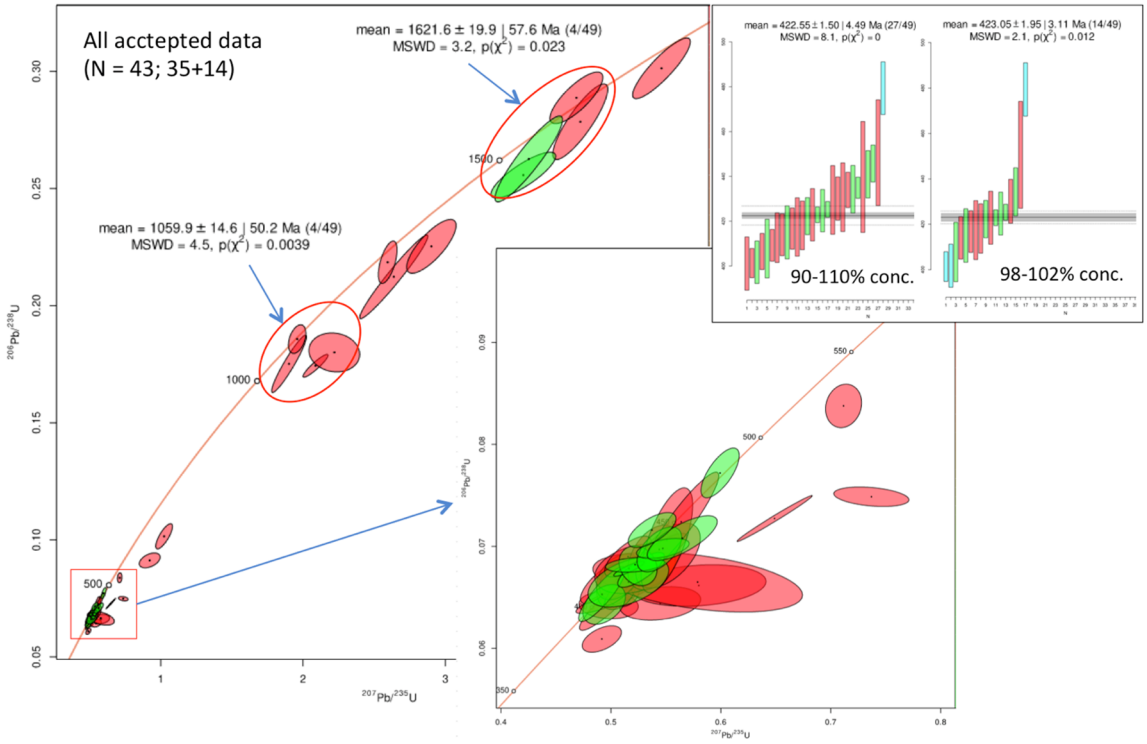

Figure 30: *Sample 546917 plotted in Wetherill-Concordia plots, showing an expansion of the ca 400 Ma interval, and inserts of weighted average $^{238}U/^{206}Pb$ ages based on specific concordance intervals (see text for explanation). Red ellipsoids: untreated grains, green ellipsoids: treated (i.e., annealed + acid leached) grains.*

567232 – Aplitic granite (Devonian)

Högboms Bjerg: 73.57083, N 22.73397 W

Sample: Aplitic granite with tabular K-feldspar and euhedral quartz micro-phenocrysts. The microgranite in the Högboms Bjerg area is recognised as part of the Devonian magmatism in Hudson Land (Haller & Koch, 1971). The granite is mainly a very fine-grained, aplitic type with a characteristic brick-red colour (Figure 31). It is typically homogeneous with a massive appearance. The granite is highly leucocratic (< 5% mafic minerals) with micro-phenocrysts of 1-2 mm white quartz. Rare examples of inclusions of dark cherty material, interpreted as baked rhyolitic xenoliths occur locally, establishing an age relationship between the granite and the associated (largely contemporaneous) rhyolitic lavas. The sample has an A-type whole-rock chemistry typical for the Devonian magmatism (Table 1).

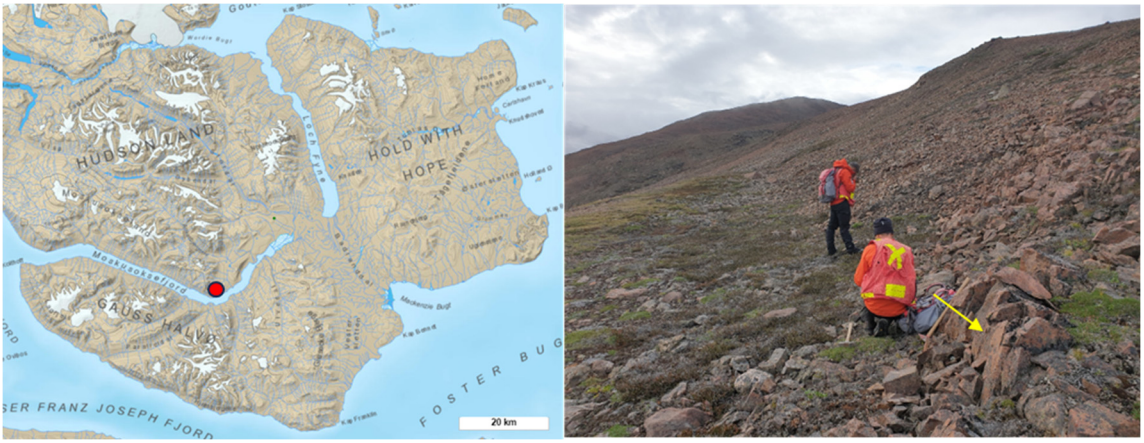

Figure 31: *Sample 567232 of aplitic granite at Högboms Bjerg.*

Zircon morphology: Grains are distinctly box-shaped, stubby, about 75 µm long with aspect ratios mostly < 1 : 2. Most grains show magmatic zonation with CL-dull cores and brighter rims.

Zircon data:
Most grains are strongly discordant and contain massive cPb (grey data) (Figure 32). A group of nine grains plot at, or very near the Concordia line and are interpreted as undisturbed. Based on the four most concordant grains a Concordia age of **397.1 ± 4.4 Ma** is calculated. This age, though based on only few grains, is interpreted as the crystallisation age of the granite. The age should be considered provisional, based on the small number of grains that it is based upon.

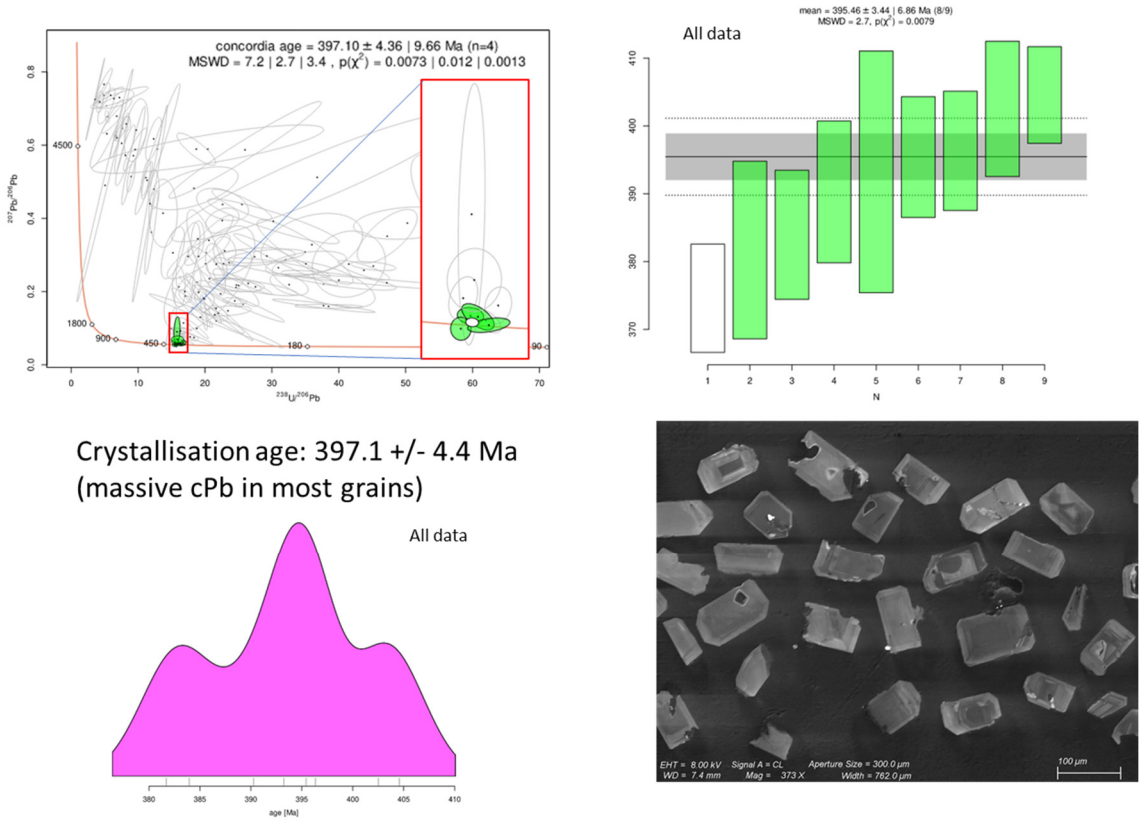

Figure 32: *Sample 567232 plotted in Tera-Wasserburg Concordia plot. Most grains are strongly discordant and contain cPb (grey data). A group of nine grains plot at or very near the Concordia and are interpreted as undisturbed. Based on the four most concordant grains a Concordia age of 397.1 ± 4.4 Ma is calculated.*

Summary of ages

The nine samples selected for zircon U-Pb dating from Clavering Ø and Hudson Land all show as a first order observation the ages expected for their assigned associations, i.e., into either 'Tonian', 'Caledonian' or 'Devonian' rocks, respectively.

The two Tonian augen granites dated from Clavering Ø yield ages of about 915 Ma and 960 Ma, which is broadly consistent with previously reported ages for these early gneissic granites (Kalsbeek et al. 2000). On a regional scale, the Tonian granites of central East Greenland are intruded into metasedimentary rocks, the Krummedal sequence, of the Hagar Bjerg Thrust Sheet and the Franz Joseph Allochthon during the Neoproterozoic orogenic event at ca. 940-910 Ma (Grenvillian orogeny) (Kalsbeek et al. 2000; Watt et al. 2000). In Clavering Ø the Tonian granites are relatively sparsely present and are seen to intrude into metasedimentary rocks of the Krummedal sequence.

Four Caledonian granites with different mineralogy and well-constrained field relationships were selected for age dating to clarify their place in the orogenic evolution. From Hudson Land two main types of granites were encountered during field mapping in 2022 and 2023, thus were targeted for age dating: 1) a K-feldspar phyric (megacrystic), moderately foliated granite (or monzogranite), and 2) a medium-grained, equigranular biotite-muscovite granite. Both types occur throughout the central eastern part of Hudson Land and always show the same internal relationship, with the equigranular granite cutting the porphyric granite. The new ages reported here confirm this age relationship as the latter is dated at 455 ± 2 Ma, whereas the former is dated at 445 ± 1 Ma. Additional preliminary age data confirm this pattern and also seem to suggest that there is a general northward younging of crystallisation ages within Hudson Land.

From Clavering Ø two granites were successfully dated, a deformed granitic vein intruding the Krummedal metasedimentary sequence in the northern part of the island, giving 431 ± 1 Ma and a weakly deformed two-mica granite in the northeastern part of the island yielding 423 ± 3 Ma. The ages appear to correlate well with the relative degrees of deformation recorded in these two granites.

Finally, a Devonian granite from the intrusive complex at Högboms Bjerg was dated to 397 ± 4 Ma which despite the limited amount of acceptable zircon data nonetheless is in generally good agreement with the sparse existing age estimates of around 380 Ma (uncertain age of Haller (1971), Hansen et al. (1987)).

Summary and evaluation/further studies

The spatial distribution of granite localities, over especially Clavering Ø and central Hudson Land, illustrates the observation made during earlier investigations that granites are more abundant than shown on presently available geological maps. The mapping campaigns in 2022-2023 at Hudson Land and Gauss Halvø have focused on delineating the extents of the various granite types in more detail. With this information, assisted by 3D photointerpretation and (locally) hyperspectral data, a more complete map will be produced for the area. Some of the outstanding questions relate to whether the individual granite outcrops are small, isolated bodies, or they are connected at depth as parts of larger bodies. A more detailed understanding of the ages of the various granites is underway through more detailed geochronological and petrological studies.

Specifically, this updated study of the East Greenland granite geochemistry has verified the main findings of Thrane et al. (2021), namely that four main groups of granites can be geochemically deciphered in central East Greenland (from oldest to youngest):

1) Tonian granites from Clavering Ø
No new Tonian samples were identified and added to this report compared to Thrane et al. (2021), and as such the findings by Thrane et al. (2021) remains valid, namely that these older granites seem to be chemically distinct from the aforementioned granites by having higher FeO_t and lower Al_2O_3, which at least in part reflects derivation from another source. Two Tonian granite samples were U-Pb dated verifying their Tonian age (523813 and 521688).

2) Caledonian monzonites from Clavering Ø
Among the Caledonian granitoids, the monzonite samples from Clavering Ø represent the most primitive included in the sample set. These rocks show unusually high K, which seems to reflect some extent of secondary enrichment processes. Nonetheless, their general mineralogy and I-type geochemistry indicate infracrustal meta-igneous rocks (e.g., amphibolite) as probable melt source, which is consistent with a subduction-setting. Two age dates of monzonite samples at 446 ± 2 Ma and 456 ± 9 Ma agree marginally within error of each other, confirming this rock unit to be late Ordovician, thus early Caledonian, predating collisional orogen.

3) Caledonian S-type granites and intermediate Devonian granites
The group of so-called ‘intermediate Devonian granites’ described in Thrane et al. (2021) are not readily possible to discriminate from the larger group of Caledonian granites based on geochemical criteria alone. Although described from field criterias as Devonian, they have the same geochemical trademarks as the Caledoinian S-type granites. It is therefore possible that the two groups are part of the same population, i.e., share similar source regions, something that could be tested by acquiring Sm-Nd isotopic data on selected samples. For the large group of Caledonian granites, a closer inspection of the geochemical data in relation to geographical distribution, intrusion type, petrography, and character of host rock and mineralogy will provide a basis for further subdivision of the large group of Caledonian granites.

This work is underway based on the detailed mapping carried out in Hudson Land in 2022 and 2023.

4) Devonian rhyolites and evolved granites
The Devonian extrusive and intrusive rocks are clearly petrogenetically related based on field observations and share same distinct geochemical characteristics of A2-type granites, such as high Nb, Ta, Y, low Sr, and negative Eu-anomaly. U-Pb zircon dating of Devonian rocks (intrusive or extrusive) appear to represent a challenge due to many zircons being disturbed, and more work is underway to obtain more reliable ages. So far, we managed to date one Devonian granite sample from Högboms Bjerg (521632) yielding a preliminary age of 397 ± 4 Ma, which is in broad accordance with previous unprecise age estimates of around 380 Ma (Hansen et al. 1987).

The East Greenland granite geochemical database which has been established through the current project will continue to develop with the planned addition of more geochemical and geochronological data on samples collected in the Hudson Land-Gauss Halvø area during field work conducted by GEUS in 2023. An update report is planned by the end of 2024.

Further analytical geochronology work will aim at refining ages, which could be done by re-analysing selected key samples for precise U-Pb dating work on the NordSIMS in Stockholm. The NordSIMS offers significantly higher resolution than the LA-ICPMS setup at GEUS, and hence dating of smaller analytes which allows for deciphering of complex textural growth domains that are often found in the granites.

Whole-rock Sm-Nd isotope work is tentatively planned in collaboration with prof. Dr. Sebastian Tappe (UiT) and will help to characterise the different source regions for the Caledonian granites on a regional scale, i.e., comparing Caledonian granites across the North Atlantic region.

References

Arc Mining and SRK exploration 2015: Geological report following 2014 exploration activities on licence 2014/07, East Greenland. Licence report, GEUS Report File Number 100019.

Bengaard, H.J. 1992: Geological map of Greenland 1:250.000, Upper Proterozoic to Devonian, East Greenland. Copenhagen: Geological Survey of Denmark and Greenland.

Bernstein, S. & Thrane, K. 2019: Field report 2019 – Clavering Ø. Internal report, Geological Survey of Denmark and Greenland.

Blevin, P. L. & Chappell, B. W. 1992: The role of magma sources, oxidation states and fractionation in determining the granite metallogeny of eastern Australia: Trans. Roy. Soc. Edinburgh: Earth Sci. 83, 305-316.

Blevin, P. L. & Chappell, B. W. 1995: Chemistry, origin and evolution of mineralised granites in the Lachlan Fold Belt, Australia; the metallogeny of I- and S-type granites. Economic Geology 90, 1604-1619.

Boyton, W.V. 1984: Geochemistry of rare earth elements: Meteorite studies. In: Henderson, P., Ed., Rare Earth Element Geochemistry, Elsevier, New York 63-114.

Chappell, B. W. & White, A. J. R. 1974: Two contrasting granite types. Pacific Geology 8, 173–174.

Escher, J.C. 2001: Geological map of Greenland, 1:500 000, Kong Oscar Fjord. Sheet 11. Copenhagen: Geological Survey of Denmark and Greenland.

Frei, D, Gerdes, A (2009) Precise and accurate in situ U–Pb dating of zircon with high sample throughput by automated LA-SF-ICP-MS. Chemical Geology, 261(3-4), 261-270.

Frost, B.R, Barnes, C.G., Collins, W.J. Arculus, R.J., Ellis, D.J. & Frost, C.D. 2001: A Geochemical Classification for Granitic Rocks, Journal of Petrology 42, 2033–2048.

Grebennikov, A.V. 2014: A-type granites and related rocks: Petrogenesis and classification. Russian Geology and Geophysics 55, 1074-1086.

Haller, J. 1971: Geology of the East Greenland Caledonides, 413 pp. New York: Inter-science Publishers.

Harpøth, O. 1984: Precious metal and tin exploration in Hudson Land and Andrees Land, Central East Greenland. Nordisk Mineselskab A/S 14/83, 50 pp.

Harpøth, O., Pedersen, J.L., Schønwandt, H.K. & Thomassen, B. 1986: The mineral occurrence of central East Greenland. Meddelelser om Grønland, Geoscience 17, 140 pp.

Hansen, B.T., Steiger, R.H., Henriksen, N. & Borchardt, B. 1987: U-Pb and Rb-Sr age determinations on Caledonian plutonic rocks in the central part of the Scoresby Sund region, East Greenland: Rapp. Grønl. Geol. U. 162, 139-151.

Higgins, A.K., Elvevold, S., Escher, J.C., Frederiksen, K.S., Gilotti, J.A., Henriksen, N., Jepsen, H.F., Jones, K.A., Kalsbeek, F., Kinny, P.D., Leslie, A.G., Smith, M.P., Thrane,

K. & Watt, G.R. 2004: The foreland-propagating thrust architecture of the East Greenland Caledonides 72°-75°N. Journal of the Geological Society, London 161,1009-1026.

Hughes, C.J. 1973: Spilites, keratophyres and the Igneous Spectrum. Geol. Mag. 109, 513-527.

Jackson SE, Pearson NJ, Griffin WL, Belousova EA (2004) The application of laser ablation-inductively coupled plasma-mass spectrometry to in situ U–Pb zircon geochronology. Chemical Geology 211, 47-69.

Jones, K.A. & Escher, J.C. 1999: Thickening and collapse history of the Caledonian crust, Clavering Ø, East Greenland. In: Higgins, A.K. & Frederiksen, K.S. (Eds) Geology of East Greenland 72-75N, mainly Caledonian: preliminary reports from the 1998 expedition. Danmarks og Grønlands Geologiske Undersøgelse rapport 1999/19, 101-110.

Kalsbeek, F., Nutman, A.P. & Taylor, P.N. 1993: Palaeoproterozoic basement province in the Caledonian fold belt of North-East Greenland. Precambrian Research 63, 163-178.

Kalsbeek, F., Thrane, K., Nutman, A.P. & Jepsen, H. 2000: Late Mesoproterozoic to early Neoproterozoic history of the East Greenland Caledonides: evidence for Grenvillian orogenesis? Journal of Geological Society, London 157, 1215-1225.

Kalsbeek, F., Jepsen, H. & Jones, K.A. 2001a: Geochemistry and petrogenesis of S-type granites in the East Greenland Caledonides. Lithos 57, 91-109.

Kalsbeek, F., Jepsen, H.F. & Nutman, A.P. 2001b: From source migmatites to plutons: tracking the origin of ca. 435 Ma S-type granites in the East Greenland Caledonian orogen. Lithos 57, 1-21.

Kalsbeek, F., Higgins, A.K., Jepsen, H.F., Frei, R. & Nutman, A.P. 2008b: Granites and granites in the East Greenland Caledonides, *in* Higgins, A.K., Gilotti, J.A., and Smith, M.P., eds., The Greenland Caledonides: Evolution of the Northeast Margin of Laurentia: Geological Society of America Memoir 202, 227–249.

Kalsbeek, F., Thrane, K., Higgins, A.K., Jepsen, H.F., Leslie, A.G., Nutman, A.P. & Frei, R. 2008a: Polyorogenic history of the East Greenland Caledonides in Higgins AK, Gilotti JA, Smidt MP eds, The Greenland Caledonides: Evolution of the Northeast Margin of Laurentia: Geological Society of America, Memoir 202, 50-72.

Keulen, N., Heredia, B., Rosa, D., Malkki, S.N., Thomsen, T.B. & Whitehead, D. 2023: Tin and tungsten mineralisations in North East and central East Greenland (ca. 70-74°N). Preliminary report based on the activities in 2022 and 2023. Danmarks og Grønlands Geologiske Undersøgelse Rapport 2023/47.

Kokfelt, T.F. 2019: Report of the field work carried out during the summer of 2019 within the framework of the Clavering Ø project. Internal report, Geological Survey of Denmark and Greenland.

Koch, L. & Haller, J. 1971: Geological map of East Greenland 72-76 N. Lat. (1:250,000). Meddelelser om Grønland 183, 26 pp. (plus 13 map sheets).

Kystol, J. & Larsen, L.M. 1999: Analytical procedures in the Rock Geochemical Laboratory of the Geological Survey of Denmark and Greenland.: Geology of Greenland Survey Bulletin 184, 59–62.

Li, X., Chi, G., Zhou, Y., Deng, T. & Zhang, J. 2017: Oxygen fugacity of Yanshanian granites in South China and implications for metallogeny. Ore Geology Reviews 88, 690-701.

Maniar, P. D. & Piccoli, P. M. 1989: Tectonic discrimination of granitoids. Geological society of America bulletin 101, 635-643.

McDonough, W. F. & Sun, S.S. 1995: The composition of the Earth. Chemical geology 120, 223-253.

Meinert, L. D. 1992: Skarns and skarn deposits. Geoscience Canada 19, 145-162.

Mittelholzer, A.E. 1941: Die Kristallingebiete von Clavering-Ø und Payer Land. (Ostgrønland). Meddelelser om Grønland 144, 42 pp.

Nielsen, B.L. & Larsen, H.C. 1974: Airborne geophysical survey in central East Greenland.: Rapport Grønlands Geologiske Undersøgelse 65, 73–76.

Nielsen, B.L. & Steenfelt, A. 1977: Distribution of radioactive elements and the recognition of uranium mineralizations in East Greenland. In: Recognition and evaluation of uraniferous areas. Int. Atomic Energy Agency, Vienna (IAEA-TC-25/3), 87-105.

Olsen, H. & Larsen, P.-H. 1993: Lithostratigraphy of the continental Devonian sediments in North-East Greenland. Bulletin Grønlands Geologiske Undersøgelse 165, 108 pp.

Paton C, Hellstrom JC, Paul P, Woodhead JD, Hergt JM (2011) Iolite: Freeware for the visualisation and processing of mass spectrometric data. Journal of Analytical Atomic Spectrometry 26, 2508-2518.

Pearce, J. A., Harris, N. B. & Tindle, A. G. 1984: Trace element discrimination diagrams for the tectonic interpretation of granitic rocks. Journal of petrology 25, 956-983.

Petrus JA, Kamber BS (2012) VizualAge: A Novel Approach to Laser Ablation ICP-MS U-Pb Geochronology Data Reduction. Geostandards and Geoanalytical Research 36, 247-270.

Rosa, D. 2019: Report of the field work carried out during the summer of 2019 within the framework of the Clavering Ø project. Internal report, Geological Survey of Denmark and Greenland.

Ryan, M.J. & Sandwall, J. 1975: Field work in the Muskusoksefjord – Kejser Franz Josephs Fjord Region of East Greenland. Nordisk Mineselskab A/S 7/75, 57 pp.

Slama J, Kosler J, Condon DJ, Crowley JL, Gerdes A, Hanchar JM, Horstwood MSA, Morris GA, Nasdala L, Norberg N, Schaltegger U, Schoene N, Tubrett MN, Whitehouse MJ (2008) Plesovice zircon – a new natural reference material for U-Pb and Hf isotopic microanalysis. Chemical Geology 249, 1-2, 1-35.

Steenfelt, A. 1982: Uranium and selected trace elements in granites from the Caledonides of East Greenland. Mineralogical Magazine 46, 201-10.

Stendal, H. 1999: Mineralisation follow-up in fault zones, Hudson Land, Gauss Halvø and Steno Land, North-East Greenland. In: Geology of East Greenland 72-75N, mainly Caledonian: preliminary reports from the 1998 expedition. Eds. By Higgins, A.K. & Frederiksen, K.S. Danmarks og Grønlands Geologiske Undersøgelse rapport 1999/19, 201-205.

Thomassen, B. & Tukianinen, T. 2010: Hyperøst 2008-09: Ground check of hyperspectral anomalies in the Werner Bjerge – Wollaston Forland region, North-East Greenland. Part 1: analytical results. Danmarks og Grønlands Geologiske Undersøgelse rapport 2010/54.

Thrane, K., Kokfelt, T., Rosa, D., Steenfelt, A. & Bernstein, S. 2021: Whole-rock geochemistry of granitic intrusions from Clavering Ø, Hudson Land and Gauss Halvø, North-East Greenland. Danmarks og Grønlands Geologiske Undersøgelse Rapport 2021/72.

Thyrsted, T. 1975: Geologien I Randbøldalen Kap Franklin Regionen Centrale Østgrønland. Internal rapport (in Danish), Geological Survey of Denmark and Greenland.

Vermeesch, P., 2018, IsoplotR: a free and open toolbox for geochronology. Geoscience Frontiers, v.9, p.1479-1493, doi: 10.1016/j.gsf.2018.04.001.

Vermeesch P (2021) On the treatment of discordant detrital zircon U–Pb data. Geochronology, 3, 247–257.

Watt, G.R., Kinny, P.D. & Friderichsen, J.D. 2000: U–Pb geochronology of Neoprotero-zoic and Caledonian tectonothermal events in the East Greenland Caledonides. Journal of the Geological Society, London, 157, 1031–1048.

Whalen, J. B., Currie, K. L., & Chappell, B. W. 1987: A-type granites: geochemical characteristics, discrimination and petrogenesis. Contributions to mineralogy and petrology 95, 407-419.

Zhao, J.-X., Shiraishi, K., Ellis, D. J. & Sheraton, J. W. 1995: Geochemical and isotopic studies of syenites from the Yamato mountains, East Antarctica: implications for the origin of syenitic magmas. Geochimica et Cosmochimica Acta 59, 1363–1382.